

3. MIDDLE MIOCENE TO PLEISTOCENE DIATOM STRATIGRAPHY OF LEG 167¹

Toshiaki Maruyama²

ABSTRACT

Ocean Drilling Program Leg 167 represents the first time since 1978 that the North American Pacific margin was drilled to study ocean history. More than 7500 m of Quaternary to middle Miocene (14 Ma) sediments were recovered from 13 sites, representing the most complete stratigraphic sequence on the California margin. Diatoms are found in most samples in variable abundance and in a moderately well-preserved state throughout the sequence, and they are often dominated by robust, dissolution-resistant species. The Neogene North Pacific diatom zonation of Yanagisawa and Akiba (1998) best divides the Miocene to Quaternary sequences, and updated ages of diatom biohorizons estimated based on the geomagnetic polarity time scale of Cande and Kent (1995) are slightly revised to adjust the differences between the other zonations. Most of the early middle Miocene through Pleistocene diatom datum levels that have been proven to be of stratigraphic utility in the North Pacific appear to be nearly isochronous within the level of resolution constrained by sample spacing. The assemblages are characterized by species typical of middle-to-high latitudes and regions of high surface-water productivity, predominantly by *Coscinodiscus marginatus*, *Stephanopyxis* species, *Proboscia barboi*, and *Thalassiothrix longissima*. Latest Miocene through Pliocene assemblages in the region of the California Current, however, are intermediate between those of subarctic and subtropical areas. As a result, neither the existing tropical nor the subarctic (high latitude) zonal schemes were applicable for this region. An interval of pronounced diatom dissolution detected throughout the Pliocene sequence apparently correspond to a relatively warmer paleoceanographic condition resulting in a slackening of the southward flow of the California Current.

INTRODUCTION

The oceanographic and climate histories of the eastern and western equatorial Pacific (Ocean Drilling Program [ODP] Legs 138 and 130, respectively) and the high-latitude North Pacific (ODP Leg 145) have already been explored with scientific drilling, but sediments reflecting the history of the California Current and the temperate North Pacific, the oceanographic link between the two regions, had not previously been recovered using modern drilling techniques. ODP Leg 167 represents the first time since 1978 that the North American Pacific margin was drilled to study ocean history (Fig. 1). The leg ship-board scientific party collected not only high-resolution records within the Pleistocene through Pliocene but also lower resolution records since the middle Miocene. Sites were drilled to collect sediments needed to study the links between the evolution of North Pacific climate and the development of the California Current system.

The California Current system is probably the best investigated eastern boundary current system in the world. Nevertheless, the response of the California Current system and associated coastal upwelling systems to climate change is poorly documented. During Leg 167, 13 sites were drilled—Sites 1010 through 1022—along the climatically sensitive California margin (Fig. 1). These sites are arrayed in a series of depth and latitudinal transects to reconstruct the Neogene history of deep, intermediate, and surface ocean circulation and to understand the paleoceanographic and paleoclimatic history of this region (Table 1).

Biostratigraphic research objectives for the California margin sites focus on a few major threads. These are (1) documenting the record of surface ocean processes in the northeastern Pacific, (2) investigating the longer term linkage between the oceanographic evolution of the northeastern Pacific and continental records of marine and terrestrial processes, and (3) defining accurate depth and age frameworks for all sites. The sediments collected on Leg 167 provide

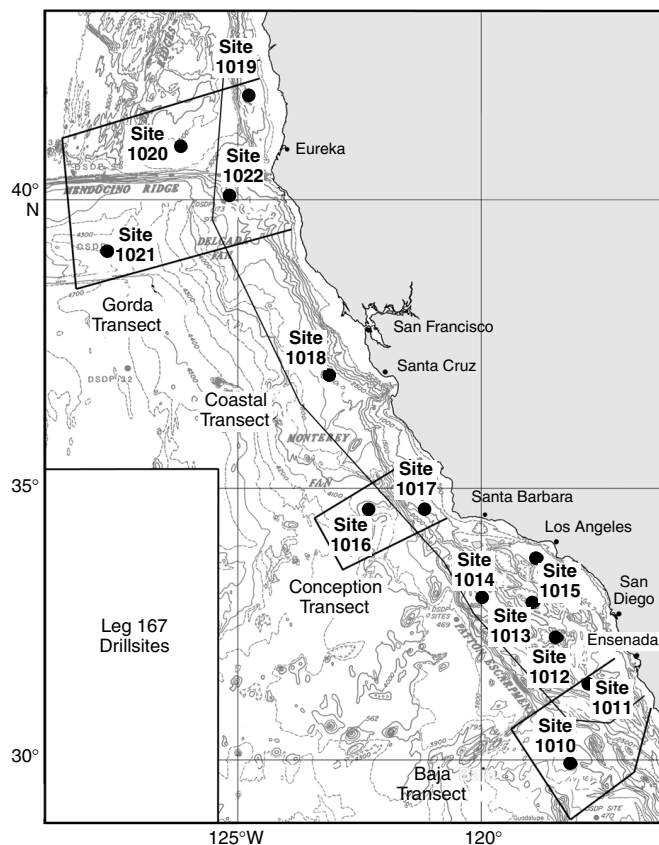


Figure 1. Location map for Leg 167 drill sites along the California margin of North America. The coastal and onshore/offshore transects of Leg 167 have been outlined. Bathymetry from Mammerickx (1989). (From Lyle, Koizumi, Richter, et al., 1997.)

¹Lyle, M., Koizumi, I., Richter, C., and Moore, T.C., Jr. (Eds.), 2000. *Proc. ODP, Sci. Results, 167*: College Station TX (Ocean Drilling Program).

²Department of Earth and Environmental Sciences, Yamagata University, 1-4-12 Kojirakawa, Yamagata, 990-8560, Japan. maruyama@sci.kj.yamagata-u.ac.jp

Table 1. Leg 167 drill sites.

Site	Location	Position	Distance from shore (km)	Water depth (m)	Sediment thickness drilled (mbsf)	Age of oldest sediment recovered	Linear sedimentation rate range (mcd/m.y.)	Name of transect		
								East-west transect	North-south transect	Depth transect
1010	Ocean crust near Guadalupe Island	29°57.90'N	209	3465	209	middle Miocene	5-24	Baja		South
1011	Animal Basin	31°16.82'N	85	2033	276	late Miocene	24-45	Baja		South
1012	East Cortes Basin	32°16.97'N	105	1783	274	late Miocene	37-80		Coastal	South
1013	San Nicolas Basin	32°48.04'N	115	1575	146	late Pliocene	34-73		Coastal	South
1014	Tanner Basin	32°49.99'N	155	1177	449	late Miocene	27-214		Coastal	South
1015	Santa Monica Basin	33°42.92'N	31	912	150	late Pleistocene				South
1016	Pelagic site, off Point Conception	34°32.41'N	148	3846	317	late Miocene	10-72	Conception		South
1017	Santa Lucia Slope	34°32.09'N	52	967	204	Pleistocene	118-204	Conception	Coastal	South
1018	Sediment drift, south of Guide Seamount	36°59.30'N	76	2476	426	late Pliocene	56-193		Coastal	North
1019	Eel River Basin	41°40.97'N	59	989	248	Pleistocene	122-498	Gorda		North
1020	Eastern flank, Gorda Ridge	41°00.05'N	167	3050	278	early Pliocene	40-120	Gorda		North
1021	Outer Delgada Fan	39°05.25'N	364	4215	310	middle Miocene	10-40	Gorda		North
1022	Delgada Slope	40°04.85'N	87	1927	388	Miocene?	~110	Gorda	Coastal	North

Note: Data from Lyle, Koizumi, Richter, et al., 1997.

one of the first direct opportunities to enhance current biostratigraphies and biochronologies to improve the temporal framework for refined paleoceanographic analysis.

Extensive Miocene to Pleistocene diatom records were recovered at several sites. The purpose of this paper is (1) to document the diatom stratigraphy at each site, (2) to test the utility of diatom datum levels in relation to the magnetostratigraphy, and (3) to present a diatom zonation for the middle Miocene through Quaternary. Because the paleomagnetic calibration of early Miocene through Pleistocene diatom datum levels in the North Pacific is generally completed (Koizumi and Tanimura, 1985; Barron and Gladenkov, 1995; Yanagisawa and Akiba, 1998), the emphasis is laid upon the testing the isochronicity of diatom datum levels in the northeastern Pacific sediments.

METHODS

Zonation

Since the pioneering works of Donahue (1970), Schrader (1973a), and Koizumi (1973a, 1973b) established the elementary framework of the Neogene diatom biostratigraphic zonation, successive revision and refinement of the North Pacific diatom stratigraphy has been developed rapidly by subsequent studies including Koizumi (1975a, 1975b, 1975c, 1975d, 1977, 1980, 1985, 1992), Burckle and Opdyke (1977), Barron (1980a, 1981, 1985b, 1992a), Akiba (1977, 1979, 1982b, 1983, 1986), Akiba, Hoshi, et al. (1982), Akiba, Yanagisawa, et al. (1982), Akiba and Ichinoseki (1983), Maruyama (1984b), Oreshkina (1985), Koizumi and Tanimura (1985), Yanagisawa (1996), and Watanabe and Takahashi (1997).

Neogene diatom zonations of Maruyama (1984b), Koizumi (1985), Akiba (1986), Barron and Gladenkov (1995), and Yanagisawa and Akiba (1998) essentially resemble each other. Akiba's (1986) paper is conceivably the best summary of the state of Miocene to Pleistocene North Pacific diatom stratigraphy, and his proposed stratigraphic zonation has been widely accepted as a standard workable scheme (Barron and Baldauf, 1995). In the high-latitude North Pacific transect (ODP Leg 145), Barron and Gladenkov (1995) succeeded in directly correlating diatom zones with magnetostratigraphy and in supplying precise ages for Neogene primary zonal marker biohorizons. Furthermore, Gladenkov and Barron (1995) confirmed an early Miocene through Oligocene diatom zonation by the nearly continuous documentation of diatom records. Recently, Yanagisawa and Akiba (1998) yielded some minor modifications to the Neogene North Pacific diatom zonation of Akiba (1986) to adjust the differences between the previously existing zonations.

The diatom zonation (Fig. 2) used for the Quaternary and Neogene closely follows the zonation of Yanagisawa and Akiba (1998) proposed for the northwest Pacific. Code numbers of Neogene North

Pacific diatom (NPD) zones were also adapted to the above-mentioned zonation with contemporary rearrangement. There is a smaller change in zonal boundaries. The top of *Denticulopsis katayamae* Zone is marked in practical sense, by the last common occurrence (LCO) of *Denticulopsis simonsenii* as suggested by Akiba (1986). Relationships between the zone name, code label, and definition are shown in Table 2. Table 3 lists age estimates for the Neogene diatom datum levels that have been found to be useful in the middle-to-high latitudes of the North Pacific. Ages are presented according to both the geomagnetic polarity time scale of Berggren et al. (1985a, 1985c) and of Cande and Kent (1992, 1995).

On board the *JOIDES Resolution*, age vs. depth plots were constructed using paleomagnetic events and other microfossil datum levels, so that the accuracy of the diatom datum levels could be basically tested (Lyle, Koizumi, Richter, et al., 1997). Although the Neogene datum levels, especially Miocene datum levels, were not directly controlled by the magnetostratigraphy, they occur in the proper sequence and apparently at the proper intervals, thus implying that they may be isochronous with other parts of the North Pacific.

In this study, a correlation between magnetostratigraphy and diatom biohorizons follows mainly Koizumi and Tanimura (1985), Koizumi (1992), and Barron and Gladenkov (1995). The ages of the primary diatom biohorizons in the text are updated based on the revised geomagnetic polarity time scale of Cande and Kent (1995) by extrapolation of each horizon within each magnetic chron. Among the geomagnetic polarity time scales (Cande and Kent, 1992, 1995; Baksi, 1993; Wei, 1995; Berggren et al., 1995a, 1995b), the severe variance in age calibration points is relatively well known. Users have to be prepared for a maximum age difference of 1.3 m.y. in the latest early Miocene because the middle Miocene is deficient in reliable age calibration points (Motoyama and Maruyama, 1998; Yanagisawa and Akiba, 1998).

In addition, exceptional diachronism across latitude was documented for a number of diatom biohorizons such as the first occurrence (FO) of *Actinocyclus ingens* f. *nodus*, the FO of *Proboscia barboi*, the FO of *Neodenticula kamschatica*, the FO of *Actinocyclus oculatus*, the FO of *Neodenticula koizumii*, and the last occurrence (LO) of *N. koizumii* (Burckle and Opdyke, 1985; Koizumi and Tanimura, 1985; Koizumi, 1992; Barron and Gladenkov, 1995).

Taxonomic studies, principally on a group commonly accepted as "marine *Denticula*" (Simonsen and Kanaya, 1961) or the genus *Denticulopsis* (Simonsen, 1979), made a remarkable advance in the Neogene North Pacific diatom biostratigraphy. Short-ranging species belonging to the three genera denominated *Denticulopsis*, *Crucidentacula*, and *Neodenticula* by Akiba and Yanagisawa (1986) provide many stratigraphically useful biohorizons (Schrader, 1973a, 1973b; Maruyama, 1984a, 1992; Akiba, 1977, 1979, 1982a, 1986; Akiba and Yanagisawa, 1986; Tanimura, 1989; Yanagisawa and Akiba, 1990).

Techniques

Ages (Ma)	Epoch / Subepoch	Chron	Polarity	Zonation	Events	North Pacific Diatom Zone	Boundary ages (Ma)
1	Quat.	C1	-	<i>N. seminae</i>	LO <i>P. curvirostris</i>	NPD 12	0.30
				<i>P. curvirostris</i>	LO <i>A. oculatus</i>	NPD 11	1.01-1.46
2	Pliocene late	C2	-	<i>A. oculatus</i>	LO <i>N. koizumii</i>	NPD 10	2.0
				<i>N. koizumii</i>	LO <i>N. kamschatica</i>	NPD 9	2.61-2.68
3	Pliocene early	C2A	-	<i>N. koizumii - N. kamschatica</i>	FO <i>N. koizumii</i>	NPD 8	3.53-3.59
4				<i>N. kamschatica</i>	FO <i>T. oestrupii</i>	NPD 7Ba	5.49
5	Pliocene late	C3	-	<i>N. kamschatica</i>	FCO <i>N. kamschatica</i>	NPD 7A	6.65
6				<i>R. californica</i>	LCO <i>R. californica</i>	NPD 7A	7.6
7	Pliocene late	C3B	-	<i>R. californica</i>	FO <i>N. kamschatica</i>	NPD 6B	8.6
8				<i>T. schraderi</i>	LCO <i>T. schraderi</i>	NPD 6A	9.16
9	Pliocene late	C4	-	<i>D. katayamae</i>	LO <i>D. katayamae</i>	NPD 5D	9.9
10				<i>D. katayamae</i>	LCO <i>D. simonsenii</i>	NPD 5D	11.5
11	Pliocene late	C4A	-	<i>D. dimorpha</i>	LO <i>D. dimorpha</i>	NPD 5C	12.9
12				<i>D. dimorpha</i>	FO <i>D. dimorpha</i>	NPD 5B	13.1
13	Pliocene early	C5	-	<i>T. yabei</i>	LCO <i>D. praedimorpha</i>	NPD 5A	14.4-14.6
14				<i>D. praedimorpha</i>	FO <i>D. praedimorpha</i>	NPD 4A	14.9
15	Pliocene middle	C5A	-	<i>D. praedimorpha</i>	LCO <i>D. praedimorpha</i>	NPD 4Bb	15.9
16				<i>C. nicobarica</i>	LCO <i>D. hyalina</i>	NPD 3B	16.3
17	Pliocene middle	C5AA	-	<i>C. nicobarica</i>	LCO <i>D. hyalina</i>	NPD 3A	16.9
18				<i>C. nicobarica</i>	FO <i>D. simonsenii</i>	NPD 2B	18.4
19	Pliocene middle	C5AB	-	<i>D. hyalina</i>	FO <i>D. simonsenii</i>	NPD 2A	20.1
20				<i>D. hyalina</i>	FO <i>D. hyalina</i>	NPD 1	22.3
21	Pliocene early	C5B	-	<i>D. lauta</i>	FO <i>D. lauta</i>	none	24.0-24.3
22				<i>D. lauta</i>	FO <i>D. praelauta</i>		
23	Pliocene early	C5C	-	<i>D. praelauta</i>	FO <i>D. praelauta</i>		
24				<i>C. kanayae</i>	FO <i>C. kanayae</i>		
25	Pliocene early	C5D	-	<i>C. sawamurae</i>	FO <i>C. sawamurae</i>		
26				<i>T. fraga</i>	FO <i>T. fraga</i>		
27	Pliocene early	C5E	-	<i>T. fraga</i>	FO <i>T. fraga</i>		
28				<i>T. praeprae</i>	LO <i>R. gelida</i>		
29	Pliocene early	C6	-	<i>T. praeprae</i>	LO <i>R. gelida</i>		
30				<i>R. gelida</i>	FO <i>T. praeprae</i>		
31	Oligo.	C6A	-	<i>R. gelida</i>	FO <i>T. praeprae</i>		
32				<i>R. gelida</i>	FO <i>T. praeprae</i>		
33	Oligo.	C6AA	-	<i>R. gelida</i>	FO <i>T. praeprae</i>		
34				<i>R. gelida</i>	FO <i>T. praeprae</i>		
35	Oligo.	C6B	-	<i>R. gelida</i>	FO <i>T. praeprae</i>		
36				<i>R. gelida</i>	FO <i>T. praeprae</i>		
37	Oligo.	C6C	-	<i>R. gelida</i>	FO <i>T. praeprae</i>		
38				<i>R. gelida</i>	FO <i>T. praeprae</i>		

Figure 2. Correlation of diatom zonation, primary zonal markers, and zonal code numbers used on Leg 167. Zone limits have been calibrated to the geochronology of Cande and Kent (1995). LO = last occurrence; FO = first occurrence; FCO = first common occurrence; LCO = last common occurrence.

The taxonomy used follows that of Koizumi (1980, 1992), Akiba (1986), Yanagisawa and Akiba (1990, 1998), Fenner (1991), Harwood and Maruyama (1992), and Akiba et al. (1993). Because it is not clear how to separate correctly preferable taxa of *Crucidentacula* and *Denticulopsis*, and because it is uncertain whether a number of secondary diatom biohorizons proposed by Yanagisawa and Akiba (1998) apply in the California margin, I have made the following groupings:

- Crucidentacula nicobarica* group = *C. paranicobarica* vars. and *C. nicobarica*;
- Denticulopsis lauta* group = *D. lauta*, *D. ichikawae*, *D. okunoii*, and *D. tanimurae*;
- D. hyalina* group = *D. praehyalina* and *D. hyalina*;
- D. simonsenii* group = *D. simonsenii* and *D. vulgaris*;
- D. katayamae* group = *D. praekatyamae* and *D. katayamae*;
- D. praedimorpha* group = *D. praedimorpha* v. *minor*, *D. barronii*, *D. praedimorpha* v. *intermedia*, *D. praedimorpha* v. *praedimorpha* and *D. praedimorpha* v. *robusta*; and
- D. dimorpha* group = *D. dimorpha* v. *dimorpha* and *D. dimorpha* v. *areolata*.

On board the *JOIDES Resolution*, strewn slides were prepared by placing a small amount of material on a slide glass, adding a few drops of distilled water, kneading the material, and extending it thinly with a toothpick. When, because of a low concentration of diatom skeletons or an induration of siliceous grains, age assignment control was required, selected samples were processed by boiling them in hydrogen peroxide and hydrochloric acid, followed by centrifuging at 1200 rpm for 2 min to remove the chemical solutions from the suspension.

Because a large amount of clay-rich sediments interfered with an identification of diatoms, almost all core-catcher samples had to be processed once again on land in the laboratory. Sample material was placed in an oven at 60°C for 24 hr, and about 2–3 g of dried material was boiled in a 200-mL beaker with about 30–50 mL of hydrogen peroxide solution (5%) for a few minutes and 10 mL of hydrochloric acid (5%) was added in small portions. Acid-treated material was made pH-neutral by repeatedly filling and decanting the beakers with distilled water and allowing 1 hr for settling. Strewn slides were prepared by spreading the pipette suspension onto a cover glass (24 × 32 mm), drying on a hot plate, and mounting in Photocuring Adhesive DB-855.

Diatoms are present throughout the sites, but with varying abundance and preservation. Whenever possible, all of the diatom taxa were tabulated without *Chaetoceros* spores. Strewn slides were examined in their entirety at a magnification of 600× for stratigraphic markers and paleoenvironmentally sensitive taxa. Identifications were checked routinely at 1000×. These abundances were recorded as follows:

- D (dominant) = more than five specimens per field of view;
- A (abundant) = two or more specimens per field of view;
- C (common) = one specimen per two fields of view;
- F (few) = one specimen per each vertical traverse;
- R (rare) = one specimen per a few vertical traverses;
- T (trace) = one specimen per several or more vertical traverses; and
- B (barren).

Preservation of diatoms was determined qualitatively as follows:

- VG (very good) = finely silicified forms present, no alteration of frustules, and some colonies of frustules preserved;
- G (good) = finely silicified forms present and no alteration of frustules observed;
- M (moderate) = finely silicified forms present with some alteration; and
- P (poor) = finely silicified forms absent or rare and fragmented, and the assemblage is dominated by robust forms.

RESULTS

The tabulated occurrences of stratigraphically important and relatively common diatom taxa are shown in Tables 4 through 13, including the sample depth both of meters below seafloor depth (mbsf) and meters composite depth (mcd). Tables 14 and 15 provide the sample, meters below seafloor depth (mbsf), and meters composite depth (mcd) constrained to stratigraphic events identified for Sites 1010 through 1022, located along the north-to-south transect, whereas Sites 1012, 1013, 1015, and 1017 were situated in the low-biosiliceous-productivity region along the California Borderland basins where a good record of calcareous microfossils was expected. The composite depth assignment follows that reported in Lyle, Koizumi, Richter, et al. (1997).

Table 2. Diatom zonation and stratigraphic markers used during Leg 167.

Code	Zone and Subzone	Category	Author	Base	Top
NPD12	<i>Neodenticula seminae</i>	Interval zone	Donahue (1970)	LO of <i>Proboscia curvirostris</i>	Present
NPD11	<i>Proboscia curvirostris</i>	Interval zone	Donahue (1970)	LO of <i>Actinocyclus oculatus</i>	LO of <i>Proboscia curvirostris</i>
NPD10	<i>Actinocyclus oculatus</i>	Interval zone	Donahue (1970)	LO of <i>Neodenticula koizumii</i>	LO of <i>Actinocyclus oculatus</i>
NPD9	<i>Neodenticula koizumii</i>	Interval zone	Koizumi (1973b)	LO of <i>Neodenticula kamschatica</i>	LO of <i>Neodenticula koizumii</i>
NPD8	<i>N. koizumii-N. kamschatica</i>	Concurrent range zone	Koizumi (1973b)	FO of <i>Neodenticula koizumii</i>	LO of <i>Neodenticula kamschatica</i>
NPD7Bb	<i>N. kamschatica-b</i>	Interval zone	Koizumi (1973a, 1973b, 1985)	FO of <i>Thalassiosira oestrupii</i> s.l.	FO of <i>Neodenticula koizumii</i>
NPD7Ba	<i>N. kamschatica-a</i>	Interval zone	Koizumi (1973a, 1973b, 1985)	LCO of <i>Rouxia californica</i>	FO of <i>Thalassiosira oestrupii</i> s.l.
NPD7A	<i>Rouxia californica</i>	Interval zone	Akiba (1986)	LCO of <i>Thalassionema schraderi</i>	LCO of <i>Rouxia californica</i>
NPD6B	<i>Thalassionema schraderi</i>	Interval zone	Akiba (1982b)	LCO of <i>Denticulopsis simonsenii</i>	LCO of <i>Thalassionema schraderi</i>
NPD6A	<i>Denticulopsis katayamae</i>	Interval zone	Maruyama (1984b)	LO of <i>Denticulopsis dimorpha</i>	LCO of <i>Denticulopsis simonsenii</i>
NPD5D	<i>D. dimorpha</i>	Taxon range zone	Maruyama (1984b), Akiba (1979)	FO of <i>Denticulopsis dimorpha</i>	LO of <i>Denticulopsis dimorpha</i>
NPD5C	<i>Thalassiosira yabei</i>	Interval zone	Maruyama (1984b), Akiba (1979)	LCO of <i>Denticulopsis praedimorpha</i>	FO of <i>Denticulopsis dimorpha</i>
NPD5B	<i>Denticulopsis praedimorpha</i>	Taxon range zone	Akiba et al. (1982a)	FO of <i>Denticulopsis praedimorpha</i>	LCO of <i>Denticulopsis praedimorpha</i>
NPD5A	<i>Crucidentricula nicobarica</i>	Interval zone	Akiba et al. (1982a)	LCO of <i>Denticulopsis hyalina</i>	FO of <i>Denticulopsis praedimorpha</i>
NPD4Bb	<i>Denticulopsis hyalina-b</i>	Interval zone	Maruyama (1984b)	FO of <i>Denticulopsis simonsenii</i>	LCO of <i>Denticulopsis hyalina</i>
NPD4Ba	<i>Denticulopsis hyalina-a</i>	Interval zone	Maruyama (1984b)	FO of <i>Denticulopsis hyalina</i>	FO of <i>Denticulopsis simonsenii</i>
NPD4A	<i>Denticulopsis lauta</i>	Lineage zone	Koizumi (1973b)	FO of <i>Denticulopsis lauta</i>	FO of <i>Denticulopsis hyalina</i>
NPD3B	<i>Denticulopsis praelauta</i>	Lineage zone	Akiba (1983, 1986)	FO of <i>Denticulopsis praelauta</i>	FO of <i>Denticulopsis lauta</i>
NPD3A	<i>Crucidentricula kanayae</i>	Interval zone	Akiba (1977)	FO of <i>Crucidentricula kanayae</i>	FO of <i>Denticulopsis praelauta</i>
NPD2B	<i>Crucidentricula sawamurae</i>	Interval zone	Gladenkov and Barron (1995)	FO of <i>Crucidentricula sawamurae</i>	FO of <i>Crucidentricula kanayae</i>
NPD2A	<i>Thalassiosira fraga</i>	Interval zone	Barron (1985a)	FO of <i>Thalassiosira fraga</i>	FO of <i>Crucidentricula sawamurae</i>
NPD1	<i>Thalassiosira praefraga</i>	Interval zone	Gladenkov and Barron (1995)	FO of <i>Thalassiosira praefraga</i>	FO of <i>Thalassiosira fraga</i>
None	<i>Rocella gelida</i>	Partial range zone	Gladenkov and Barron (1995)	FO of <i>Rocella gelida</i>	FO of <i>Thalassiosira praefraga</i>

Notes: Modified from Yanagisawa and Akiba, 1998. The boundary between Subzone NPD4Bb and Zone NPD5A can be also recognized by the FCO of *Denticulopsis simonsenii*. LO = last occurrence, FO = first occurrence, LCO = last common occurrence, FCO = first common occurrence.

Site 1010

Site 1010 is the deep-water site (3465 m) of the southern depth transect (Baja Transect) and is situated on 14- to 15-Ma basaltic basement. Six holes were cored at Site 1010 in the southern region of the California Current. The sedimentary sequence recovered at Site 1010 consists of an apparently continuous 210-m-thick interval of Quaternary to middle middle Miocene sediments.

The section includes an upper 82-m-thick sequence containing trace to absent diatoms, from the Quaternary through the latest Miocene. Paleomagnetic studies obtained a detailed magnetostratigraphy from the Brunhes to the top of Chron C3Bn (7 Ma). In the lower part of the interval, Chron C3A can be recognized from 61 to 75 mbsf, indicating an age assignment of 5.89–6.94 Ma. This is underlain by a 48-m-thick sequence of late Miocene to late middle Miocene age marked by variable but often common diatoms and an almost complete absence of planktonic foraminifers. This, in turn, is underlain by a 55-m-thick sequence of rapidly deposited diatom ooze of middle middle Miocene age.

Diatoms are rare to abundant and moderately well to well preserved throughout the middle Miocene through upper Miocene section (Table 4). Samples 167-1010C-10H-3, 20–21 cm, through 11H-3, 20–21 cm, are placed in the *Thalassionema schraderi* Zone (NPD 6B), where the topmost sample indicates not only the LCO of *T. schraderi* but also the end of high production in diatom assemblages at the middle late Miocene. Although the deep-sea hiatus NH6 aged 7.4–8.4 Ma (Keller and Barron, 1987), is widespread in the North Pacific (Barron, 1980a), this event was not found because of the poor preservation of diatoms in both Holes 1010C and 1010E.

Both the LO of *D. katayamae* and the LCO of *D. simonsenii* are recorded simultaneously in Sample 167-1010C-11H-5, 21–22 cm, which marks the top of the *D. katayamae* Zone (NPD 6A). The boundary between the *D. katayamae* Zone and the underlying *D. dimorpha* Zone (NPD 6A/5D) is assigned between Samples 167-1010C-11H-CC and 12H-3, 20–21 cm, based upon the LO of *D. dimorpha*. Zones NPD 6A through 5D (8.6–9.9 Ma) are greatly compressed from 97.2 to 103.7 mbsf, especially the unique horizon of 103.7 mbsf, which represents the total range of *D. dimorpha* in Hole 1010C. The FO of *D. katayamae*, which should be the uppermost event settled within Zone NPD 5D, coincides with the base of overlying Zone NPD 6A.

The interval from Samples 167-1010C-12H-5, 21–22 cm, through 14H-5, 20–22 cm, is assigned to the *Thalassiosira yabei* Zone (NPD 5C). The LCO of *Denticulopsis praedimorpha* in Sample 167-1010C-

14H-CC marks the boundary between the *T. yabei* Zone and the underlying *D. praedimorpha* Zone (NPD 5B). A special feature of Site 1010 was the recovery of an unusually thick middle Miocene section assignable to the interval of the *D. praedimorpha* Zone (NPD 5B) through the underlying *Crucidentricula nicobarica* Zone (NPD 5A). The FO of *D. praedimorpha*, defining the base of Zone NPD 5B, is assigned in Sample 167-1010C-17H-CC. The interval of Zone NPD 5B is equivalent to the total range of *D. praedimorpha* definitely, having an estimated age of 11.5–12.9 Ma. Correspondingly, the same two zones were also observed in the 40-m-thick interval from Samples 167-1010E-14H-CC through 18H-CC. Assigned ages based on diatoms and other microfossil groups are similar between Holes 1010C and 1010E.

The coincidence of the LCO of *D. hyalina* with the FCO of *D. simonsenii* is assigned between Samples 167-1010C-19X-CC and 20X-3, 75–76 cm, and marks the boundary between the *C. nicobarica* Zone (NPD 5A) and the *D. hyalina* Zone (NPD 4B). Based upon the FO of *D. simonsenii*, Zone NPD 4 can be divided into two subzones (Yanagisawa and Akiba, 1998), but the basal barren sequence from Sample 167-1010C-20X-CC through 23X-CC interrupts a full and particular investigation at Site 1010. Though *D. simonsenii* are not found at all, the lowest sample can be placed within Subzone NPD 4Bb because of the common occurrence of *D. hyalina* without the presence of *D. lauta*. Likewise in Hole 1010E, the lowest Sample 167-1010E-19X-CC contains *D. hyalina* and can be correlated with the *D. hyalina* Zone (NPD 4B). The base of the sedimentary sequence at Site 1010, probably corresponding to the middle middle Miocene *D. hyalina* Zone, exhibits an age between 13.1 and 14.6 Ma.

Barron (1985b) noticed that the FO of *D. "hustedtii"* (= *simonsenii*) is too diachronous to be useful in lower middle latitudes. The first consistent dominance of *D. "hustedtii"* over *D. hyalina* is widely known as the dominance transition of *D. hyalina* to *D. "hustedtii"* and appears to be isochronous in the middle- to high-latitude North Pacific. Because of the latitudinal diachronism of the FO of *D. "hustedtii"*, Barron (1985b) speculated that the FCO of *D. "hustedtii"* at middle-to-high latitudes probably corresponds with the FO of *D. "hustedtii"* in the warmer low-latitude Pacific. In Hole 1010C at 29°57.90'N, the FO of *D. simonsenii* is coincident with the abrupt transition from *D. hyalina* to *D. simonsenii*, which agrees with stratigraphic occurrences of these taxa in Deep Sea Drilling Project (DSDP) Leg 63, Hole 470 at 28°54.46'N (Barron, 1981).

Diatom datum levels indicate continuous and relatively rapid sediment accumulation rates within the middle Miocene, when the sub-

Table 3. Magnetic calibration and age estimates of diatom events useful for biostratigraphy in the Neogene through Quaternary periods of the North Pacific.

Event	Datum	BKFV85 (Ma)	CK92 (Ma)	CK95 (Ma)	Chron	Source
* LO	<i>Proboscia curvirostris</i>	0.3-0.35	0.30	0.30	C1n	Koizumi (1992)
LO	<i>Thalassiosira jouseae</i>	0.26-0.39	0.30-0.41	0.30-0.41	C1n	Koizumi and Tanimura (1985)
LO	<i>Rhizosolenia matuyamai</i>	0.85-0.97	0.91-1.04	0.91-1.06	C1r.1n	Koizumi and Tanimura (1985)
FO	<i>Rhizosolenia matuyamai</i>	0.91-1.05	0.98-1.12	0.99-1.14	C1r.1n	Koizumi and Tanimura (1985)
* LO	<i>Actinocyclus oculatus</i>	0.93-1.33	1.00-1.44	1.01-1.46	C1r.1n	Koizumi and Tanimura (1985)
FO	<i>Proboscia curvirostris</i>	1.5	1.58		C1r.2r	Koizumi and Tanimura (1985)
LO	<i>Coscinodiscus pustulatus</i>	1.7	1.8			Barron (1980a)
LO	<i>Pyxidicula horridus</i>	1.7	1.8-2.0	1.8-2.0		Barron (1992a)
LO	<i>Thalassiosira antiqua</i>	1.43-1.70	1.5-1.8	1.52-1.8		Koizumi and Tanimura (1985)
FO	<i>Fragilariopsis doliolus</i>	1.89-2.00	2	2	C2r.1r	Barron (1992a)
* LO	<i>Neodenticula koizumii</i>	1.9	2.0	2.0	C2r.1r	Koizumi (1992)
LO	<i>Pyxidicula pustulata</i>	2.0	2.0-2.2	2.0-2.14		Barron (1980a)
LO	<i>Thalassiosira convexa</i>	2.3	2.4	2.35	C2r.1r	Barron (1992a)
* LO	<i>Neodenticula kamschatica</i>	2.50-2.58	2.63-2.7	2.61-2.68	C2An.1n	Koizumi and Tanimura (1985)
LCO	<i>Neodenticula kamschatica</i>	2.50-2.58	2.63-2.7	2.61-2.68		Barron and Gladenkov (1995)
FO	<i>Neodenticula seminiae</i>	2.6	2.7	2.68	C2An.1n	Koizumi (1992)
LO	<i>Thalassiosira marujamica</i>		3.1-3.2	3.08-3.2	C2An.1r to .2n	Barron and Gladenkov (1995)
LO	<i>Thalassiosira jacksonii</i>	3.1	3.1-3.4	3.08-3.41	C2An.1r to .3n	Koizumi (1992)
* FO	<i>Neodenticula koizumii</i>	3.6	3.51-3.85	3.53-3.95	C2Ar	Koizumi and Tanimura (1985)
FO	<i>Actinocyclus oculatus</i>	3.7	3.6-3.9	3.64-4.01	C2Ar	Koizumi (1992)
FO	<i>Thalassiosira latimarginata</i>	4.9	4.9	5.07	C3n.4n	Barron and Gladenkov (1995)
* FO	<i>Thalassiosira oestrupii</i>	5.1	5.3	5.49	C3r	Barron (1992a)
LO	<i>Rouxia californica</i>	5.2	5.5	5.9		Barron (1992a)
LO	<i>Thalassiosira miocenica</i>	5.35	5.8	6.0	C3An.1n	Koizumi and Tanimura (1985)
FO	<i>Thalassiosira praeoestrupii</i>	5.54	5.95	6.1	C3An.1r	Barron and Gladenkov (1995)
LO	<i>Thalassiosira praekonvexa</i>	5.8	6.3		C3An.2n	Barron (1992a)
FCO	<i>Neodenticula kamschatica</i>			6.4		Yanagisawa and Akiba (1998)
FO	<i>Thalassiosira miocenica</i>	6.1	6.2	6.4	C3An.2n	Barron (1992a)
* LCO	<i>Rouxia californica</i>	6.1	6.46	6.65		Akiba (1986)
LO	<i>Cavitatus jouseanus</i>		6.5-6.6	6.7-6.8	C3Ar	Barron and Gladenkov (1995)
FO	<i>Thalassiosira jacksonii</i>	6.4	6.8			Barron (1992a)
FO	<i>Nitzschia reinholdii</i>	6.5	7.2-7.3	7.4-7.5	C4n.1n	Barron and Gladenkov (1995)
FO	<i>Neodenticula kamschatica</i>	6.6	7.1-7.2	7.3-7.4	C3Br	Barron and Gladenkov (1995)
* LCO	<i>Thalassionema schraderi</i>	6.7	7.4	7.6	C4n.1r	Barron and Gladenkov (1995)
LO	<i>Thalassiosira minutissima</i>	7.5	8.2			Barron (1992a)
FCO	<i>Thalassionema schraderi</i>			8.4		Yanagisawa and Akiba (1998)
FO	<i>Thalassiosira antiqua</i>	7.6	8.3	8.5		Barron (1992a)
LO	<i>Denticulopsis katayamae</i>	7.6	8.3	8.5		Barron (1992a)
FO	<i>Thalassiosira marujamica</i>	7.8-7.9	8.4-8.5			Barron (1992a)
* LCO	<i>Denticulopsis simonsenii</i>	8.0	8.4	8.6	C4r.2r	Barron and Gladenkov (1995)
LO	<i>Lithodesmium reynoldsii</i>	8.1	8.7			Barron (1992a)
* LO	<i>Denticulopsis dimorpha</i>	8.4	9	9.16	C4Ar.1r	Barron and Gladenkov (1995)
FO	<i>Denticulopsis katayamae</i>	8.7	9.1	9.26	C4Ar.1n	Barron and Gladenkov (1995)
FO	<i>Thalassionema schraderi</i>		9.3	9.5	C4Ar	Barron and Gladenkov (1995)
FO	<i>Thalassiosira minutissima</i>	9.0	9.6			Barron (1992a)
* FO	<i>Denticulopsis dimorpha</i>	8.9	9.8	9.9	C5n.2n	Barron and Gladenkov (1995)
LO	<i>Nitzschia heteropolica</i>		10.7-10.9	10.8-11.0	ca.C5n.2n base	Barron and Gladenkov (1995)
LO	<i>Medialia splendida</i>		10.7-10.9	10.8-11.0	ca.C5n.2n base	Barron and Gladenkov (1995)
* LCO	<i>Denticulopsis praedimorpha</i>	10.4	11.4	11.5	C5r.2n	Barron and Gladenkov (1995)
FO	<i>Hemidiscus cuneiformis</i>	11.4	11.7			Barron (1992a)
FO	<i>Thalassiosira brunii</i>	11.5	11.8			Barron (1992a)
FO	<i>Proboscia barboi</i>	11.2	12.2	12.3	C5An.2n	Barron and Gladenkov (1995)
LO	<i>Crucidentacula nicobarica</i>	12.2	12.4	12.5		Barron (1992a)
* FO	<i>Denticulopsis praedimorpha</i>	12.6	12.8	12.9	C5Ar.3r	Gersonde and Burckle (1990)
* FCO	<i>Denticulopsis simonsenii</i>	13.65	13.1	13.1	C5AAr	Barron (1992a)
* LCO	<i>Denticulopsis hyalina</i>	13.65	13.1	13.1		Yanagisawa and Akiba (1998)
LO	<i>Thalassiosira praeyabei</i>	13.4	13.4			Barron (1992a)
FO	<i>Thalassiosira grunowii</i>	13.75	13.7			Barron (1992a)
* FO	<i>Denticulopsis simonsenii</i>	14.3	14.4-14.6	14.4-14.6	C5ADn	Barron and Gladenkov (1995)
FO	<i>Thalassiosira praeyabei</i>	14.8	14.7			Barron (1992a)
LO	<i>Crucidentacula kanayae</i>	14.8	14.7			Barron (1992a)
* FO	<i>Denticulopsis hyalina</i>	15	14.9	14.9	C5Bn.1r	Barron and Gladenkov (1995)
FO	<i>Actinocyclus ingens nodus</i>	15.2	15.1	15.1-15.6		Barron (1992a)
LO	<i>Denticulopsis praelauta</i>	15.3-15.7	15.2-15.6	15.7		Barron (1992a)
* FO	<i>Denticulopsis lauta</i>	16	15.9	15.9		Barron (1992a)
* FO	<i>Denticulopsis praelauta</i>	16.3	16.3	16.3		Barron (1992a)
* FO	<i>Crucidentacula kanayae</i>	18	16.9	16.9	C5Cr	Barron and Gladenkov (1995)
FO	<i>Actinocyclus ingens</i>	17.9	17.6			Barron (1992a)
* FO	<i>Crucidentacula sawamurae</i>	17.8	18.4	18.4	C5En	Barron (1992a)
FO	<i>Thalassiosira fraga</i>	20.3-20.4	20.1	20.3		Barron and Gladenkov (1995)

Notes: Based on the time scales of Berggren et al. (1985b) and Cande and Kent (1992, 1995). BKFV85 = Berggren et al., 1985b; CK92 = Cande and Kent, 1992; CK95 = Cande and Kent, 1995. FO = first occurrence, LO = last occurrence, FCO = first common or consistent occurrence. LCO = last common or consistent occurrence. * = datums marking zonal boundaries.

arctic North Pacific assemblages are dominated typically by *Denticulopsis simonsenii*, *D. praedimorpha*, and *D. hyalina*. Furthermore temperate to subtropical indexes such as *Annellus californicus*, *Coscinodiscus lewianus*, *Craspedodiscus coscinodiscus*, and *Crucidentacula nicobarica* persistently occur from Zone NP4 through the lower part of Zone NP5B.

Thalassiothrix longissima and *Thalassionema nitzschoides* are especially abundant in the middle middle Miocene sequence and are indicative of high oceanic productivity associated with an intense up-

welling province. Abundant occurrences of *Coscinodiscus marginatus* and *Proboscia barboi*, suggesting the coastal upwelling conditions, break out sporadically in harmony with the persistence of the oceanic mass production. The rapidly deposited diatom oozes of middle middle Miocene age are indicative of extensive upwelling of cool waters associated with the California Current.

Because of the modern distribution of *Coscinodiscus marginatus* and *Proboscia barboi* in the North Pacific (Sancetta and Silvestri, 1986; Takahashi, 1986) and the increased abundances of *C. marginatus*

Table 5. Distribution and relative abundances of diatoms, Hole 1011B.

Geologic age	North Pacific diatom zone	Numeric age (Ma)*	Core, section, interval (cm)	Sample depth (mbsf)	Offset (m)	Composite depth (mcd)	Group abundance	Preservation	Environment, type of upwelling	<i>Actinocyclus ehrenbergii</i> vars.	<i>Actinocyclus ellipticus</i>	<i>Actinocyclus ingens</i>	<i>Actinocyclus ingens</i> f. <i>ingens</i>	<i>Actinocyclus ingens</i> f. <i>nodus</i>	<i>Actinocyclus</i> cf. <i>oculatus</i>	<i>Actinocyclus ochotensis</i>	<i>Actinocyclus tsugaruensis</i>	<i>Actinocyclus</i> sp.	<i>Actinopychus senarius</i>	<i>Amphora</i> sp.	<i>Aulacoseira granulata</i>	<i>Azpeitia endoi</i>	<i>Azpeitia nodulifera</i>	<i>Cocconeis californica</i>	<i>Cocconeis scutellum</i>	<i>Coscinodiscus marginatus</i>	<i>Coscinodiscus marginatus</i> f. <i>fossilis</i>	<i>Coscinodiscus asteromphalus</i>	<i>Coscinodiscus</i> sp.	<i>Denticulopsis lauta</i> s.l.	<i>Denticulopsis dimorpha</i>	<i>Denticulopsis hustedtii</i> (elliptical)	<i>Denticulopsis hyalina</i>	<i>Denticulopsis katayamae</i>						
Pleistocene	Unzoned		167-1011B-1H-CC	8.40	0.00	8.40	T	P																																
			2H-CC	17.90	0.53	18.43	T	P																																
			3H-CC	27.40	3.24	30.64	T	P																																
			4H-CC	36.90	4.04	40.94	T	P																																
			5H-CC	46.40	4.58	50.98	R	P																																
			6H-CC	55.90	5.28	61.18	T	P																																
			7H-CC	65.40	6.52	71.92	T	P																																
			8H-CC	74.90	6.32	81.22	T	P																																
			9H-CC	84.40	6.22	90.62	T	P																																
			10H-CC	93.90	6.92	100.82	T	P																																
Pliocene	Unzoned		11H-CC	103.40	7.04	110.44	T	P																																
			12H-CC	112.90	8.24	121.14	T	P																																
			13H-CC	122.40	8.96	131.36	T	P																																
			14H-CC	131.90	10.30	142.20	T	P																																
			15H-CC	137.90	10.94	148.84	B																																	
			16X-CC	146.50	10.94	157.44	B																																	
			17X-CC	156.20	10.56	166.76	R	P																																
			18X-CC	165.70	10.56	176.26	R	P																																
			19X-3, 21-22	168.91	12.12	181.03	R	P																																
			19X-5, 21-22	171.91	12.12	184.03	R	P																																
late Miocene	NPD 7A	7.6	19X-CC	175.40	12.12	187.52	F	M																																
			20X-3, 21-22	178.61	14.44	193.05	R	P																																
			20X-5, 21-22	181.61	14.44	196.05	C	P																																
			20X-CC	185.00	14.44	199.44	F	P																																
			21X-3, 21-22	188.21	14.44	202.65	T	P																																
			21X-5, 21-22	191.21	14.44	205.65	R	P																																
			21X-CC	194.60	14.44	209.04	C	M																																
			22X-3, 20-21	197.80	14.44	212.24	R	P																																
			22X-5, 20-21	200.80	14.44	215.24	R	P																																
			22X-CC	204.30	14.44	218.74	F	P																																
	23X-3, 20-21	207.50	14.44	221.94	R	P																																		
	23X-5, 20-21	210.50	14.44	224.94	R	P																																		
	23X-CC	213.90	14.44	228.34	A	G			Coastal/oceanic																															
	24X-3, 21-22	217.11	14.44	231.55	C	P			Coastal	T																														
	24X-5, 21-22	220.11	14.44	234.55	C	P			Coastal																															
	24X-CC	223.50	14.44	237.94	A	G			Coastal																															
	25X-3, 20-22	226.70	14.44	241.14	C	P			Coastal																															
	25X-5, 19-21	229.69	14.44	244.13	C	P			Coastal																															
	25X-CC	233.20	14.44	247.64	A	G			Coastal/oceanic																															
	26X-3, 20-21	236.40	14.44	250.84	C	P			Coastal																															
26X-5, 20-21	239.40	14.44	253.84	A	M			Coastal/oceanic																																
26X-CC	242.80	14.44	257.24	A	G			Coastal/oceanic																																
27X-3, 21-22	246.01	14.44	260.45	C	M			Coastal																																
27X-5, 21-22	249.01	14.44	263.45	A	M			Coastal	R	T																														
27X-CC	252.40	14.44	266.84	A	G			Coastal/oceanic																																
28X-3, 21-22	255.61	14.44	270.05	A	G			Oceanic																																
28X-5, 21-22	258.61	14.44	273.05	C	M																																			
28X-CC	262.10	14.44	276.54	A	G			Oceanic																																
29X-1, 4-7	262.14	14.44	276.58	C	M																																			
29X-CC	271.70	14.44	286.14	A	G			Oceanic																																

Notes: * = Cande and Kent (1995). Shaded area = barren interval. Abundance: A = abundant, C = common, F = few, R = rare, T = trace, and B = barren. Preservation: G = good, M = moderate, and P = poor. For complete definition of terms, see "Techniques" section of this chapter.

Table 6. Distribution and relative abundances of diatoms, Hole 1014A.

Geologic age	North Pacific diatom zone	Core, section	Sample depth (mbsf)	Offset (m)	Composite depth (mcd)	Group abundance	Preservation	Environment, type of upwelling	<i>Actinocyclus ingens</i>	<i>Actinocyclus ingens f. nodus</i>	<i>Actinocyclus oculatus</i>	<i>Actinocyclus tenellus</i>	<i>Actinocyclus tsugaruensis</i>	<i>Actinopychus senarius</i>	<i>Actinopychus splendens</i>	<i>Aulacoseira granulata</i>	<i>Auliscus</i> sp.	<i>Aspetitia nodulifera</i>	<i>Cavitatus jouseanus</i>	<i>Cocconeis decipiens</i>	<i>Cocconeis scutellum</i>	<i>Coscinodiscus asteromphalus</i>	<i>Coscinodiscus lewisianus</i>	<i>Coscinodiscus marginatus</i>	<i>Coscinodiscus marginatus f. fossilis</i>	<i>Coscinodiscus</i> sp.	<i>Craspedodiscus coscinodiscus</i>	<i>Crucidentacula nicobarica</i>	<i>Crucidentacula cf. punctata</i>	<i>Denticulopsis dimorpha</i>	<i>Denticulopsis hyalina</i>	<i>Denticulopsis katayamae</i>	<i>Denticulopsis lauta</i>	<i>Denticulopsis lauta</i> s.l.	<i>Denticulopsis prae-dimorpha</i>	<i>Denticulopsis prae-lauta</i>	<i>Denticulopsis simonsenii</i>	<i>Diploneis smithii</i>						
Quaternary	NPD 12	167-1014A-1H-CC	3.10	0.00	3.10	T	P		T	T																																		
		2H-CC	12.60	0.65	13.25	T	P		T																																			
		3H-CC	22.10	1.16	23.26	T	P		T	T																																		
		4H-CC	31.60	1.31	32.91	T	P		T																																			
		5H-CC	41.40	1.60	43.00	T	P		T																																			
		6H-CC	50.60	2.97	53.57	R	P		T						T					T																								
		7X-CC	54.30	3.00	57.30	T	P		T	T																																		
		8X-CC	64.00	2.67	66.67	T	P		T																																			
		9X-CC	73.80	2.03	75.83	T	P		T																																			
	NPD 11	10X-CC	83.50	2.31	85.81	T	P		T																																			
		11X-CC	93.10	1.91	95.01	T	P		T	T																																		
		12X-CC	102.80	2.21	105.01	T	P		T	T																																		
		13X-CC	112.40	1.96	114.36	T	P		T																																			
		14X-CC	122.00	0.12	122.12	T	P		T	T	T																																	
		15X-CC	131.60	-3.64	127.96	T	P		T	T	T																																	
		16X-CC	141.20	-7.00	134.20	R	P		T	T																																		
		17X-CC	150.80	-4.74	146.06	T	P		T																																			
		18X-CC	160.40	-3.87	156.53	T	P		T																																			
late Pliocene	NPD 10	19X-CC	170.00	-3.87	166.13	T	P		T																																			
		20X-CC	179.60	-4.56	175.04	R	P		T																																			
		21X-CC	189.20	-4.56	184.64	T	P		T	T	T																																	
		22X-CC	198.80	-4.49	194.31	A	M	Coastal	R																																			
		23X-CC	208.40	-4.49	203.91	R	P		T	T																																		
		24X-CC	218.00	-6.60	211.40	C	P		R	R																																		
		25X-CC	223.50	-6.60	216.90	R	P		T																																			
		26X-CC	227.70	-6.60	221.10	R	P		T	T																																		
		27X-CC	237.30	-6.60	230.70	T	P		T	T																																		
	NPD 9	28X-CC	246.90	-6.60	240.30	T	P		T	T																																		
		29X-CC	250.10	-6.60	243.50	T	P		T																																			
		30X-CC	256.60	-6.60	250.00	R	P		T																																			
		31X-CC	266.20	-6.60	259.60	T	P		T	T																																		
		32X-CC	275.80	-6.60	269.20	F	P		R	R																																		
		33X-CC	285.50	-6.60	278.90	R	P		T																																			
		34X-CC	295.10	-6.60	288.50	R	P		T	T																																		
		35X-CC	304.80	-6.60	298.20	T	P		T	T																																		
		36X-CC	314.40	-6.60	307.80	T	P		T	T	T																																	
NPD 8	37X-CC	324.10	-6.60	317.50	R	P		T	T	T																																		
	38X-CC	333.70	-6.60	327.10	T	P		T	T																																			
	39X-CC	343.40	-6.60	336.80	R	P		T	T	T																																		
	40X-CC	353.00	-6.60	346.40	T	P		T	T																																			
	41X-CC	362.60	-6.60	356.00	T	P		T																																				
	42X-CC	372.20	-6.60	365.60	T	P		T																																				
	43X-CC	381.80	-6.60	375.20	†																																							
	44X-CC	391.00	-6.60	384.40	R	P		T	T																																			
	45X-CC	401.00	-6.60	394.40	R	P		T	T	T																																		
early Pliocene	NPD 7?	46X-CC	410.50	-6.60	403.90	R	P		T	T																																		
		47X-CC	420.50	-6.60	413.90	R	P		T	T																																		
		48X-CC	429.80	-6.60	423.20	R	P		T	T																																		

Table 9 (continued).

Geologic age	North Pacific diatom zone	Numeric age (Ma)*	Core, section	Sample depth (mbsf)	Offset (m)	Composite depth (mcd)	Group abundance	Preservation	Environment, type of upwelling	<i>Navicula</i> sp.	<i>Neodenticula kamschatkica</i>	<i>Neodenticula koizumii</i>	<i>Neodenticula seminiae</i>	<i>Neodenticula cf. seminiae</i>	N. sp. A sensu Akiba and Yanagisawa	<i>Nitzschia marina</i>	<i>Nitzschia reinholdii</i>	<i>Opephora</i> sp.	<i>Paralia sulcata</i>	<i>Proboscia barboi</i>	<i>Proboscia curvirostris</i>	<i>Rhaphoneis</i> sp.	<i>Stephanodiscus asraeca</i>	<i>Stephanopyxis dimorpha</i>	<i>Stephanopyxis turris</i>	<i>Thalassionema nitzschoides</i>	<i>Thalassionema robusta</i>	<i>Thalassiostra eccentrica</i>	<i>Thalassiostra leptopus</i>	<i>Thalassiostra nidulus</i>	<i>Thalassiostra oestrupii</i>	<i>Thalassiostra</i> sp.	<i>Thalassiothrix longissima</i>	<i>Centric</i> sp.1	Resting spores						
Pleistocene	NPD 12	0.30	167-1019C-																																						
			1H-CC	8.30	0.00	8.30	R	P				T																													
			2H-CC	17.80	0.01	17.81	F	P																																	
			3H-CC	27.30	0.12	27.42	R	P																																	
			4H-CC	36.80	2.12	38.92	R	P																																	
			5H-CC	46.30	3.09	49.39	F	P																																	
			6H-CC	55.80	1.51	57.31	C	P/M																																	
			7H-CC	65.30	1.48	66.78	A	P/M	Coastal/oceanic																																
			8H-CC	74.80	1.70	76.50	A	M/G	Coastal/oceanic																																
			9X-CC	84.30	3.86	88.16	R	M																																	
			10X-CC	94.10	2.94	97.04	C	M	Coastal/oceanic																																
			11X-CC	103.70	2.94	106.64	A	M/G	Coastal/oceanic																																
	12X-CC	113.30	2.94	116.24	R	P																																			
	13X-CC	122.90	2.94	125.84	C	P																																			
	14X-CC	132.50	4.88	137.38	F	P																																			
	15X-CC	142.10	5.70	147.80	C	P	Coastal																																		
	16X-CC	151.70	4.72	156.42	C	M	Coastal/oceanic																																		
	17X-CC	161.30	1.68	162.98	C	M	Coastal/oceanic																																		
	18X-CC	170.90	3.30	174.20	A	M	Coastal/oceanic																																		
	19X-CC	180.50	3.30	183.80	A	M	Coastal/oceanic																																		
	20X-CC	190.10	3.30	193.40	C	M	Coastal																																		
	21X-CC	199.70	3.30	203.00	F	P/M																																			
	22X-CC	209.30	3.30	212.60	R	P																																			
	23X-CC	219.00	3.30	222.30	A	M/G	Coastal/oceanic																																		
	24X-CC	228.60	3.30	231.90	A	M/G	Coastal/oceanic																																		
	25X-CC	238.20	3.30	241.50	A	M/G	Coastal/oceanic																																		
26X-CC	247.90	3.30	251.20	R	P																																				

Table 12 (continued).

Geologic age	North Pacific diatom zone	Numeric age (Ma5*)	Core, section, interval (cm)	Sample depth (mbsf)	Offset (m)	Composite depth (mcd)	Group abundance	Preservation	Environment, type of upwelling	<i>Denticulopsis</i> cf. <i>dimorpha</i>	<i>Denticulopsis</i> <i>hustedtii</i> (elliptical)	<i>Denticulopsis</i> <i>hyalina</i>	<i>Denticulopsis</i> <i>katayamae</i>	<i>Denticulopsis</i> cf. <i>katayamae</i>	<i>Denticulopsis</i> <i>lauta</i> s.s.	<i>Denticulopsis</i> <i>praedimorpha</i>	<i>Denticulopsis</i> <i>simonsenii</i>	<i>Grammatophora</i> sp.	<i>Hemiaulus</i> <i>polymorphus</i>	<i>Hemidiscus</i> <i>cuneiformis</i>	<i>Neodenticula</i> <i>kamtschatica</i>	<i>Neodenticula</i> <i>koizumii</i>	<i>Neodenticula</i> cf. <i>koizumii</i>	<i>Neodenticula</i> <i>seminae</i>	<i>N.</i> sp. A sensu Akiba and Yanagisawa	<i>Nitzschia</i> <i>fossilis</i>	<i>Nitzschia</i> <i>heteropolica</i>	<i>Nitzschia</i> <i>pitocena</i>	<i>Nitzschia</i> <i>porteri</i>	<i>Nitzschia</i> <i>reinholdii</i>	<i>Nitzschia</i> <i>rolandii</i>	<i>Nitzschia</i> sp.	<i>Paralia</i> <i>sulcata</i>	<i>Proboscia</i> <i>barboi</i>	<i>Proboscia</i> <i>praebarboi</i>	<i>Proboscia</i> sp.	<i>Rhaphoneis</i> sp.	<i>Rhizosolenia</i> <i>hebetata</i> f. <i>hiemalis</i>	<i>Rhizosolenia</i> <i>mitocnica</i>		
Quaternary	Unzoned	2.0?	167-1021B-1H-CC	8.00	0.00	8.00	B		Clay																																
			2H-CC	17.50	1.18	18.68	T	P	Clay																																
			3H-CC	27.00	1.94	28.94	T	P	Clay																																
			4H-CC	36.50	2.50	39.00	B		Clay																																
			5H-CC	46.00	4.02	50.02	T	P	Clay																																
			6H-CC	55.50	4.76	60.26	C	P	Dissolution																																
			7H-CC	65.00	5.69	70.69	F	P	Clay																																
			8H-CC	74.50	6.55	81.05	C	P/M	Oceanic																																
			9H-CC	84.00	8.71	92.71	R	P	Dissolution																																
			late Pliocene	NPD 9 - NPD 8	3.5?	10H-CC	93.50	12.75	106.25	T	P	Clay + nanno																													
11H-CC	103.00	13.15				116.15	T	P	Clay + nanno																																
12H-CC	112.50	14.31				126.81	R	P	Clay + dissolution																																
13H-CC	122.00	14.29				136.29	T	P	Clay + dissolution																																
14H-CC	131.50	13.43				144.93	T	P	Clay + dissolution																																
15H-CC	141.00	14.13				155.13	A	P	Clay + oceanic																																
16H-CC	150.50	14.95				165.45	R	P	Clay + dissolution																																
17H-CC	160.00	15.53				175.53	R	P																																	
18H-CC	169.50	15.41				184.91	A	P	Clay + upwelling																																
19X-CC	175.40	15.41				190.81	F	P	Clay + dissolution																																
early Pliocene	NPD 7B	<5.49	20X-CC	185.00	15.41	200.41	A	P	Clay																																
			21X-3, 20-22	188.20	15.41	203.61	R	P																																	
			21X-CC	194.70	15.41	210.11	R	P	Clay																																
			22X-2, 20-22	196.40	15.41	211.81	R	P																																	
			22X-5, 10-12	200.80	15.41	216.21	R	P																																	
			22X-CC	204.30	15.41	219.71	R	P																																	
			23X-2, 20-22	206.00	15.41	221.41	F	P																																	
			23X-5, 20-22	210.50	15.41	225.91	A	P/M	Oceanic																																
			23X-CC	214.00	15.41	229.41	A	P	Oceanic																																
			24X-2, 20-22	215.70	15.41	231.11	A	P/M	Oceanic																																
late Miocene	NPD 7A	7.6	24X-5, 20-22	220.20	15.41	235.61	A	P/M	Oceanic																																
			24X-CC	223.60	15.41	239.01	A	P/M	Oceanic																																
			25X-2, 18-20	225.28	15.41	240.69	A	P/M	Oceanic																																
			25X-5, 18-20	229.78	15.41	245.19	A	P	Oceanic																																
			25X-CC	233.20	15.41	248.61	A	P	Oceanic																																
			26X-2, 92-94	235.62	15.41	251.03	A	G	Oceanic																																
			26X-5, 93-95	240.13	15.41	255.54	A	G	Oceanic																																
			26X-CC	242.80	15.41	258.21	C	P	Oceanic																																
			27X-2, 12-14	244.42	15.41	259.83	A	G	Oceanic																																
			27X-5, 12-14	248.92	15.41	264.33	C	M/G	Oceanic																																
late Miocene	NPD 6B	9.16 9.26	27X-CC	252.40	15.41	267.81	C	M	Oceanic																																
			28X-2, 25-27	254.15	15.41	269.56	C	M	Oceanic																																
			28X-5, 12-14	258.52	15.41	273.93	C	M	Oceanic																																
			28X-CC	262.10	15.41	277.51	C	P/M	Oceanic																																
			29X-2, 6-8	263.66	15.41	279.07	A	P/M	Oceanic																																
			29X-5, 20-22	268.30	15.41	283.71	A	P/M	Oceanic																																
			29X-CC	271.70	15.41	287.11	C	P/M	Dissolution																																
			30X-2, 18-20	273.38	15.41	288.79	R	P	Dissolution																																
			30X-5, 20-22	277.90	15.41	293.31	R	P	Dissolution																																
			30X-CC	281.30	15.41	296.71	R	P	Dissolution																																

Table 12 (continued).

Geologic age	North Pacific diatom zone	Numeric age (Ma5*)	Core, section, interval (cm)	Sample depth (mbsf)	Offset (m)	Composite depth (mcd)	Group abundance	Preservation	Environment, type of upwelling							
middle Miocene	NPD 5B	12.5? 12.8? <12.9	167-1021B-32X-CC 33X-2, 20-22 33X-5, 15-17 33X-CC	300.50	15.41	315.91	A	M	Oceanic	<i>Denticulopsis</i> cf. <i>dimorpha</i>						
				302.20	15.41	317.61	A	M/G	Oceanic	<i>Denticulopsis</i> <i>hustedtii</i> (elliptical)	R					
				306.65	15.41	322.06	A	M/G	Oceanic	<i>Denticulopsis</i> <i>hyalina</i>						
				310.20	15.41	325.61	A	M/G	Oceanic	<i>Denticulopsis</i> <i>kateyamae</i>						
											<i>Denticulopsis</i> cf. <i>kateyamae</i>					
											<i>Denticulopsis</i> <i>lauta</i> s.l.					
											<i>Denticulopsis</i> <i>praedimorpha</i>		F	C		
											<i>Denticulopsis</i> <i>simonsenii</i>		C	C		
											<i>Grammatophora</i> sp.		C	C		
											<i>Hemiantulus polymorphus</i>		C	C		
											<i>Hemidiscus cuneiformis</i>					
											<i>Neodenticula kamtschatica</i>					
							<i>Neodenticula koizumii</i>									
							<i>Neodenticula</i> cf. <i>koizumii</i>									
							<i>Neodenticula seminata</i>									
							N. sp. A sensu Akiba and Yanagisawa									
							<i>Nitzschia fossilis</i>									
							<i>Nitzschia heteropolica</i>									
							<i>Nitzschia pliocena</i>									
							<i>Nitzschia porteri</i>									
							<i>Nitzschia reinholdii</i>									
							<i>Nitzschia rolandii</i>									
							<i>Nitzschia</i> sp.									
							<i>Paralia sulcata</i>									
							<i>Proboscia barboi</i>				R					
							<i>Proboscia praearboi</i>				A					
							<i>Proboscia</i> sp.				R					
							<i>Rhaphoneis</i> sp.				R					
							<i>Rhizosolenia hebetata</i> f. <i>hiemalis</i>				R					
							<i>Rhizosolenia miocenica</i>				A					

Table 12 (continued).

Geologic age	North Pacific diatom zone	Numeric age (Ma5*)	Core, section, interval (cm)	Sample depth (mbsf)	Offset (m)	Composite depth (mcd)	Group abundance	Preservation	Environment, type of upwelling	<i>Rhizosolenia styliformis</i>	<i>Rossetia paleacea</i>	<i>Rouxia californica</i>	<i>Stephanopyxis dimorpha</i>	<i>Stephanopyxis turris</i>	<i>Synedra</i> spp.	<i>Thalassionema hirosakiensis</i>	<i>Thalassionema nitschoides</i>	<i>Thalassionema nitschoides v. parva</i>	<i>Thalassionema robusta</i>	<i>Thalassionema schraderi</i>	<i>Thalassionema</i> spp.	<i>Thalassiosira antiqua</i>	<i>Thalassiosira convexa</i>	<i>Thalassiosira cf. convexa</i>	<i>Thalassiosira eccentrica</i>	<i>Thalassiosira grunowii</i>	<i>Thalassiosira leptopus</i>	<i>Thalassiosira oestrupii</i>	<i>Thalassiosira yabei</i>	<i>Thalassiothrix longissima</i>	<i>Thalassiothrix</i> spp.	<i>Centric</i> sp. 1						
Quaternary	Unzoned	2.0?	167-1021B-1H-CC	8.00	0.00	8.00	B		Clay																													
			2H-CC	17.50	1.18	18.68	T	P		Clay																												
late Pliocene	NPD 9 - NPD 8	3.5?	3H-CC	27.00	1.94	28.94	T	P	Clay																													
			4H-CC	36.50	2.50	39.00	B		Clay																													
			5H-CC	46.00	4.02	50.02	T	P		Clay																												
			6H-CC	55.50	4.76	60.26	C	P		Dissolution																												
			7H-CC	65.00	5.69	70.69	F	P		Clay																												
			8H-CC	74.50	6.55	81.05	C	P/M		Oceanic																												
			9H-CC	84.00	8.71	92.71	R	P		Dissolution	R																											
			10H-CC	93.50	12.75	106.25	T	P		Clay + nanno																												
			11H-CC	103.00	13.15	116.15	T	P		Clay + nanno																												
			early Pliocene	NPD 7B	<5.49	12H-CC	112.50	14.31	126.81	R	P	Clay + dissolution																										
13H-CC	122.00	14.29				136.29	T	P	Clay + dissolution																													
14H-CC	131.50	13.43				144.93	T	P	Clay + dissolution																													
15H-CC	141.00	14.13				155.13	A	P	Clay + oceanic																													
16H-CC	150.50	14.95				165.45	R	P	Clay + dissolution																													
17H-CC	160.00	15.53				175.53	R	P																														
18H-CC	169.50	15.41				184.91	A	P	Clay + upwelling																													
19X-CC	175.40	15.41				190.81	F	P	Clay + dissolution																													
20X-CC	185.00	15.41				200.41	A	P	Clay																													
late Miocene	NPD 7A	7.6				21X-3, 20-22	188.20	15.41	203.61	R	P																											
			21X-CC	194.70	15.41	210.11	R	P	Clay																													
			22X-2, 20-22	196.40	15.41	211.81	R	P																														
			22X-5, 10-12	200.80	15.41	216.21	R	P																														
			22X-CC	204.30	15.41	219.71	R	P																														
			23X-2, 20-22	206.00	15.41	221.41	F	P																														
			23X-5, 20-22	210.50	15.41	225.91	A	P/M	Oceanic																													
			23X-CC	214.00	15.41	229.41	A	P	Oceanic																													
			24X-2, 20-22	215.70	15.41	231.11	A	P/M	Oceanic																													
			24X-5, 20-22	220.20	15.41	235.61	A	P/M	Oceanic																													
			24X-CC	223.60	15.41	239.01	A	P/M	Oceanic																													
			25X-2, 18-20	225.28	15.41	240.69	A	P/M	Oceanic																													
			25X-5, 18-20	229.78	15.41	245.19	A	P	Oceanic																													
			25X-CC	233.20	15.41	248.61	A	P	Oceanic																													
			26X-2, 92-94	235.62	15.41	251.03	A	G	Oceanic																													
			26X-5, 93-95	240.13	15.41	255.54	A	G	Oceanic																													
			26X-CC	242.80	15.41	258.21	C	P	Oceanic																													
			27X-2, 12-14	244.42	15.41	259.83	A	G	Oceanic																													
			27X-5, 12-14	248.92	15.41	264.33	C	M/G	Oceanic																													
			27X-CC	252.40	15.41	267.81	C	M	Oceanic																													
28X-2, 25-27	254.15	15.41	269.56	C	M	Oceanic																																
28X-5, 12-14	258.52	15.41	273.93	C	M	Oceanic																																
28X-CC	262.10	15.41	277.51	C	P/M	Oceanic																																
29X-2, 6-8	263.66	15.41	279.07	A	P/M	Oceanic																																
29X-5, 20-22	268.30	15.41	283.71	A	P/M	Oceanic																																
29X-CC	271.70	15.41	287.11	C	P/M	Dissolution																																
30X-2, 18-20	273.38	15.41	288.79	R	P	Dissolution																																
30X-5, 20-22	277.90	15.41	293.31	R	P	Dissolution																																
30X-CC	281.30	15.41	296.71	R	P	Dissolution																																
31X-2, 15-17	282.95	15.41	298.36	R	P	Dissolution																																
31X-5, 20-22	287.50	15.41	302.91	R	P	Dissolution																																
31X-CC	290.90	15.41	306.31	R	P	Dissolution																																
		11.5	32X-3, 57-59	294.47	15.41	309.88	C	M	Oceanic	R					R											R												

Table 12 (continued).

Geologic age	North Pacific diatom zone	Numeric age (Ma ^{5*})	Core, section, interval (cm)	Sample depth (mbsf)	Offset (m)	Composite depth (mcd)	Group abundance	Preservation	Environment, type of upwelling	<i>Rhizosolenia styliformis</i> <i>Rossetella paleacea</i> <i>Rouxia californica</i> <i>Stephanopyxis dimorpha</i> <i>Stephanopyxis turris</i> <i>Synedra</i> spp. <i>Thalassionema hirotsukiensis</i> <i>Thalassionema nitzschioides</i> <i>Thalassionema nitzschioides</i> v. <i>parva</i> <i>Thalassionema robusta</i> <i>Thalassionema schraderi</i> <i>Thalassionema</i> spp. <i>Thalassiosira antiqua</i> <i>Thalassiosira convexa</i> <i>Thalassiosira</i> cf. <i>convexa</i> <i>Thalassiosira eccentrica</i> <i>Thalassiosira grunowii</i> <i>Thalassiosira leptopus</i> <i>Thalassiosira ostrupii</i> <i>Thalassiosira yabei</i> <i>Thalassiothrix longissima</i> <i>Thalassiothrix</i> spp. <i>Centric</i> sp.1
middle Miocene	NPD 5B	12.5? 12.8? <12.9	167-1021B-32X-CC 33X-2, 20-22 33X-5, 15-17 33X-CC	300.50 302.20 306.65 310.20	15.41 15.41 15.41 15.41	315.91 317.61 322.06 325.61	A A A A	M M/G M/G M/G	Oceanic Oceanic Oceanic Oceanic	R R F C C R R R C R R R R F A A A A

Table 13 (continued).

Geologic age	North Pacific diatom zone	Numeric age (Ma)*	Core, section	Sample depth (mbsf)	Offset (m)	Composite depth (mcd)	Group abundance	Preservation	Environment, type of upwelling	<i>Nitzschia navicularis</i>	<i>Nitzschia reinholdii</i>	<i>Nitzschia</i> sp.	<i>Paralia sulcata</i>	<i>Proboscia barboi</i>	<i>Rhaphoneis</i> spp.	<i>Rhizosolenia styliformis</i>	<i>Stephanopyxis dimorpha</i>	<i>Stephanopyxis turris</i>	<i>Synedra</i> spp.	<i>Thalassionema nitzschioides</i>	<i>Thalassionema nitzschioides</i> v. <i>parva</i>	<i>Thalassionema robusta</i>	<i>Thalassionema schraderi</i>	<i>Thalassiosira antiqua</i>	<i>Thalassiosira convexa</i>	<i>Thalassiosira</i> cf. <i>convexa</i>	<i>Thalassiosira eccentrica</i>	<i>Thalassiosira leptopus</i>	<i>Thalassiosira temperi</i>	<i>Thalassiosira oestrupii</i>	<i>Thalassiosira</i> sp.	<i>Thalassiothrix longissima</i>	<i>Thalassiothrix</i> spp.							
late Pliocene	NPD 9	>2.0	167-1022A-	1H-CC	4.50	0.12	4.62	R	P	Coastal																														
			2H-CC	14.00	0.44	14.44	A	M/G	Coastal	R																														
			3H-CC	23.50	1.16	24.66	A	P/M	Coastal																															
			4H-CC	33.00	0.11	33.11	C	P/M	Coastal/oceanic																															
			5H-CC	42.50	0.09	42.59	C	M	Coastal	T																														
			6H-CC	52.00	1.83	53.83	A	M/G	Coastal/oceanic																															
			7H-CC	61.50	2.55	64.05	A	M	Coastal/oceanic	R																														
			8H-CC	71.00	4.76	75.76	A	M/G	Coastal/oceanic																															
			9H-CC	80.50	4.97	85.47	C	M	Coastal/oceanic																															
	NPD 8	2.6?	10H-CC	90.00	4.54	94.54	C	P/M	Coastal																															
			11H-CC	99.50	5.46	104.96	F	P/M	Coastal																															
			12H-CC	109.00	5.48	114.48	C	M	Coastal																															
			13H-CC	118.50	5.85	124.35	C	P/M	Coastal																															
			14H-CC	128.00	7.52	135.52	C	P/M	Coastal	T																														
			15H-CC	137.50	9.42	146.92	C	P/M	Coastal	T																														
			16H-CC	147.00	9.70	156.70	C	P/M	Coastal																															
			17H-CC	156.50	12.94	169.44	A	P/M	Oceanic																															
			18H-CC	166.00	12.94	178.94	R	P	Oceanic																															
early Pliocene	NPD 7	2.6?	167-1022C-	19X-CC	174.80	10.98	185.78	R	P	Coastal	T																													
			20X-CC	184.40	10.98	195.38	C	P	Coastal																															
			21X-CC	194.00	10.98	204.98	R	P	Coastal																															
			22X-CC	203.60	10.98	214.58	R	P	Coastal																															
			23X-CC	213.20	10.98	224.18	C	P/M	Oceanic																															
			24X-CC	222.90	10.98	233.88	A	P/M	Oceanic																															
			25X-CC	232.50	10.98	243.48	A	P/M	Oceanic																															
			26X-CC	242.10	10.98	253.08	A	P/M	Coastal/oceanic																															
			27X-CC	251.80	10.98	262.78	A	M	Coastal/oceanic																															
			28X-CC	261.40	10.98	272.38	A	M	Coastal/oceanic																															
	Barren	<5.49	29X-CC	271.00	10.98	281.98	A	M	Coastal																															
			30X-CC	280.60	10.98	291.58	A	P/M	Coastal/oceanic																															
			31X-CC	290.30	10.98	301.28	A	P/M	Coastal/oceanic																															
			32X-CC	299.90	10.98	310.88	A	P/M	Coastal																															
			33X-CC	309.60	10.98	320.58	A	M	Coastal																															
			34X-CC	319.30	10.98	330.28	A	M	Coastal	R																														
			35X-CC	328.90	10.98	339.88	A	P/M	Coastal	R																														
			36X-CC	338.60	10.98	349.58	A	M	Coastal	R																														
			37X-CC	348.20	10.98	359.18	A	P/M	Coastal	R																														
			38X-CC	357.80	10.98	368.78	A	P	Coastal	F																														

Table 14. Age and stratigraphic position of middle Miocene through Quaternary diatom datum levels, Leg 167.

Event	Datum	BKFV85 (Ma)	CK95 (Ma)	Hole 1022A		Hole 1021B		Hole 1020C	
				Interval	Depth (mbsf)	Interval (cm)	Depth (mbsf)	Interval	Depth (mbsf)
* LO	<i>Proboscia curvirostris</i>	0.3-0.35	0.30	—	—	—	—	5H-CC to 6H-CC	42.30-51.80
LO	<i>Rhizosolenia matuyamai</i>	0.85-0.97	0.91-1.06	—	—	—	—	—	—
FO	<i>Rhizosolenia matuyamai</i>	0.91-1.05	0.99-1.14	—	—	—	—	—	—
* LO	<i>Actinocyclus oculatus</i>	0.93-1.33	1.01-1.46	—	—	—	—	14H-CC to 15H-CC	127.80-137.30
FO	<i>Proboscia curvirostris</i>	1.5	—	—	—	—	—	14H-CC to 15H-CC	127.80-137.30
FO	<i>Fragilariopsis doliola</i>	1.89-2.00	2	—	—	—	—	19X-CC to 20X-CC	175.50-185.10
* LO	<i>Neodenticula koizumii</i>	1.9	2.0	—	—	—	—	19X-CC to 20X-CC	175.50-185.10
LO	<i>Thalassiosira convexa</i>	2.3	2.35	4H-CC to 5H-CC	33.00-42.50	—	—	22X-CC to 23X-CC	204.30-213.90
* LO	<i>Neodenticula kamschatica</i>	2.50-2.58	2.61-2.68	—	—	—	—	—	—
LCO	<i>Neodenticula kamschatica</i>	2.50-2.58	2.61-2.68	9H-CC to 10H-CC	80.50-90.00	—	—	—	—
FO	<i>Neodenticula seminae</i>	2.6	2.68	(7H-CC to 8H-CC)	(61.50-71.00)	—	—	—	—
* FO	<i>Neodenticula koizumii</i>	3.6	3.53-3.95	15H-CC to 16H-CC	137.50-147.00	(8H-CC to 9H-CC)	(74.50-84.00)	—	—
* FO	<i>Thalassiosira oestrupii</i>	5.1	5.49	—	—	(15H-CC to 16H-CC)	(141.00-150.50)	—	—
LO	<i>Rouxia californica</i>	5.2	5.9	—	—	(19X-CC to 20X-CC)	(175.40-185.00)	—	—
FCO	<i>Neodenticula kamschatica</i>	—	6.4	—	—	(15H-CC to 16H-CC)	(141.00-150.50)	—	—
* LCO	<i>Rouxia californica</i>	6.1	6.65	—	—	(23X-2, 20-22 to 23X-5, 20-22)	(206.00-210.50)	—	—
LO	<i>Cavittatus jouseanus</i>	—	6.7-6.8	—	—	(23X-2, 20-22 to 23X-5, 20-22)	(206.00-210.50)	—	—
* LCO	<i>Thalassionema schraderi</i>	6.7	7.6	—	—	23X-CC to 24X-2, 20-22	214.00-215.70	—	—
FCO	<i>Thalassionema schraderi</i>	8.0	8.4	—	—	26X-2, 92-94 to 26X-5, 93-95	235.62-240.13	—	—
LO	<i>Denticulopsis katayamae</i>	7.6	8.5	—	—	(26X-CC to 27X-2, 12-14)	(242.80-244.42)	—	—
* LCO	<i>Denticulopsis simonsenii</i>	8.0	8.6	—	—	26X-2, 92-94 to 26X-5, 93-95	235.62-240.13	—	—
* LO	<i>Denticulopsis dimorpha</i>	8.4	9.16	—	—	27X-2, 12-14 to 27X-5, 12-14	244.42-248.92	—	—
FO	<i>Denticulopsis katayamae</i>	8.7	9.26	—	—	27X-CC to 28X-2, 25-27	252.40-254.15	—	—
FO	<i>Thalassionema schraderi</i>	—	9.5	—	—	28X-CC to 29X-2, 6-8	262.10-263.66	—	—
* FO	<i>Denticulopsis dimorpha</i>	8.9	9.9	—	—	28X-CC to 29X-2, 6-8	262.10-263.66	—	—
* LCO	<i>Denticulopsis praedimorpha</i>	10.4	11.5	—	—	31X-5, 20-22 to 31X-CC	287.50-290.90	—	—
FO	<i>Hemidiscus cuneiformis</i>	11.4	—	—	—	—	—	—	—
LO	<i>Crucidenticula nicobarica</i>	12.2	12.5	—	—	33X-2, 20-22 to 33X-5, 15-17	302.20-306.65	—	—
* FO	<i>Denticulopsis praedimorpha</i>	12.6	12.9	—	—	—	—	—	—
* FCO	<i>Denticulopsis simonsenii</i>	13.65	13.1	—	—	—	—	—	—
* LCO	<i>Denticulopsis hyalina</i>	13.65	13.1	—	—	—	—	—	—

Notes: Diatom events are calibrated to the time scales of Berggren et al. (1985b) and Cande and Kent (1995). BKFV85 = Berggren et al., 1985 time scale. CK95 = Cande and Kent, 1995 time scale. * = zonal boundaries. LO = last occurrence, FO = first occurrence, LCO = last common or consistent occurrence; FCO = first common or consistent occurrence. Data in parentheses represent uncertainty as to stratigraphic position. — = no data.

Table 14 (continued).

Event	Datum	Hole 1020B		Hole 1019C		Hole 1018A		Hole 1016A	
		Interval	Depth (mbsf)	Interval	Depth (mbsf)	Interval	Depth (mbsf)	Interval	Depth (mbsf)
* LO	<i>Proboscia curvirostris</i>	4H-CC to 5H-CC	36.30-45.80	4H-CC to 5H-CC	36.80-46.30	7H-CC to 8H-CC	61.90-71.40	3H-CC to 4H-CC	26.60-36.10
LO	<i>Rhizosolenia matuyamai</i>	—	—	—	—	—	—	4H-CC to 5H-CC	36.10-45.60
FO	<i>Rhizosolenia matuyamai</i>	—	—	—	—	—	—	5H-CC to 6H-CC	45.60-55.10
* LO	<i>Actinocyclus oculatus</i>	13H-CC to 14H-CC	121.80-131.30	—	—	10H-CC to 11X-CC	90.40-99.10	(6H-CC to 7H-CC)	(55.10-64.60)
FO	<i>Proboscia curvirostris</i>	14H-CC to 15H-CC	131.30-140.80	—	—	20X-CC to 21X-CC	185.70-195.30	—	—
FO	<i>Fragilariopsis dohliola</i>	18H-CC to 19X-CC	169.30-178.90	—	—	—	—	—	—
* LO	<i>Neodenticula koizumii</i>	18H-CC to 19X-CC	169.30-178.90	—	—	25X-CC to 26X-CC	233.80-243.50	(11X-CC to 12X-CC)	(96.30-106.00)
LO	<i>Thalassiosira convexa</i>	23X-CC to 25X-CC	217.30-236.60	—	—	31X-CC to 32X-CC	291.50-301.10	—	—
* LO	<i>Neodenticula kantschatica</i>	—	—	—	—	38X-CC to 39X-CC	359.00-368.70	—	—
LCO	<i>Neodenticula kantschatica</i>	—	—	—	—	44X-CC to 45X-CC	416.70-426.20	—	—
FO	<i>Neodenticula seminae</i>	—	—	—	—	—	—	—	—
* FO	<i>Neodenticula koizumii</i>	—	—	—	—	—	—	—	—
* FO	<i>Thalassiosira oestrupii</i>	—	—	—	—	—	—	(29X-CC to 30X-CC)	(269.50-279.20)
LO	<i>Rouxia californica</i>	—	—	—	—	—	—	—	—
FCO	<i>Neodenticula kantschatica</i>	—	—	—	—	—	—	—	—
* LCO	<i>Rouxia californica</i>	—	—	—	—	—	—	—	—
LO	<i>Cavitatus jouseanus</i>	—	—	—	—	—	—	—	—
* LCO	<i>Thalassionema schraderi</i>	—	—	—	—	—	—	—	—
FCO	<i>Thalassionema schraderi</i>	—	—	—	—	—	—	—	—
LO	<i>Denticulopsis katayamae</i>	—	—	—	—	—	—	—	—
* LCO	<i>Denticulopsis simonsenii</i>	—	—	—	—	—	—	—	—
* LO	<i>Denticulopsis dimorpha</i>	—	—	—	—	—	—	—	—
FO	<i>Denticulopsis katayamae</i>	—	—	—	—	—	—	—	—
FO	<i>Thalassionema schraderi</i>	—	—	—	—	—	—	—	—
* FO	<i>Denticulopsis dimorpha</i>	—	—	—	—	—	—	—	—
* LCO	<i>Denticulopsis praedimorpha</i>	—	—	—	—	—	—	—	—
FO	<i>Hemidiscus cuneiformis</i>	—	—	—	—	—	—	—	—
LO	<i>Crucidenticula nicobarica</i>	—	—	—	—	—	—	—	—
* FO	<i>Denticulopsis praedimorpha</i>	—	—	—	—	—	—	—	—
* FCO	<i>Denticulopsis simonsenii</i>	—	—	—	—	—	—	—	—
* LCO	<i>Denticulopsis hyalina</i>	—	—	—	—	—	—	—	—

Table 14 (continued).

Event	Datum	Hole 1014A		Hole 1011B		Hole 1010C	
		Interval	Depth (mbsf)	Interval (cm)	Depth (mbsf)	Interval (cm)	Depth (mbsf)
* LO	<i>Proboscia curvirostris</i>	—	—	—	—	—	—
LO	<i>Rhizosolenia matuyamai</i>	—	—	—	—	—	—
FO	<i>Rhizosolenia matuyamai</i>	—	—	—	—	—	—
* LO	<i>Actinocyclus oculatus</i>	12X-CC to 13X-CC	102.80-112.40	—	—	—	—
FO	<i>Proboscia curvirostris</i>	—	—	—	—	—	—
FO	<i>Fragilariopsis doliola</i>	—	—	—	—	—	—
* LO	<i>Neodenticula koizumii</i>	—	—	—	—	—	—
LO	<i>Thalassiosira convexa</i>	(24X-CC to 25X-CC)	(218.00-223.50)	—	—	—	—
* LO	<i>Neodenticula kamschatica</i>	(38X-CC to 39X-CC)	(333.70-343.40)	—	—	—	—
LCO	<i>Neodenticula kamschatica</i>	—	—	—	—	—	—
FO	<i>Neodenticula seminae</i>	—	—	—	—	—	—
* FO	<i>Neodenticula koizumii</i>	—	—	—	—	—	—
* FO	<i>Thalassiosira oestrupii</i>	—	—	—	—	—	—
LO	<i>Rouxia californica</i>	—	—	—	—	—	—
FCO	<i>Neodenticula kamschatica</i>	—	—	—	—	—	—
* LCO	<i>Rouxia californica</i>	—	—	—	—	—	—
LO	<i>Cavitatus jouseanus</i>	—	—	—	—	—	—
* LCO	<i>Thalassionema schraderi</i>	—	—	23X-3, 20-21 to 23X-5, 20-21	207.50-210.50	9H-CC to 10H-3, 20-21	81.50-84.70
FCO	<i>Thalassionema schraderi</i>	—	—	25X-CC to 26X-3, 20-21	233.20-236.40	—	—
LO	<i>Denticulopsis katayamae</i>	—	—	26X-5, 20-21 to 26X-CC	239.40-242.80	11H-3, 20-21 to 11H-5, 21-22	94.20-97.20
* LCO	<i>Denticulopsis simonsenii</i>	—	—	26X-5, 20-21 to 26X-CC	239.40-242.80	11H-3, 20-21 to 11H-5, 21-22	94.20-97.20
* LO	<i>Denticulopsis dimorpha</i>	—	—	28X-5, 21-22 to 28X-CC	258.61-262.10	11H-CC to 12H-3, 20-21	100.50-103.70
FO	<i>Denticulopsis katayamae</i>	—	—	—	—	11H-CC to 12H-3, 20-21	100.50-103.70
FO	<i>Thalassionema schraderi</i>	—	—	—	—	—	—
* FO	<i>Denticulopsis dimorpha</i>	—	—	—	—	12H-3, 20-21 to 12H-5, 21-22	103.70-106.70
* LCO	<i>Denticulopsis praedimorpha</i>	—	—	—	—	14H-5, 20-22 to 14H-CC	125.70-129.00
FO	<i>Hemidiscus cuneiformis</i>	—	—	—	—	(13H-5, 21-22 to 13H-CC)	(116.21-119.50)
LO	<i>Crucidenticula nicobarica</i>	—	—	—	—	(17H-5, 21-22 to 17H-CC)	(154.21-157.50)
* FO	<i>Denticulopsis praedimorpha</i>	—	—	—	—	17H-CC to 18X-3, 21-22	157.50-160.71
* FCO	<i>Denticulopsis simonsenii</i>	—	—	—	—	19X-CC to 20X-3, 75-76	174.90-178.65
* LCO	<i>Denticulopsis hyalina</i>	—	—	—	—	19X-CC to 20X-3, 75-76	174.90-178.65

Table 15. Age and composite depth constraints of stratigraphically useful diatom datum levels, Leg 167.

Event	Datum	BKFV85 (Ma)	CK95 (Ma)	Hole 1022A		Hole 1021B		Hole 1020C		Hole 1020B		Hole 1019C	
				Top (mcd)	Bottom (mcd)	Top (mcd)	Bottom (mcd)	Top (mcd)	Bottom (mcd)	Top (mcd)	Bottom (mcd)	Top (mcd)	Bottom (mcd)
* LO	<i>Proboscia curvirostris</i>	0.3-0.35	0.30	—	—	—	—	46.12	56.62	38.38	48.96	38.92	49.39
LO	<i>Rhizosolenia matuyamai</i>	0.85-0.97	0.91-1.06	—	—	—	—	—	—	—	—	—	—
FO	<i>Rhizosolenia matuyamai</i>	0.91-1.05	0.99-1.14	—	—	—	—	—	—	—	—	—	—
* LO	<i>Actinocyclus oculatus</i>	0.93-1.33	1.01-1.46	—	—	—	—	135.68	147.51	136.68	146.28	—	—
FO	<i>Proboscia curvirostris</i>	1.5	—	—	—	—	—	135.68	147.51	146.28	155.78	—	—
FO	<i>Fragilariopsis doliola</i>	1.89-2.00	2	—	—	—	—	189.87	201.09	186.43	196.79	—	—
* LO	<i>Neodenticula koizumii</i>	1.9	2.0	—	—	—	—	189.87	201.09	186.43	196.79	—	—
LO	<i>Thalassiosira convexa</i>	2.3	2.35	33.11	42.59	—	—	222.21	232.35	239.33	255.67	—	—
* LO	<i>Neodenticula kamschatica</i>	2.50-2.58	2.61-2.68	—	—	—	—	—	—	—	—	—	—
LCO	<i>Neodenticula kamschatica</i>	2.50-2.58	2.61-2.68	85.47	94.54	—	—	—	—	—	—	—	—
FO	<i>Neodenticula seminae</i>	2.6	2.68	(64.05)	(75.76)	—	—	—	—	—	—	—	—
* FO	<i>Neodenticula koizumii</i>	3.6	3.53-3.95	146.92	156.70	(81.05)	(92.71)	—	—	—	—	—	—
* FO	<i>Thalassiosira oestrupii</i>	5.1	5.49	—	—	(155.13)	(165.45)	—	—	—	—	—	—
LO	<i>Rouxia californica</i>	5.2	5.9	—	—	(190.81)	(200.41)	—	—	—	—	—	—
FCO	<i>Neodenticula kamschatica</i>	—	6.4	—	—	(155.13)	(165.45)	—	—	—	—	—	—
* LCO	<i>Rouxia californica</i>	6.1	6.65	—	—	(221.41)	(225.91)	—	—	—	—	—	—
LO	<i>Cavitatus jouseanus</i>	—	6.7-6.8	—	—	(221.41)	(225.91)	—	—	—	—	—	—
* LCO	<i>Thalassionema schraderi</i>	6.7	7.6	—	—	229.41	231.11	—	—	—	—	—	—
FCO	<i>Thalassionema schraderi</i>	8.0	8.4	—	—	251.03	255.54	—	—	—	—	—	—
LO	<i>Denticulopsis katayamae</i>	7.6	8.5	—	—	(258.21)	(259.83)	—	—	—	—	—	—
* LCO	<i>Denticulopsis simonsenii</i>	8.0	8.6	—	—	251.03	255.54	—	—	—	—	—	—
* LO	<i>Denticulopsis dimorpha</i>	8.4	9.16	—	—	259.83	264.33	—	—	—	—	—	—
FO	<i>Denticulopsis katayamae</i>	8.7	9.26	—	—	267.81	269.56	—	—	—	—	—	—
FO	<i>Thalassionema schraderi</i>	—	9.5	—	—	277.51	279.07	—	—	—	—	—	—
* FO	<i>Denticulopsis dimorpha</i>	8.9	9.9	—	—	277.51	279.07	—	—	—	—	—	—
* LCO	<i>Denticulopsis praedimorpha</i>	10.4	11.5	—	—	302.91	306.31	—	—	—	—	—	—
FO	<i>Hemidiscus cuneiformis</i>	11.4	—	—	—	—	—	—	—	—	—	—	—
LO	<i>Crucidentacula nicobarica</i>	12.2	12.5	—	—	317.61	322.06	—	—	—	—	—	—
* FO	<i>Denticulopsis praedimorpha</i>	12.6	12.9	—	—	—	—	—	—	—	—	—	—
* FCO	<i>Denticulopsis simonsenii</i>	13.65	13.1	—	—	—	—	—	—	—	—	—	—
* LCO	<i>Denticulopsis hyalina</i>	13.65	13.1	—	—	—	—	—	—	—	—	—	—

Notes: Diatom events are calibrated to the time scales of Berggren et al. (1985b) and Cande and Kent (1995). BKFV85 = Berggren et al., 1985 time scale. CK95 = Cande and Kent, 1995 time scale. * = zonal boundaries. LO = last occurrence, FO = first occurrence, LCO = last common or consistent occurrence; FCO = first common or consistent occurrence. Data in parentheses represent uncertainty as to stratigraphic position. — = no data.

Table 15 (continued).

Event	Datum	Hole 1018A		Hole 1016A		Hole 1014A		Hole 1011B		Hole 1010C	
		Top (mcd)	Bottom (mcd)	Top (mcd)	Bottom (mcd)	Top (mcd)	Bottom (mcd)	Top (mcd)	Bottom (mcd)	Top (mcd)	Bottom (mcd)
* LO	<i>Proboscia curvirostris</i>	68.51	78.84	27.80	37.70	—	—	—	—	—	—
LO	<i>Rhizosolenia matuyamai</i>	—	—	37.7	48.12	—	—	—	—	—	—
FO	<i>Rhizosolenia matuyamai</i>	—	—	48.12	57.84	—	—	—	—	—	—
* LO	<i>Actinocyclus oculatus</i>	99.34	109.27	(57.84)	(67.84)	105.01	114.36	—	—	—	—
FO	<i>Proboscia curvirostris</i>	202.67	212.27	—	—	—	—	—	—	—	—
FO	<i>Fragilariopsis doliola</i>	—	—	—	—	—	—	—	—	—	—
* LO	<i>Neodenticula koizumii</i>	254.03	263.73	(105.54)	(115.78)	—	—	—	—	—	—
LO	<i>Thalassiosira convexa</i>	311.19	320.79	—	—	(211.40)	(216.90)	—	—	—	—
* LO	<i>Neodenticula kamschatica</i>	378.69	388.39	—	—	(327.10)	(336.80)	—	—	—	—
LCO	<i>Neodenticula kamschatica</i>	436.39	445.89	—	—	—	—	—	—	—	—
FO	<i>Neodenticula seminae</i>	—	—	—	—	—	—	—	—	—	—
* FO	<i>Neodenticula koizumii</i>	—	—	—	—	—	—	—	—	—	—
* FO	<i>Thalassiosira oestrupii</i>	—	—	(297.90)	(307.60)	—	—	—	—	—	—
LO	<i>Rouxia californica</i>	—	—	—	—	—	—	—	—	—	—
FCO	<i>Neodenticula kamschatica</i>	—	—	—	—	—	—	—	—	—	—
* LCO	<i>Rouxia californica</i>	—	—	—	—	—	—	—	—	—	—
LO	<i>Cavitatus jouseanus</i>	—	—	—	—	—	—	—	—	—	—
* LCO	<i>Thalassionema schraderi</i>	—	—	—	—	—	—	221.94	224.94	89.23	93.23
FCO	<i>Thalassionema schraderi</i>	—	—	—	—	—	—	247.64	250.84	—	—
LO	<i>Denticulopsis katayamae</i>	—	—	—	—	—	—	253.84	257.24	103.63	106.63
* LCO	<i>Denticulopsis simonsenii</i>	—	—	—	—	—	—	253.84	257.24	103.63	106.63
* LO	<i>Denticulopsis dimorpha</i>	—	—	—	—	—	—	273.05	276.54	109.93	114.21
FO	<i>Denticulopsis katayamae</i>	—	—	—	—	—	—	—	—	109.93	114.21
FO	<i>Thalassionema schraderi</i>	—	—	—	—	—	—	—	—	—	—
* FO	<i>Denticulopsis dimorpha</i>	—	—	—	—	—	—	—	—	114.21	117.21
* LCO	<i>Denticulopsis praedimorpha</i>	—	—	—	—	—	—	—	—	138.75	142.05
FO	<i>Hemidiscus cuneiformis</i>	—	—	—	—	—	—	—	—	(128.28)	(131.57)
LO	<i>Crucidentacula nicobarica</i>	—	—	—	—	—	—	—	—	(166.97)	(170.26)
* FO	<i>Denticulopsis praedimorpha</i>	—	—	—	—	—	—	—	—	170.26	174.47
* FCO	<i>Denticulopsis simonsenii</i>	—	—	—	—	—	—	—	—	190.65	194.98
* LCO	<i>Denticulopsis hyalina</i>	—	—	—	—	—	—	—	—	190.65	194.98

erally uncommon assemblages of planktonic foraminifers and few to abundant calcareous nannofossils. Below this interval, a 61-m-thick sequence of rapidly deposited diatom-rich sediments of late Miocene age was recovered.

Diatoms are abundant to common and display excellent to good preservation in chiefly the lowermost seven cores of Hole 1011B (210.5–271.7 mbsf). Diatom assemblages are typical of the subarctic

region of the North Pacific and can be zoned readily using the North Pacific diatom zonation (Table 5). The interval from Sample 167-1011B-19X-CC through 23X-3, 20–21 cm, corresponds to the *Rouxia californica* Zone (NPD 7A) based upon sporadic occurrences of *R. californica*. Persistent reworking of early late Miocene forms of *D. katayamae*, *D. dimorpha*, and conceivably *D. simonsenii* occur within the uppermost Miocene NPD 7A Zone. The LCO of *Thalassionema*

schraderi is recognized in Sample 167-1011B-23X-5, 20–21 cm, and marks the top of the *T. schraderi* Zone (NPD 6B).

A complete sequence from the *T. schraderi* Zone (NPD 6B) down to the *Denticulopsis dimorpha* Zone (NPD 5D) was recovered through Samples 167-1011B-23X-5, 20–21 cm, to 29X-CC, which falls within the middle late Miocene. The coincidence of the LCO of the *Denticulopsis simonsenii* group and the LO of *Denticulopsis katayamae* in Sample 167-1011B-26X-CC marks the boundary between the *Thalassionema schraderi* Zone (NPD 6B) and the underlying *Denticulopsis katayamae* Zone (NPD 6A). Akiba (1986) adopted the former event dated at 8.6 Ma as the zonal boundary because of the practical difficulty in morphological identification, whereas Yanagisawa and Akiba (1998) used the latter at 8.5 Ma as was defined originally by Maruyama (1984b). If a careful examination is allowed, the latter should be perfect as the boundary. But from the point of view of realistic decision making, support for the former should not be abandoned immediately. Above these events, the FCO of *T. schraderi* (8.4 Ma) is assigned to Sample 167-1011B-25X-CC.

The top of the *Denticulopsis dimorpha* Zone (NPD 5D) has been placed between Samples 167-1011B-28X-5, 21–22 cm, and 28X-CC at the LO of *D. dimorpha* at 9.16 Ma. The presence of *D. dimorpha* accompanied by *D. katayamae* in the lowest sample, 167-1011B-29X-CC, indicates that the base of the cored section at Site 1011 is assuredly younger than 9.26 Ma, an assignment that is consistent with that of the radiolarians.

Assemblages examined from Samples 167-1011B-23X-5, 20–21 cm, through 28X-3, 21–22 cm, are commonly dominated by *Coscinodiscus marginatus*, a large, robust centric diatom that is resistant to dissolution and transportation. Long needle-like diatoms such as *Thalassionema nitzschioides*, *T. schraderi*, and *Thalassiothrix longissima* occasionally exhibit abundant occurrences in accord with *C. marginatus*. These samples fall just below the 64-m-thick, diatom-scarce interval and represent an almost entire sequence of the NPD 6B through 6A zones. Increased abundances of *C. marginatus* shows evidence for strong upwelling conditions during the late Miocene at Site 1011.

On the other hand, the diatom-poor sequence from the latest Miocene to the early Pliocene indicates warm-temperate to cool-subtropical conditions with a weakening of the upwelling system. Although cold-water *Neodenticula* species always dominate diatom assemblages wherever subarctic zonation prospered in the late Miocene through Pleistocene age, they are completely absent, nor are there characteristics of temperate to subtropical markers in Hole 1011B. Moreover, the scarcity of diatoms in the clay-rich, upper part of the sequence at Site 1011 as well as Site 1010 results from ecological exclusion or chemical decomposition from the relatively warm coastal waters during the late Pliocene through Quaternary.

Sites 1012, 1013, 1015, and 1017

Sites 1012, 1013, 1015, and 1017 comprise the Pliocene through Quaternary sequences with very little diatoms, so they are explained together. Stratigraphic documentation of diatom fossils are presented in the Leg 167 *Initial Reports* volume (Lyle, Koizumi, Richter, et al., 1997).

The sedimentary sequence recovered from the two holes at Site 1012 consists of an apparently continuous 264-m-thick interval of upper lower Pliocene to Quaternary sediments. Also, three holes were cored at Site 1013, recovering an apparently continuous sequence of late late Pliocene (2.7 Ma) through Quaternary age. Site 1012 is located at a distance 105 km from the shore, and similarly Site 1013 is 115 km off the coast. Diatoms are barren to few in all sections from the Pliocene through Quaternary interval at both Sites 1012 and 1013. All diatom assemblages are poorly preserved, and neither the North Pacific diatom zonation nor the standard diatom datum levels were recognized in any part of the holes.

The poorly preserved assemblages are commonly accompanied by abundant sponge spicules. Large, robust, and fresh biosiliceous

skeletons are resistant to dissolution and transportation. Diatoms recovered from both sites contain consistent, but typically few, reworked planktonic diatoms from pelagic middle Miocene sediment sequences. These specimens include many diagnostic cool-water taxa such as *Actinocyclus ingens* and *Denticulopsis* spp. Persistent and scattered common occurrences of reworked specimens as well as numerous sponge spicules indicate strong incursions of marginal shallow waters that are associated with seafloor erosion from Baja California during the latest Cenozoic or from the tops of California Borderland ridges.

Site 1015 in the Santa Monica Basin is the only Leg 167 site located within an inner borderland basin at a water depth of 901 mbsf. Diatoms are either absent or occur only in trace amounts throughout the upper Quaternary sequence at Site 1015. Reworked Miocene taxa are very poorly preserved and are of no value for biostratigraphy through the distal turbidites extended onto Site 1015. The uppermost core-catcher samples of Holes 1015A and 1015B (Samples 167-1015A-1H-CC and 167-1015B-1H-CC) contain common to few siliceous bands dislodged from the girdles of diatom cells.

Site 1017 is located about 50 km west of Point Arguello on the continental slope at 955-m water depth. It is the shallow-water drill site in the Conception Transect (35°N), near an important upwelling center off Point Conception. Five holes were cored to a maximum depth of 204.2 mbsf, recovering an apparently continuous interval of Quaternary age.

Site 1017 exhibits a characteristic biosiliceous component made up of trace amounts of fragmented diatoms, rare reworked diatoms of middle Miocene age, and common fresh sponge spicules. Thus, Site 1017 resembles Sites 1012, 1013, and 1014. These mixtures suggest a persistence of reworking of relatively shallow-water components during the Pleistocene. Although sparse occurrences are documented of *Actinocyclus oculatus* in Sample 167-1017B-11H-CC and of *Proboscia curvirostris* in Sample 167-1017B-12H-CC, diatom biostratigraphy is ineffective at Site 1017.

Site 1014

Site 1014 is located in Tanner Basin, within the outer band of California Borderland basins. Four holes were cored with the advanced piston corer (APC) and extended core barrel (XCB) to a maximum depth of 449.0 mbsf. The sedimentary sequence recovered from Site 1014 consists of a well-dated, apparently continuous, 325-m-thick interval of upper Pliocene to Quaternary sediments, underlain by a relatively poorly dated 124-m-thick sequence of lower Pliocene to possibly latest Miocene age. The sediments consist predominantly of calcareous nannofossils, foraminifers, and siliciclastic clays. A well-constrained biostratigraphy and chronology for all holes at Site 1014 is provided by a combination of calcareous nannofossil, planktonic foraminifer, and radiolarian datums for the upper Pliocene and Quaternary.

Few diatoms occur in the Pliocene and Quaternary section at Site 1014 (Table 6). All diatom assemblages are poorly preserved, and, as at Sites 1012 and 1013, neither the Leg 167 North Pacific diatom zonation nor the standard diatom datum levels was recognized in Holes 1014A and 1014B. Poorly preserved assemblages are commonly accompanied by abundant fresh sponge spicules, rare radiolarians, and reworked planktonic diatoms, forming an unusual biosiliceous assemblage.

A stratigraphic interval younger than Sample 167-1014A-12X-CC contains assemblages lacking *Actinocyclus oculatus*, and is assignable to the *Proboscia curvirostris* Zone (NPD 11) through the *N. seminae* Zone (NPD 12). Sparse occurrences of *A. oculatus* throughout Samples 167-1014A-13H-CC to 38H-CC suggest weakly a range of late Pliocene to early Pleistocene (~4.0–1.0 Ma), and a possible boundary between Zones NPD 10/11 is indicated by the last occurrence (LO) of *A. oculatus* at 1.01–1.46 Ma in Sample 167-1014A-13X-CC (112.4 mbsf). Paleomagnetic investigation revealed a good magnetostratigraphic record down to 100 mbsf and allowed the iden-

tification of the Brunhes and Jaramillo normal-polarity intervals. The chronostratigraphic boundary of Chron C1r.1n (Jaramillo onset) at 1.07 Ma is reported from 86 to 87 mbsf at both Holes 1014B and 1014D, suggesting that the evaluation of the age of the LO of *A. oculus* is not completely incorrect but narrowly reasonable.

The diatom assemblage in Sample 167-1014A-39X-CC contains *Hemidiscus cuneiformis*, *Thalassiosira* cf. *leptopus*, and *Coscinodiscus* sp., but lacks *Neodenticula* spp., *Nitzschia reinholdii*, and another *Nitzschia* sp. The assemblage is typical of neither the subarctic North Pacific nor equatorial East Pacific Ocean, but rather of the relatively warm-temperate surface water that might be extended along the west coast of California at the time. Moreover, subarctic index species such as *Neodenticula kamtschatica*, *N. koizumii*, and *N. seminae* occur in traces throughout the section, which indicate relative warmth around Site 1014 from the early Pliocene through the late Pleistocene.

More than 20 m of the section, from 179 to 199 mbsf, includes abundant to few specimens of both *Coscinodiscus marginatus* and *Proboscia barboi* (Samples 167-1014A-20X-CC through 22X-CC and 167-1014B-22X through 24X-CC). These diatom elements are so large and robust that their assemblage is resistant to dissolution and fragmentation. They are also characteristic of bordering upwelling (see "Site 1010" section, this chapter), indicative of high-productivity episodes during the late Pliocene on the continental margin (Table 6).

Persistent reworking of many diagnostic cool-water taxa such as *Actinocyclus ingens*, *A. ingens* v. *nodus*, and *Denticulopsis* spp., documented in the Pleistocene through upper Pliocene section from Site 1014, represents strong incursions of marginal shallow waters, inducing seafloor erosion. Reworked specimens, which are commonly dissolved and fragmented, suggest that they might be derived from the corresponding sediment sequences of Luisian through Mohnian age in the Monterey Formation of California (Poore et al., 1981).

During DSDP Leg 63 off southern California, Barron (1981) also reported a diatom-poor interval, containing only rare, poorly preserved specimens reworked from the Miocene, between lowermost Pliocene and upper Pliocene diatomaceous sediments at both Holes 467 (33°50.97'N) and 469 (32°37.00'N) near Hole 1014 (32°49.99'N). Barron (1981) also explained that a slackening of the California Current during a period of relative warming caused reduced upwelling with resultant decreased diatom productivity.

Site 1016

Site 1016 is located about 150 km west of Point Conception and forms the deep-water drill site (water depth of 3834 mbsl) on the Conception Transect (35°N). Site 1016 occupies an important transitional zone for modern diatom flora and provides material to investigate paleoceanographic conditions near the center of the California Current. The sedimentary sequence recovered from the four holes at Site 1016 consists of a well-dated, apparently continuous, 308-m-thick interval ranging from the upper Miocene to the Quaternary. At the base of Hole 1016A, cored to a maximum depth of 316.5 mbsf, slow drilling and poor recovery were encountered in massive chert and porcellanite layers starting at 298 mbsf. Magnetic intensities were below the noise level of the magnetometer and precluded the establishment of a magnetic polarity stratigraphy aboard ship.

Diatoms are generally common to abundant and poorly to well preserved in the upper Miocene through Pleistocene section above 290 mbsf at Site 1016 (Table 7). In contrast to Sites 1011 through 1015, typical Quaternary assemblages are well preserved and easily zoned from Cores 167-1016A-1H through 11H. The LO of the *Proboscia curvirostris* (0.30 Ma) falls between Samples 167-1016A-3H-CC and 4H-CC, where it differentiates the *N. seminae* Zone (NPD 12) from the underlying *P. curvirostris* Zone (NPD 11). The zonal boundary between the NPD 12/11 zones is also determined in Holes 1016B and 1016D. A rare occurrence of *Rhizosolenia matuyamai* in Sample 167-1016A-5H-CC is dated as 0.91–1.14 Ma and indicates a tight cor-

relation with a short interval spanning the normal-polarity Jaramillo subchron (Barron, 1980b; Barron and Gladenkov, 1995). The solitary occurrence of *R. matuyamai* has been used to tentatively place the boundary between the *P. curvirostris* and *A. oculus* Zones (NPD 11/10). The FO of *P. curvirostris* in Sample 167-1016A-6H-CC can be detected from the middle part of Zone NPD 10 accordingly. Because the Pliocene/Pleistocene boundary is placed between 55.1 and 55.8 mbsf by a combination of calcareous nannofossils and planktonic foraminifer biostratigraphy, the NPD 11/10 boundary in Hole 1016A should lie between Samples 167-1016A-4H-CC and 5H-CC. Consequently, the last rare occurrence of *A. oculus* in Sample 167-1016A-7H-CC is stratigraphically too low to mark the top of the *A. oculus* Zone (NPD 10).

Following Koizumi (1992), the base of the *A. oculus* Zone (NPD 10) and top of the underlying *Neodenticula koizumii* Zone (NPD 9) are defined by the LO of *N. koizumii* (2.0 Ma). The LO of *Thalassiosira convexa* (2.4 Ma) occurs just below the LO of *N. koizumii* (Barron and Gladenkov, 1995). These latest Pliocene events were documented in Samples 167-1016A-11X-CC through 12X-CC, but occurrences of these species are too sparse to provide high stratigraphic reliability at Site 1016. Despite an abundance of diatoms in sediments between Samples 167-1016A-11X-CC (96.3 mbsf) and 31X-CC (288.8 mbsf), three zones of the late Pliocene through latest Miocene age—the *N. koizumii* Zone (NPD 9), the underlying *N. koizumii* -*N. kamtschatica* Zone (NPD 8), and the lowest *N. kamtschatica* Zone (NPD 7)—could not be clearly defined because of the absence of zonal marker species *N. koizumii* and *N. kamtschatica*. Barron and Baldauf (1986) reported that it is inappropriate to use the *N. kamtschatica* Zone (NPD 7) in California and substituted two zones defined by Barron (1981): the *Nitzschia reinholdii* Zone and the overlying *Thalassiosira oestrupii* Zone. The combination of calcareous nannofossils and planktonic foraminifers provided a well-constrained biostratigraphy and chronology for Hole 1016A, and fairly placed the lower/upper Pliocene boundary between 154.5 and 157.45 mbsf and the upper Miocene/lower Pliocene boundary between 182.8 and 192.3 mbsf.

The 190-m-thick diatomaceous interval from 96.3 to 288.8 mbsf at Site 1016 includes abundant representatives of *Coscinodiscus marginatus*, *Proboscia barboi*, *Thalassionema nitzschioides*, and *Thalassiothrix longissima*, which are characteristic of oceanic-to-marginal upwelling systems and indicative of high coastal productivity. The diatom assemblages contain scattered and consistent representatives of warm-water taxa such as *Hemidiscus cuneiformis*, *Thalassiosira convexa*, *Azpeitia nodulifera*, and *N. reinholdii*. These assemblages are typical of neither the subarctic North Pacific nor the equatorial eastern Pacific, but rather the relatively warm-temperate surface waters that extend along the northeastern Pacific rim off California.

Such diatom assemblages suggest two major episodes of strong upwelling during the upper Miocene (from 182 to 288 mbsf) and the upper Pliocene (from 96 to 154 mbsf). These two episodes are separated by an interval marked by low sedimentation rates during the early Pliocene (from 163 to 173 mbsf). Although age vs. depth plots for Holes 1016A and 1016B show high sedimentation rates from the Quaternary to the upper Pliocene and for the upper Miocene (Lyle, Koizumi, Richter, et al., 1997), sedimentation rates were drastically lower for the lower to mid-Pliocene, indicating decreased vertical advection of deep waters.

The coexistence of both *N. reinholdii* and *N. pliocena* in Sample 167-1016A-31X-CC at 288.8 mbsf indicates that the base of the diatomaceous interval in Hole 1016A may be younger than 7.3 Ma. Surface waters at Site 1016 have maintained intermediate properties between subarctic cold waters and subtropical warm waters during the latest Miocene through Pliocene. Oceanic-to-marginal upwelling caused high diatom productivity between both fronts along the eastern rim of the temperate North Pacific. An almost continuous absence of cold-water *Neodenticula* spp. reflects a transitional provincialism of the diatom flora, suggesting warm conditions during the late Miocene through late Pliocene.

Site 1018

Site 1018 is located about 75 km west of Santa Cruz, California, on a sediment drift just south of Guide Seamount at a water depth of 2477 mbsl. It provides continuity in the Leg 167 sites from the central California margin between the Gorda Transect at 40°N and the southern California transects. The sedimentary sequence recovered from the four holes at Site 1018 consists of a well-dated, apparently continuous 426-m-thick interval of uppermost lower Pliocene to Quaternary sediments. All the microfossil groups at Site 1018 are clearly dominated by cool, high-latitude elements throughout the late Neogene. Site 1018 is sufficiently far north in the California Current to exclude most to all subtropical elements, even during interglacial episodes. Diatoms are dominated by subarctic forms, however, with the addition of much less abundant temperate elements.

Diatoms are generally common to abundant and poorly to moderately well preserved throughout the Quaternary through upper Pliocene section recovered at Site 1018 (Table 8). In the uppermost parts of the Quaternary section, however, diatoms are few because of increases in clay minerals and silt grains. Diatom assemblages from all core-catcher samples consist almost entirely of oceanic species, occasionally including littoral benthic forms. They are mainly of the subarctic North Pacific Ocean, although such warm-water taxa as *Hemidiscus cuneiformis*, *Nitzschia reinholdii*, *Fragilariopsis doliola*, *Azpeitia nodulifera*, and *Thalassiosira convexa* are typically present throughout the section. The core-catcher samples examined range from the Quaternary *Neodenticula seminae* Zone (NPD 12) to the late Pliocene *Neodenticula koizumii-Neodenticula kamtschatica* Zone (NPD 8). The Neogene North Pacific Ocean diatom zones are readily distinguishable, and standard diatom datum levels were used to recognize these zones.

The boundary between the late Quaternary *N. seminae* and *Probosciasia curvirostris* Zones (NPD 12/11) is clearly indicated by the LO of *P. curvirostris* around 70 mbsf in Holes 1018A, 1018C, and 1018D. This event is detected from between Cores 167-1018A-7H-CC and 8H-CC, 167-1018C-8H-CC and 9H-CC, and 167-1018D-7H-CC and 8H-CC. The continuous occurrence of *F. doliola* is observed from Zone NPD 11 down to the upper part of Zone NPD 10 (Samples 167-1018A-8H-CC through 15X-CC). This species is one of the most diagnostic forms within the low-latitude diatom zonation (Baldauf and Iwai, 1995), and its stratigraphic distribution probably indicates the proximity of warm surface waters.

The LO of *Actinocyclus oculatus* in Sample 167-1018A-11X-CC marks the boundary between the *P. curvirostris* and *A. oculatus* Zones (NPD 11/10) in Hole 1018A, but it is not detected in Holes 1018C and 1018D. Within Zone NPD 10, the FO of *P. curvirostris* between Samples 167-1018A-20X-CC and 21X-CC may be useful for subdividing this zone. This datum, with an assigned age of 1.58 Ma, is tentatively adapted as a zonal boundary between Zones NPD 11 and 10 (between Samples 167-1018C-20X-CC and 21X-CC) in Hole 1018C, because the LO of *A. oculatus* was not observed. Both paleomagnetic records and the short range of *Rhizosolenia matuyamai* in Sample 167-1018C-16X-CC, which ranges from only 0.91 to 1.14 Ma, supports this biostratigraphic determination. Positive paleomagnetic inclinations in the top 88 mbsf, which most likely represent the Brunhes Chron, approve of diatom sequence through Zones NPD 12 to 11. Below the normal polarity interval, an interpretation of the inclination record was not possible because of the low magnetic intensity and core disturbance by XCB coring.

Koizumi (1992) proposed that the base of the *A. oculatus* Zone (NPD 10) and top of the underlying *N. koizumii* Zone (NPD 9) be defined by the LO of *N. koizumii*. This latest Pliocene event at 2.0 Ma occurs between Cores 25X-CC and 26X-CC in both Holes 1018A and 1018C. The LO of *T. convexa* (2.35 Ma) is documented in the middle of Zone NPD 9 between Samples 167-1018A-31X-CC and 32X-CC. The LO of *N. kamtschatica* and its last common occurrence (LCO) are narrowly assignable between Samples 167-1018A-38X-

CC and 39X-CC, and between 44X-CC and 45X-CC, respectively. Although Barron and Gladenkov (1995) adopted the LCO event as the top of Zone NPD 8, the LO of *N. kamtschatica* is so generally used by Akiba (1986), Koizumi (1992), and Yanagisawa and Akiba (1998) that here it was chosen to mark the top of the underlying *N. koizumii-N. kamtschatica* Zone (NPD 8) in Hole 1018A.

The lowest record of *N. seminae* in Sample 167-1018A-42X-CC is situated between the LO of *N. kamtschatica* and its LCO within the topmost of Zone NPD 8 in Hole 1018A. According to Yanagisawa and Akiba (1998), the FO of *N. seminae* should be defined by the FO of its closed copula and can be estimated at about 2.4 Ma above the LO of *Neodenticula kamtschatica* at DSDP Hole 438A off northeastern Honshu, Japan. However, Koizumi (1992) and Barron and Gladenkov (1995) reported that the FO of *N. seminae* coincides with the LO of *N. kamtschatica* in the Japan Sea and in the high-latitude western North Pacific, respectively. On the other hand, Koizumi and Tanimura (1985) recognized that event within the *N. koizumii-N. kamtschatica* Zone (NPD 8).

These discrepancies indicate both that the LCO and/or LO of *N. kamtschatica* are diachronous and appear to be earlier off California than in the subarctic region, and that *N. seminae* cannot be distinguished from *N. koizumii* based solely on valve morphology. Yanagisawa and Akiba (1998) note that the type of copula is a key to the final decision to differentiate clearly *N. seminae*, with a closed copula, from *N. koizumii*, with an open copula. Moreover, they report the presence of an evolutionary intermediate form referred to as *Neodenticula* sp. A by Akiba and Yanagisawa (1986), which makes it more difficult to differentiate the two species. The taxonomic refinement among three taxa of *Neodenticula* would contribute to biostratigraphic establishment across the Zone NPD 9/8 boundary, though the stratigraphic distribution of the closed copula of *Neodenticula* (= FO of *N. seminae*) was not investigated during Leg 167.

In contrast to the late Pliocene to Quaternary diatom assemblages at Site 1016, those of Site 1018 contain consistent, but typically few, neritic diatoms. These taxa include representatives of the littoral benthic genera *Cocconeis*, *Cymbella*, *Epithemia*, *Eunotia*, and *Gomphonema* and are taken as evidence for sediment transported from the west coast continental shelf or from the top of Guide Seamount, if the latter was within the photic zone. The transport of these diatoms must have been contemporaneous with higher input of terrigenous sediments because reworked diatoms are extremely rare in Site 1018 sediments.

In the uppermost Pliocene to lower Pleistocene, the diatom assemblages are marked by rare-to-common *N. seminae*, few-to-common *P. barboi*, and few-to-abundant *Stephanopyxis* species, which are indicative of high oceanic-to-marginal productivity. The abundant fragments of *Thalassiothrix* species, conspicuously common occurrence of *C. marginatus*, and large numbers of siliceous bands dislodged from diatom girdles sometimes found in this interval, especially during the latest Pliocene, may indicate surface water, reflecting coastal upwelling associated with climatic change.

Site 1019

Site 1019 is located about 60 km west of Crescent City, California, in the Eel River Basin at a water depth of 977 mbsl. It is the near-shore drill site of the Gorda Transect. The five holes at Site 1019 recovered an apparently continuous sediment sequence of the late Quaternary. The age of the base of Hole 1019C at 247.8 mbsf is well constrained at ~900 ka.

Two characteristic North Pacific diatom zones of the *Neodenticula seminae* Zone (NPD 12) to the *Probosciasia curvirostris* Zone (NPD 11) were recognized in the Quaternary section at Site 1019. Diatoms are rare to abundant and poorly to moderately well preserved throughout the sequence (Table 9). The last consistent occurrence of *P. curvirostris* in Sample 167-1019C-5H-CC marks the boundary between the *N. seminae* and *P. curvirostris* Zones (NPD 12/11) in Hole 1019C. This

boundary in Hole 1019D occurs slightly higher (between Samples 167-1019D-3H-CC and 4H-CC) than in Hole 1019C. Positive paleomagnetic inclinations of the top 75 mbsf most likely represent the Brunhes Chron and support these diatom zonation.

Radiolarians are completely dominated by subarctic forms, whereas diatoms are dominated by cool, high-latitude, North Pacific assemblages, with limited subtropical forms. The cold-water representative *N. seminae* occurs throughout most of the sequence and is indicative of Zone NPD 11 but not of Zone NPD 12. Despite the relatively high-latitude location of this site, warm-water taxa such as *Fragilariopsis doliola* and *Nitzschia reinholdii* are sporadically but persistently present in the section except in the uppermost Zone NPD 12. Fine-grained sand turbidites, which were observed to be more common in the latest part of the sequence younger than ~400 ka (above 42 mbsf), explain why diatom assemblages within Zone NPD 12 seem broken and reduced.

Both the persistent occurrence of *P. curvirostris* and the absence of *Rhizosolenia matuyamai* in the lowest part of the sequence (Samples 167-1019C-23X-CC to 25X-CC) indicate that an age of the base in Hole 1019C is younger than the condensed range of the latter species from 0.91 down to 1.14 Ma. Such distribution of diatoms cooperate with the evolutionary transition in a radiolarian bioseries between 199.7 and 190.1 mbsf, which is well dated between 0.9 and 0.8 Ma based upon magnetostratigraphic intercalibration.

Both *N. seminae* and *Stephanopyxis* species are characteristic of coastal upwelling and exhibit highly variable abundance throughout the sequence. Coincidence of common-to-abundant occurrences of these taxa, corresponding to high-productivity, seems likely to reflect paleoclimatic oscillations as glaciation expanded in the Northern Hemisphere.

Site 1020

Site 1020 is located on the east flank of the Gorda Ridge at a water depth of 3038 mbsl. It is about 170 km west of Eureka, California, and forms the deep-water drill site on the Gorda Transect. The site is located on an abyssal hill that trends northeast and rises ~50 m above the surrounding seafloor on 5.1-Ma ocean crust. The sedimentary sequence recovered from the four holes at Site 1020 consists of an apparently continuous 279-m-thick interval of upper lower Pliocene to Quaternary sediments. A well-constrained biostratigraphy and chronology are provided by a combination of paleomagnetic reversals and microfossil datums. Calcareous nannofossils indicate that the base of Hole 1020B is 3.79 Ma in age.

Except for a barren interval immediately above basaltic basement, all samples from Site 1020 were readily placed within the subarctic diatom zonation of the North Pacific (Tables 10, 11). Sparse occurrences of temperate taxa, such as *Hemidiscus cuneiformis*, *Nitzschia reinholdii*, *N. marina*, and *Thalassiosira convexa*, indicate the influence of temperate water masses from the south during the late Pliocene through early Quaternary. Despite the location of Site 1020 in relatively deep water (>3000 m depth), diatom assemblages in the sequence above 140 mbsf are not typical of hemipelagic environments but show considerable resemblance to the assemblages encountered at nearshore Site 1019. The drill sites were situated almost certainly near the core of the northern region of the California Current during the critical time interval when the Northern Hemisphere glaciation developed. However, cold-water representatives belonging to the genus *Neodenticula* especially reveal low abundances throughout the sequence.

Diatoms are few to common and poorly to moderately well preserved throughout the upper Quaternary section recovered at Site 1020. Abundant clay diluted the diatoms, and almost all are strongly etched and fragmented by dissolution, except for robust forms of *Stephanopyxis turris* and *S. dimorpha*. In contrast, the lower Quaternary through upper Pliocene interval below 140 mbsf is diatomaceous, and diatoms in this interval are common to abundant and gen-

erally moderately to well preserved. Diatoms are represented by open-ocean forms not characteristic of coastal upwelling regions, except during the late Pliocene when upwelling forms are present in relatively high frequencies. The abundant occurrence of robust taxa, such as *Coscinodiscus marginatus*, *Proboscia barboi* (see "Site 1010" section, this chapter), *Stephanopyxis* spp., and *Thalassiothrix* spp., suggests an increase in coastal upwelling intensity during the late Pliocene through the beginning of the earliest Pleistocene.

The boundary between the late Quaternary *Neodenticula seminae* and *Proboscia curvirostris* Zones (NPD 12/11) is indicated by the LO of *P. curvirostris* in Samples 167-1020B-5H-CC and 167-1020C-6H-CC, respectively. The biostratigraphic interval through Zone NPD 12 and the uppermost part of Zone NPD 11 corresponds well to positive inclinations above 78 mbsf in Holes 1020B and 1020C, representing Chron C1n (Brunhes).

The LO of *Actinocyclus oculatus* in Samples 167-1020B-14H-CC and 167-1020C-15H-CC marks the boundary between the *P. curvirostris* and *A. oculatus* Zones (NPD 11/10) in these holes. This boundary is estimated to be between 1.01 and 1.46 Ma in the subarctic region as its LCO by Barron and Gladenkov (1995). The FO of *P. curvirostris* with an age of 1.58 Ma is recognized between core-catcher samples 14H-CC and 15H-CC in both Holes 1020B and 1020C. The normal-polarity Jaramillo Subchron (C1r.1n, 0.99–1.07 Ma) at about 89 to 98 mbsf in Hole 1020B supports an age older than 1 Ma for the LO of *A. oculatus* at Site 1020.

Koizumi (1992) proposed that the LO of *Neodenticula koizumii* clearly defines the base of the *A. oculatus* Zone (NPD 10) and the top of the underlying *N. koizumii* Zone (NPD 9). This latest Pliocene event at ~2.0 Ma falls between Samples 167-1020B-18H-CC and 19X-CC, and between Samples 167-1020C-19X-CC and 20X-CC, respectively. The occurrence of *Fragilariopsis doliola* in Samples 167-1020B-18H-CC and 167-1020C-19X-CC supports the recognition of the NPD 10/9 boundary, because the FO of that species has an estimated age of 1.9 Ma in the eastern equatorial Pacific (Baldauf and Iwai, 1995). Continuous common occurrences of *Neodenticula kamtschatica*, which verify the underlying *N. koizumii*-*N. kamtschatica* Zone (NPD 8), were not found at Site 1020. The LO of *T. convexa*, dated at 2.35 Ma, is assignable in Samples 167-1020B-25X-CC and 167-1020C-23X-CC, just above the barren interval.

Site 1021

Site 1021 is the deep-water drill site of the Gorda Transect. It is located about 100 km south of the Mendocino Fracture Zone on 29.6-Ma crust in 4213-m-deep water. Four holes were cored at Site 1021 to a maximum depth of 310.1 mbsf, recovering a well-dated, apparently continuous interval of uppermost middle Miocene to Quaternary (12.9–0 Ma) sediments. Dominant lithologies are clay, clay with nannofossils, nannofossil ooze, clayey diatomite, and diatom clay mixed sediment. The upper part of the sequence is characterized by a dominance of clay and calcareous nannofossils, whereas diatoms form the main biogenic component in the lower part.

The sedimentation rate for the last 10 m.y. was remarkably constant at ~30 m/m.y., but it was lower during the late middle Miocene (10–12.9 Ma). A complete magnetostratigraphy was determined in Holes 1021B and 1021C. All chrons from the Brunhes (C1n) to the onset of C3n.4n (Thvera subchron) at 5.23 Ma could be identified in the upper 160 mbsf. The microfossil groups are dominated by cool, high-latitude elements from the latest Miocene through the Quaternary. However, diatom assemblages are typical of hemipelagic sedimentary sequences of temperate middle latitudes, and the standard North Pacific diatom zonation has been adapted for use at Hole 1021B (Table 12). Both diatoms and radiolarians indicate that upwelling was strong during the middle through late Miocene.

Diatoms are generally common to abundant and moderately to well preserved in the middle and early late Miocene. In the Quaternary, lower Pliocene, and uppermost Miocene, diatoms are mostly

rare and poorly preserved as a result of dissolution. Reworked forms and neritic assemblages are not important at this site. Sparse occurrences of subtropical taxa including *Actinocyclus ellipticus*, *Azpeitia nodulifera*, *Crucidentacula nicobarica*, *C. punctata*, and *Hemidiscus cuneiformis* suggest the influence of relatively warmer waters during the middle and early late Miocene.

A poorly preserved interval from 55.5 to 84.0 mbsf is generally correlative with the late Pliocene zones from the *Neodenticula koizumii* Zone (NPD 9) to the underlying *N. koizumii-Neodenticula kamtschatica* Zone (NPD 8), based on the presence of *N. kamtschatica*, *Thalassiosira convexa*, *Neodenticula* sp. A of Akiba and Yanagisawa (1986), and consistent *N. koizumii*. A couple of samples from 167-1021-14H-CC and 15H-CC (131.5–141.0 mbsf) are assigned to the *N. kamtschatica* Zone (NPD 7B), based on the presence of rare *N. kamtschatica* and *Thalassiosira oestrupii*.

Characteristic early Pliocene subarctic assemblages dominated by *N. kamtschatica* and *Coscinodiscus marginatus* are missing at Site 1021 because of the warm-temperate conditions. Thus, it is inferred that an unzoned interval between Samples 167-1021B-16H-CC and 23X-2, 20–22 cm, probably including the Miocene/Pliocene boundary, is equivalent in age to the lower part the *N. kamtschatica* Zone (NPD 7B) through the upper part of the *Rouxia californica* Zone (NPD 7A). Samples 167-1021B-23X-5, 20–22 cm, and 23X-CC are tentatively placed in Zone NPD 7A.

A complete sequence of diatom zones from the late Miocene *Thalassionema schraderi* Zone (NPD 6B) to the middle Miocene *Denticulopsis praedimorpha* Zone (NPD 5B) was penetrated in the lower half part (>214 mbsf) of Hole 1021B. The LCO of *T. schraderi* in Sample 167-1021B-24X-2, 20–22 cm, marks the boundary between the NPD 7A and the underlying the *T. schraderi* Zone (NPD 6B). From Zones NPD 7A through 6B, both characteristics of *R. californica* and *T. schraderi*, occur importunately but not so abundantly. The LCO of *D. simonsenii* is assigned to between Samples 167-1021B-26X-2, 92–94 cm, and 26X-5, 93–95 cm, where the NPD 6B/6A boundary is obviously placed. The LO of *D. katayamae* is not determined clearly because of an interpolation of poorly preserved horizon.

Assemblages in Samples 167-1021-27X-5, 12–14 cm, through 28X-CC (248.9–262.1 mbsf) containing *Denticulopsis dimorpha* are assigned to the early late Miocene *D. dimorpha* Zone (NPD 5D). Within Zone NPD 5D, Sample 167-1021B-27X-CC records the FO of *D. katayamae*, and Sample 167-1021B-28X-CC contains the FO of *T. schraderi*. The consistent occurrence of *D. praedimorpha* in Samples 167-1021B-31X-CC through 33X-CC corresponds to the *D. praedimorpha* Zone (NPD 5B) and indicates that the top of the zone is established by the LCO (LO) of that species at 290.9 mbsf.

Between Zones NPD 5D and 5B, the *Thalassiosira yabei* Zone (NPD 5C) lies between Samples 167-1021B-29X-2, 6–8 cm, and 167-1021B-31X-5, 20–22 cm. Although *D. praedimorpha* persists until the lower half of Zone NPD 5C, an evolutionary lineage from *D. praedimorpha* to *D. dimorpha* does not occur as in the mid-latitude northwestern Pacific. *Crucidentacula nicobarica* occurs in the bottom Samples 167-1021B-33X-5, 15–17 cm, and 33X-CC, and in addition *D. praedimorpha* still remains commonly, which surely indicates that the base of Hole 1021B is settled in age between 12.5 and 12.9 Ma (Barron and Gladenkov, 1995) or between 12.7–12.8 and 12.9 Ma (Yanagisawa and Akiba, 1998).

Specimens of *Thalassiothrix*, including *T. longissima*, are especially abundant and large in middle to late Miocene assemblages, indicating high oceanic productivity during this time. Simultaneously, *Coscinodiscus marginatus* and *Proboscica barboi* exhibit common-to-abundant frequencies, showing evidence for intense upwelling conditions (see “Site 1010” section, this chapter). In contrast, specimens of *Denticulopsis* are mainly represented by small size compared with those in diatom assemblages from the northwest Pacific, but coastal environments represented by a large quantity of *Stephanopyxis* species are never indicated at Site 1021.

Two periods of intense upwelling conditions are remarkable during the latest Miocene through the late middle Miocene. One corresponds to Zone NPD 7A down to the uppermost of Zone NPD 5C, and the other represents almost the entire Zone NPD 5B in the basal part of Hole 1021B. An interval of poorly preserved assemblages, probably resulting from strong dissolution, lies between the upwelling intervals. Such genera as *Denticulopsis* and *Neodenticula*, characteristic of subarctic oceanic environments, are small or scarce throughout most of the sequence, suggesting weak and episodic southward extension of the California Current at this location.

Site 1022

Site 1022 is situated on the continental slope just south of the Mendocino Fracture Zone about 90 km from Cape Mendocino. The drill site is located at a water depth of 1926 mbsl on a sliver of continental crust that may have been transferred to the Pacific Plate during the Oligocene. Three holes were cored at Site 1022, to a maximum depth of 387.8 mbsf, recovering an interval of Quaternary to late/early Pliocene age.

The Quaternary is represented by only a very thin (<1 m) veneer of sediments overlying the upper Pliocene. Both diatoms and radiolarians show evidence of strong upwelling throughout the Pliocene at Site 1022. A diagenetic boundary occurs at 360 mbsf, where diatomite is transformed into interbedded siliceous mudstone and chert. Low magnetic intensities and a drilling-induced overprint precluded the establishment of a magnetic chronostratigraphy.

Diatoms are generally common to abundant and poorly to moderately well preserved throughout the sequence. Pliocene diatom assemblages recovered from Holes 1022A and 1022C are dominated by cool temperate to subarctic taxa, with subtropical elements very seldom. Littoral forms and reworked assemblages are not significant at this site.

The standard North Pacific diatom zonation is difficult to use at Site 1022 despite the relatively northern locality at 40°N (Table 13). Whereas the upper Pliocene sequence at Site 1022 is the most diatomaceous of all Leg 167 sites, such diagnostic markers as *Neodenticula seminae*, *Neodenticula koizumii*, and *Neodenticula kamtschatica* are consistently trace to rare.

The late Pliocene zonal boundary between Zones NPD 9 and NPD 8 is difficult to place because of very rare occurrences of *N. kamtschatica*. The boundary is tentatively placed at the LO (= LCO) of *N. kamtschatica* between Samples 167-1022A-9H-CC and 10H-CC. The LO of *T. convexa* is assigned to Sample 167-1022A-5H-CC at 42.5 mbsf within the middle part of Zone NPD 9. The first occurrences of *N. seminae* and *N. sp. A* sensu Akiba and Yanagisawa are assigned to Sample 167-1022A-7H-CC at 61.5 mbsf and 8H-CC at 71.0 mbsf, respectively, just above the LO of *N. kamtschatica* at 90.0 mbsf. The FO of *N. koizumii* (top of Zone NPD 7), which is close to the lower/upper Pliocene boundary, occurs between Samples 167-1022A-15H-CC and 16H-CC.

Diatom species characteristic of upwelling conditions are sometimes dominant throughout the sequence, exhibiting clear oscillations associated with oceanic/coastal environmental changes. Radiolarians indicate a prevalence of strong coastal upwelling, whereas the diatoms reflect oscillations between strong coastal upwelling and occasional oceanic upwelling. The former is characterized by abundant, large *Coscinodiscus marginatus* and *Stephanopyxis* species; on the other hand, the latter is marked by abundant *Thalassiothrix longissima* and *Proboscica barboi*.

Hole 1022A consists of 166 m of upper Pliocene through possible uppermost lower Pliocene sediments. Continuous occurrences of *N. koizumii* in Hole 1022A prove the topmost core-catcher sample to be older than 2.0 Ma, and the lowest sample to be just older than 3.5–3.9 Ma. Co-occurrences of *N. kamtschatica*, *Nitzschia reinholdii*, and *Thalassiosira oestrupii* through Samples 167-1022C-31X-CC to 38X-CC support that the lowermost sample is younger than 5.49 Ma

certainly. On board the *JOIDES Resolution*, planktonic foraminifers indicate that the top of the sequence is >2.25 Ma and that the base of Hole 1022A is older than 3.3 Ma. Calcareous nannofossils also provide data on the age of the base of Hole 1022A to be <3.8 Ma. Most of the microfossil groups well constrain the total age range of the sedimentary sequence recovered from Site 1022.

DISCUSSION

The diatom zonation described in Yanagisawa and Akiba (1998) was used along the California margin. Tables 2 and 3 and Figure 2 summarize the lower Miocene to Quaternary diatom zonation and zonal datum levels used to date samples from Leg 167. Tables 14 and 15 epitomize the stratigraphic and areal occurrences and the chronol-

ogy of important diatom datum levels in a south-to-north transect from Sites 1010 to 1022 along the California margin. Figures 3 through 11 give the stratigraphic distribution of environmental characteristics in Leg 167, and Figure 12 summarizes diatom zonal data to correlate among all holes along the north-to-south direction.

Miocene Datum Levels

Based on available synthesis studies (Koizumi, 1985; Akiba, 1986; Barron, 1992a; Yanagisawa and Akiba, 1998), the following Miocene datum levels appear to be essentially isochronous and widely applicable in the North Pacific through Leg 167: the FCO of *Denticulopsis simonsenii* (13.1 Ma), the FO of *D. praedimorpha* (12.9 Ma), the LCO of *D. praedimorpha* (11.5 Ma), the FO of *D. dimorpha* (9.9 Ma), the FO of *Thalassionema schraderi* (9.5 Ma), the LO of *D. di-*

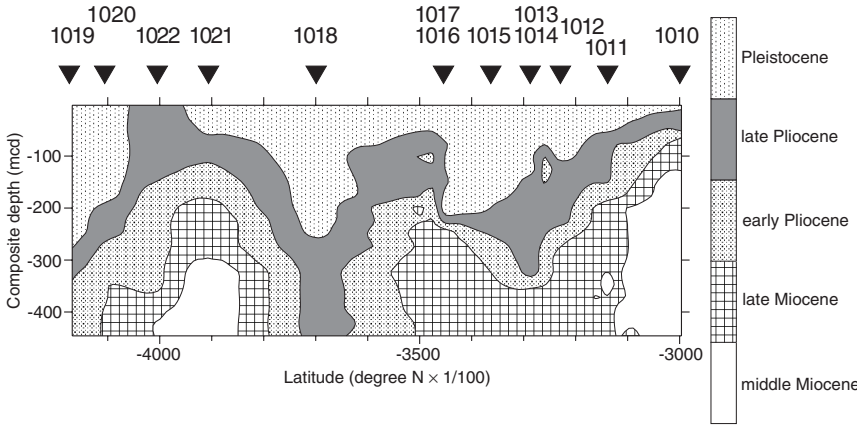


Figure 3. Geologic age correlation among the Leg 167 sites along the California margin. Age determination depends on the diatom biostratigraphy and the other microfossil results.

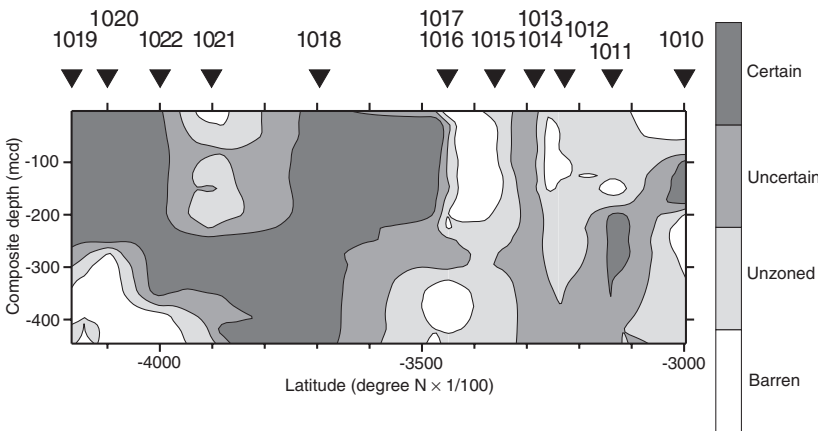


Figure 4. Results of diatom zonation among the Leg 167 sites along the California margin.

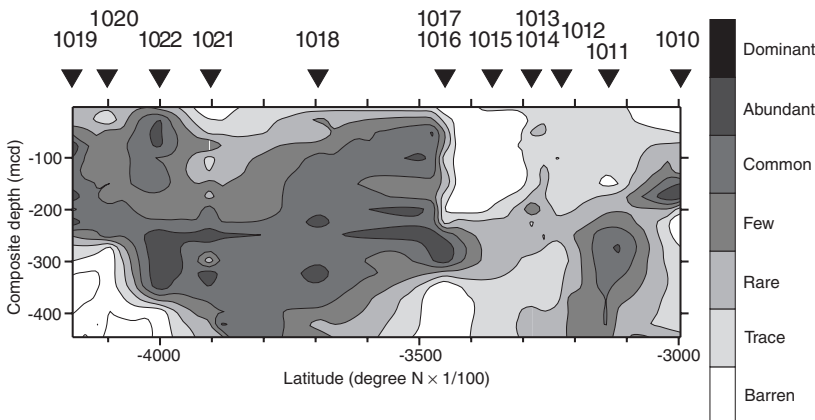


Figure 5. Distribution of group abundance of diatom assemblages among the Leg 167 sites along the California margin.

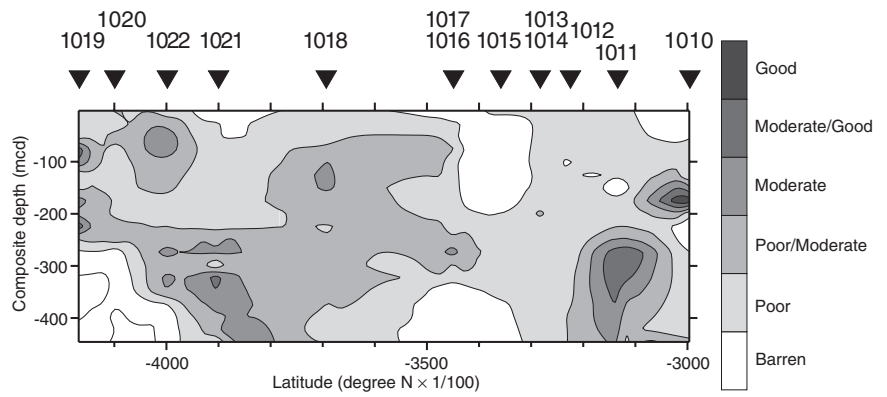


Figure 6. Distribution of preservation of diatom assemblages among the Leg 167 sites along the California margin.

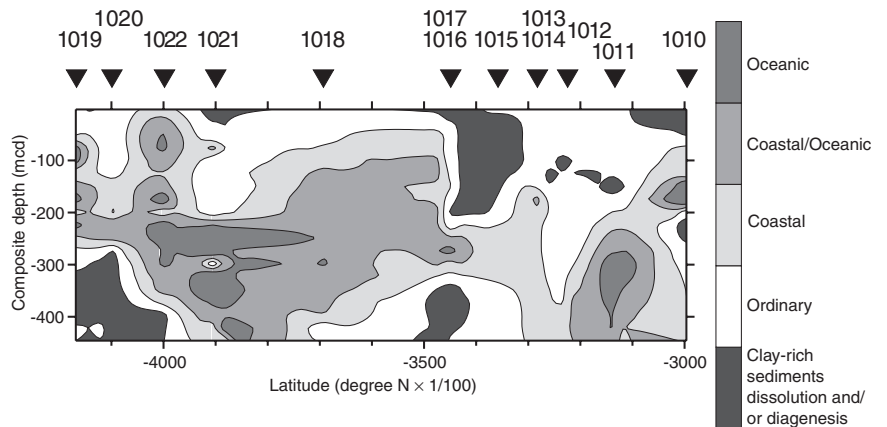


Figure 7. Paleoceanographic characteristics of upwelling and sediment clastics among the Leg 167 sites along the California margin.

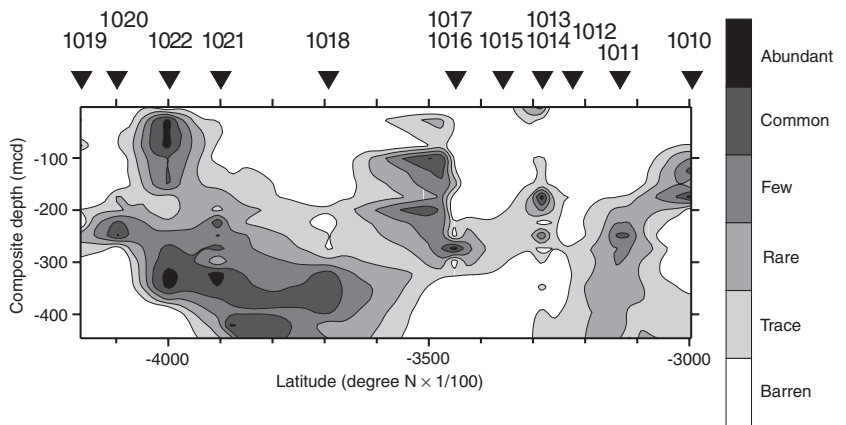


Figure 8. Distribution of the robust taxon *Coscinodiscus marginatus* among the Leg 167 sites along the California margin.

morpha (9.16 Ma), the LCO of *D. simonsenii* (8.6 Ma), the FCO of *T. schraderi* (8.4 Ma), the LCO of *T. schraderi* (7.6 Ma), the LCO of *Rouxia californica* (6.65 Ma), the FCO of *Neodenticula kamschatica* (6.4 Ma), and the FO of *T. oestrupii* (5.49 Ma).

All these datum levels have been recognized to be of the essence of various North Pacific diatom zonation (Koizumi, 1992; Barron and Gladenkov, 1995). It should be mentioned, however, that one of the North Pacific diagnostic species, *Neodenticula kamschatica*, is effectively excluded from California waters, and so the practical use of the *N. kamschatica* Zone (NPD 7) is almost not allowed for the California region sediments. According to Barron (1989, 1992a), the FO of *N. kamschatica* is delayed in California (~5.3 Ma), whereas *Rouxia californica* has an earlier LO (~6.5 Ma).

The FO of *Probosia barboi* (12.3 Ma) near the Zone NPD 5A/5B boundary and the LO of *Denticulopsis katayamae* (8.5 Ma) immedi-

ately below the top of Zone NPD 6A seem to be isochronous among Sites 1010, 1011, and 1021, but these events of cold-water taxa are slightly earlier in the North Pacific. Likewise, some of the FOs and LOs of warm-water diatom taxa appear to modulate across latitude in the North Pacific. Particularly, the LO of *Crucidentricula nicobarica* (12.5 Ma), the FO of *Hemidiscus cuneiformis* (11.5 Ma), the FO of *Nitzschia fossilis* (8.7 Ma), and the FO of *N. reinholdii* (7.4–7.5 Ma) gave some indication of their biostratigraphic uncertainty, but confirmation of their diachroneity must await magnetostratigraphic studies across middle latitudes in the North Pacific.

At Site 1010, warm-water diatoms such as *Actinocyclus ellipticus*, *Annellus californicus*, and *Craspedodiscus coscinodiscus* are relatively consistent in an interval from Subzone NPD 4Bb through the lower part of Zone NPD 5B. The restricted few-to-common occurrences of *Azpeitia nodulifera* within this interval support the possibil-

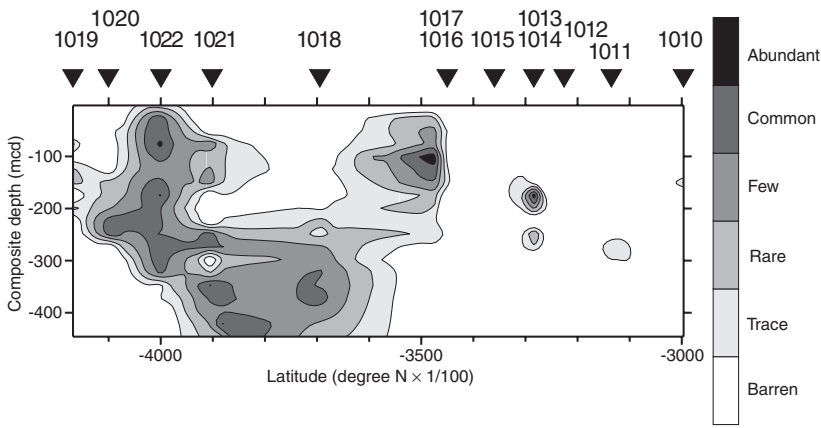


Figure 9. Distribution of *Proboscia barboi* among the Leg 167 sites along the California margin.

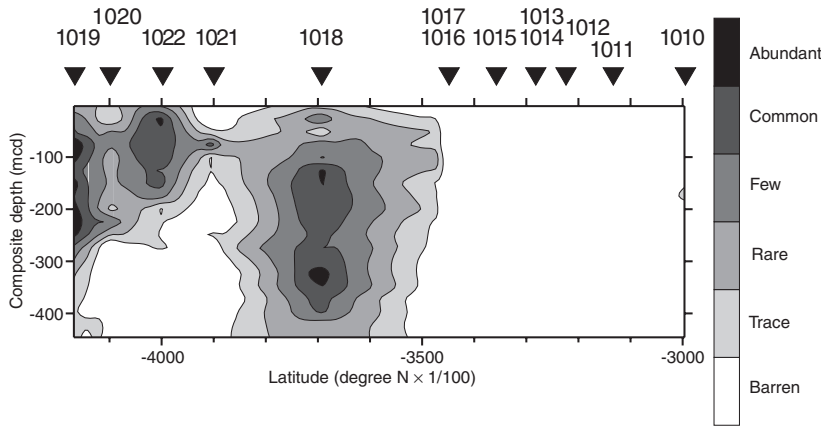


Figure 10. Distribution of the robust *Stephanopyxis* species among the Leg 167 sites along the California margin. Graphic data are based on the sum of relative frequencies of *S. dimorpha* and *S. turris*.

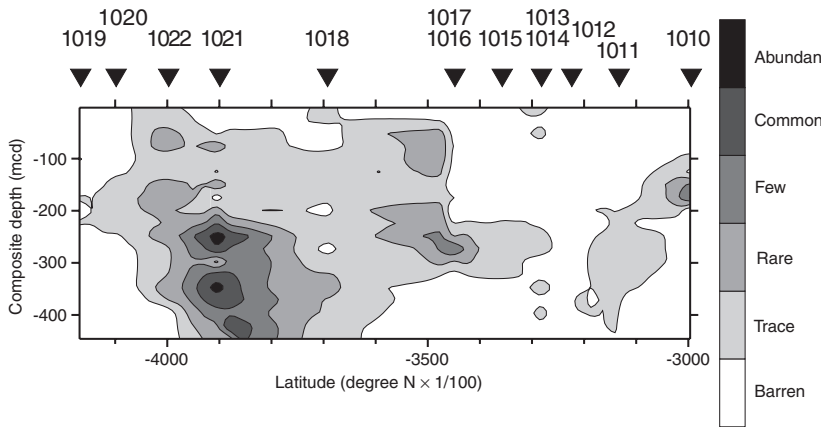


Figure 11. Distribution of the spindle taxa of *Thalassionema* and *Thalassiothrix* species among the Leg 167 sites along the California margin. Graphic data are based on the sum of relative frequencies of *Thalassionema nitzschioides*, *Thalassiothrix longissima*, and *Thalassiothrix* spp.

ity that warming conditions prevailed during this period (~13.1–12.0 Ma). At Site 1021 off northern California, the consistent presence of *Actinocyclus ellipticus* f. *javanica*, *Azpeitia nodulifera*, and *Crucidenticula punctata* within the correlative interval in Zone NPD 5B also support a relative warming trend compared to younger intervals of the Miocene deposits. At Site 1021 the relative warm interval (~12.8–12.0 Ma) is separated from the late Miocene cool interval (~7–10 Ma) by a dissolution interval between Cores 167-1021B-29X and 167-1021B-31X.

Prominent dissolution intervals similar to Hole 1021B occur in Subzone c of the *Denticulopsis hustedtii*–*D. lauta* Zone of Barron (1981) at that time, which is almost equivalent to Zone NPD 5C, in both DSDP Leg 63, Hole 470 at 28°54.46'N and Hole 472 at 23°00.35'N off Baja California. Preservation in the diatomaceous middle Miocene section is generally good to moderate, with the ex-

ception of DSDP Leg 63 Cores 470-13, and 472-9 through 472-10, respectively, where poorly preserved diatoms are present. As for the water depth, there is a similarity among the three holes, which are located at deeper seafloor >3500 mbsl; that is, Hole 470 at 3549 mbsl, Hole 472 at 3831 mbsl, and Hole 1021B at 4213 mbsl, respectively. Pronounced diatom dissolution is not due to silica diagenesis (Barron, 1981), but it is interpreted to be evidence of the onset of deep-to-intermediate water exchange along the California margin caused by slackening of the deep water circulation.

The FO of *Nitzschia reinholdii* is a secondary stratigraphic marker that is useful in the low-latitude Pacific. Barron (1985a, 1992a) assigned an age of 7.3 Ma for this event, which ought to fall within Zone NPD 7A. From Sites 1016, 1021, and 1022, the sporadic distribution of this species was observed above from Zone NPD 7A, so little can be said about its first occurrence.

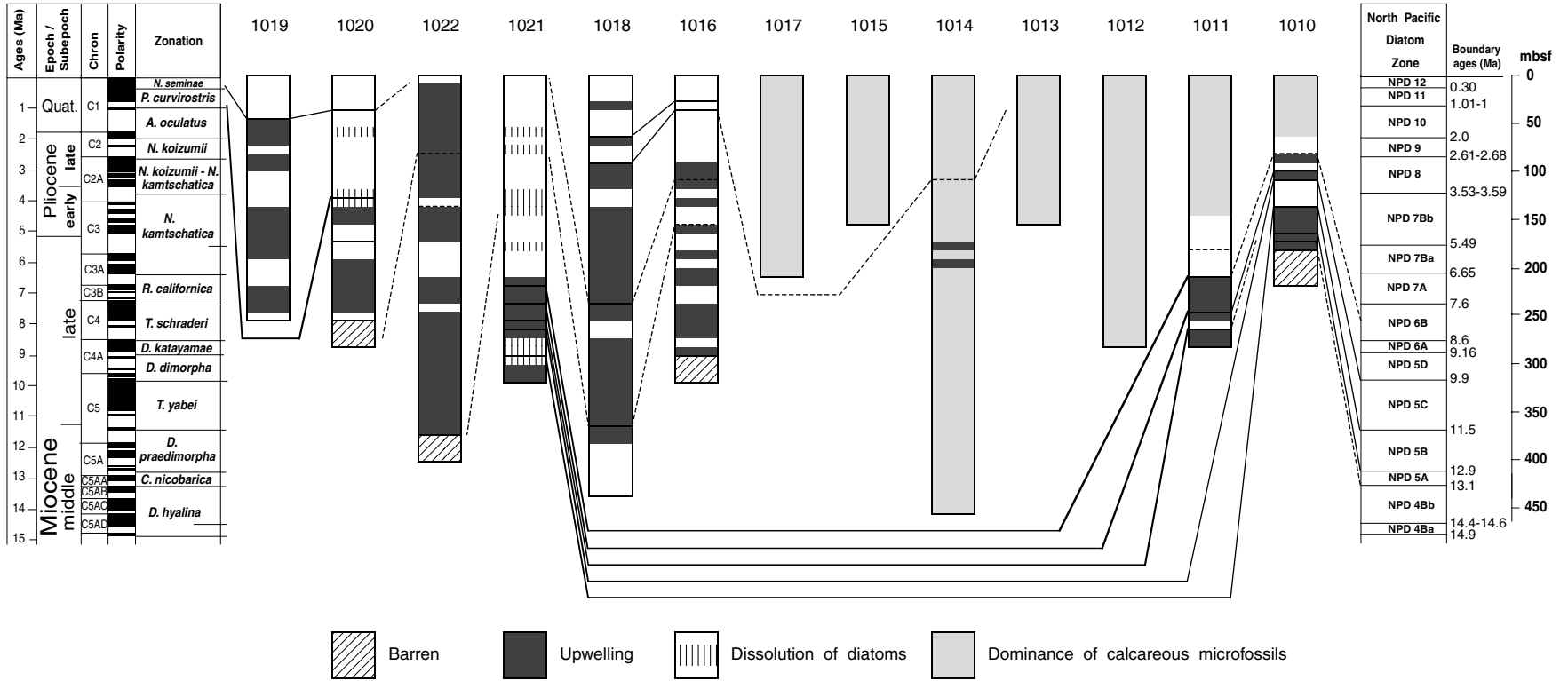


Figure 12. Summary of diatom zonal data for Leg 167.

The FO of the *T. oestrupii* group was observed in Holes 1016A and 1021B. Stratigraphic usefulness of this event was recognized as a secondary zonal marker in the North Pacific. Barron (1981) actually defined a *Thalassiosira oestrupii* Zone, whose base is defined by its FO, estimated at 5.49 Ma. This zone was used for the low- to mid-latitude Pacific, but it is difficult to make the zone up for a standard piece of the North Pacific zonation.

Pliocene and Pleistocene Datum Levels

The following subtropical warm-water, age-diagnostic species are scarce in Leg 167 sediments: *Fragilariopsis doliola*, *Nitzschia reinholdii*, *Rhizosolenia praebergonii*, *Nitzschia jouseae*, and *Thalassiosira miocenica*. Therefore, the subtropical zonation of Baldauf and Iwai (1995) could not be applied to the Pliocene through Pleistocene sediments recovered from the California margin.

Not surprisingly, continuous common occurrences of *Neodenticula kamtschatica*, which characterize the diatom assemblages from topmost Miocene through Pliocene duration, were not found at most sites of Leg 167, according to expectation by previous studies of Barron and Baldauf (1986) and Barron (1989, 1992b). However, the FO of *Neodenticula koizumii* (3.53–3.95 Ma), the FO of *Neodenticula seminae* (2.68 Ma), the LO of *N. kamtschatica* (2.61–2.68 Ma), the LO of *Thalassiosira convexa* (2.35 Ma), the LO of *N. koizumii* (2.0 Ma), the FO of *Fragilariopsis doliola* (2 Ma), the FO of *Proboscia curvirostris* (1.5 Ma), the LO of *Actinocyclus oculatus* (1.01–1.46 Ma), the FO of *Rhizosolenia matuyamai* (0.99–1.14 Ma), the LO of *R. matuyamai* (0.91–1.06 Ma), and the LO of *P. curvirostris* (0.30 Ma) appear to be nearly isochronous along the California margin in Leg 167.

As recognized by Koizumi and Tanimura (1985), the FO of *Neodenticula koizumii* is diachronous across latitude ranging from about 3.95–3.53 Ma. Barron and Gladenkov (1995) regret the widespread use of this datum level in North Pacific diatom stratigraphy where it marks the top of the *N. kamtschatica* Zone (NPD 7) and the base of the overlying *N. koizumii*-*N. kamtschatica* Zone (NPD 8). They hoped accordingly that the FO of *Actinocyclus oculatus* (3.6–4.0 Ma) might prove to be a more reliable stratigraphic marker than the FO of *N. koizumii* in the middle part of the Pliocene north of about 40°N.

Valves of *A. oculatus* are easier to identify at low magnification in the light microscope because of their commonly blue interference colors and distinctive areolar pattern. Similarly, the more robust nature of the valves of *A. oculatus*, compared with those of *N. koizumii*, would suggest that it should be less susceptible to dissolution. However, *A. oculatus* is very sparse and sporadic in Leg 167 sediments, and probably is more common in pelagic regions of the North Pacific and the Bering Sea.

Moreover, Yanagisawa and Akiba (1998) argued that the morphology of *N. koizumii* has given rise to a taxonomic problem between its LO and the FO of *Neodenticula seminae*, defining the top of the *N. koizumii* Zone (NPD 9) and the base of the overlying *A. oculatus* Zone (NPD 10). Koizumi's (1992) proposal to use the LO of *N. koizumii* to mark the top of the *N. koizumii* Zone (NPD 9) appears to be justified in place of the LO of warm-water taxon *Fragilariopsis doliola*. This zonal boundary falls just below the Pliocene/Pleistocene boundary in the mid- to high-latitude North Pacific.

The FO of *Fragilariopsis doliola* is observed from Zone NPD 10 at Sites 1018 and 1020. This event in the low-latitude Pacific has been calibrated with the middle of the Olduvai Subchron and has an age of 1.90 Ma (Baldauf and Iwai, 1995). In addition, it is diachronous between the low and middle latitudes, with age estimates ranging from 1.8 to 2.0 Ma in the northwest Pacific (Koizumi and Tanimura, 1985). The FO of *F. doliola* is slightly younger than the base of Zone NPD 10 estimated at 1.9 Ma in Leg 167.

It also should be emphasized that *N. kamtschatica* can be very sparse and sporadic in Leg 167 sediments, so that recognition of its LO at about 2.6 Ma may be very difficult to verify the boundary be-

tween Zones NPD 8/9. The LO of *Thalassiosira convexa* correlates to an interval directly above Chron 2An and has an estimated age of 2.35 Ma in the equatorial Pacific (Baldauf and Iwai, 1995). This event also was recognized at Sites 1014, 1018, 1020, and 1022 along the California margin, but a poor magnetic record prohibited age estimates.

All of these results uphold the insistence of Baldauf and Iwai (1995) and Barron and Gladenkov (1995) that quantitative studies accompanied by paleomagnetostatigraphy are necessary to adequately resolve age estimates of the Pliocene and Pleistocene diatom datum levels in the North Pacific.

Interval of Poor Diatom Preservation

In present-day waters off California, diatoms owe their abundance to coastal upwelling of nutrient-rich waters, which is driven by the persistent southward winds that are associated with the southward-flowing California Current. Slackening of the California Current during El Niño periods results in a diminished southerly current, decreased upwelling, and diminished diatom production. Because the preservation and abundance of diatoms in sediments is directly related to their abundance in the overlying surface waters, a decline in spring diatom productivity caused by a slackening of the California Current would result in a decreased diatom sedimentation rate and in a decline in diatom preservation in seafloor sediments. Consequently, we can trust that intervals of poor diatom preservation in pelagic sediments off California would correspond to a slackening of the southward flow of the California Current.

An interval of poor diatom preservation, containing only rare, poorly preserved diatoms, is present throughout much of the latest Miocene through Pliocene prior to Zone NPD 10 (2.6 Ma) at Leg 167 sites off California (Figs. 3–6, 12). Diatom stratigraphy reveals the diatomaceous interval from middle to late Miocene, but in the overlying units diatoms quickly disappear upsection as the terrigenous component increases at typically 7.0 Ma. Similarly, the early Pliocene diatom record of California is very poorly known due to increased terrigenous dilution in onshore sections, the widespread presence of hiatuses or condensed intervals in both onshore and offshore sections, and the pervasive appearance of dissolution in sequences south of about 40°N.

Barron (1981, 1992b) interpreted that this diatom-poor interval, mainly a dissolution interval, coincides with a period of high-latitude warming or deglaciation and it is taken as evidence of decreased southerly flow of the California Current and a reduction in upwelling off California during the middle part of the Pliocene. He also inferred that the intervals of diatom dissolution correspond to August sea-surface temperatures in excess of about 17°C.

This interval of poor diatom preservation is obviously detected at Sites 1010, 1011, 1014, 1018, and 1021, indicating stagnation of the mid-latitude surface waters (Figs. 3, 4, 12). At Sites 1010 and 1011 off southern California, poor diatom preservation begins between Zones NPD 6B and 7A, where it is estimated at ~7 Ma. Likewise, at the northern Site 1021 the beginning of the poor diatom preservation can be identified between Zones NPD 7A and 7B. Presumably, both rapid progress of cooling, symbolized by a global fall in sea level, and successive warming caused a decline in diatom abundance in the surface waters above Sites 1010, 1011, and 1021 and resulted in poor diatom preservation.

Dissolution of diatom assemblages is typical in the early Pliocene and early part of the late Pliocene, indicating a marked decline in the production of diatoms in surface waters. The onset of diatom dissolution at Sites 1021 off northern California at the Miocene/Pliocene boundary perhaps within Zone NPD 7B coincides with the start of a global fall in sea level in the period of major cooling.

The northward flow of the warm waters along the western Pacific rim might be so extremely weakened that the clockwise circulation pattern passing across the mid-latitude North Pacific declines abruptly

at the same time. Relatively warmer waters originating from equatorial waters accumulated off central North America accordingly, and these stagnant waters also screened out the California margin from a direct supply of cold waters from the counterclockwise circulation in the Gulf of Alaska. The southward flow of the California Current probably slackened at this time, resulting in reduced coastal upwelling and diatom blooms in offshore areas.

Nevertheless, abundant diatoms persisted in the deeper Site 1016 (distance of 148 km from shore, water depth 3846 m) in the central California region as well as at the more northerly Site 1022 (distance of 87 km from shore, water depth 1927 m). A reduction in upwelling off California during the middle part of the Pliocene had less effect on Sites 1016 and 1022 (Figs. 7, 9, 11, 12).

The onset of poor diatom preservation at nearshore southern Sites 1010 and 1011 in the latest Miocene may signal a generalized narrowing of the entire California Current system rather than further high-latitude warming. Diatom production probably continued in these coastal waters, but diatom sedimentation was almost completely masked by the clay-rich clastics from the California Borderland (Fig. 7).

Well-preserved diatoms did not return to Sites 1016, 1018, 1020, and 1022 until 2.6 Ma, almost corresponding to the NPD 8/9 boundary. At Site 1018 off central California, the interval of poor diatom preservation immediately before 2.6 Ma may indicate a generalized narrowing of the California Current rather than further high-latitude warming, because diatoms also disappear from Sites 1010 and 1011 off southern California at this same time and do not appear again in younger sediments (Figs. 3, 4, 5, 12). Off central to northern California common-to-abundant distribution of such dissolution-resistant taxa as *Coscinodiscus marginatus* and *Stephanopyxis* spp. were consistently recorded at Sites 1018 through 1022 during the late Pliocene Zone NPD 8 to the Pleistocene Zone NPD 11, and especially the late Pliocene duration from Zones NPD 8 to NPD 9 (Figs. 8, 10).

The warm waters (Kuroshio Current) come into collision toward the front of the cold-water mass (Oyashio Current) with low rapidity in the northwest Pacific off Japan, and then change their flow direction to the east. In contrast, in the northeastern Pacific somewhat warm waters crossing the middle latitudes flow abreast with the cold waters driven from the Gulf of Alaska, and then drifted toward the south from offshore Oregon. The weaker the power of traversing waters, the less able the California Current is to flow to the south. Accordingly, paleoceanographic provincialism expands greatly between the California margin and the high-latitude northeastern Pacific. In present-day oceanography off California, current waters come from the mid-latitude North Pacific, except in summer, when fleet waters originating from the Gulf of Alaska directly invade along the California margin.

Reduced upwelling with resultant decreased diatom productivity is a possible explanation for the scarcity of diatoms within the middle part of the Pliocene Epoch off California. The interval of poor diatom preservation fairly corresponds to the duration from Event C to Event D of Barron (1998). He explained that the Event C at about 4.5 Ma is characterized by the onset of a period of sustained high-latitude warming that lasted at least 1 m.y. Diatom sedimentation rates increased at higher latitudes of the northwest Pacific, whereas they declined off northeast Japan and were apparently waning off California. During this climatically warm period, large quantities of relatively warm, saline surface waters penetrated further to the north (Barron, 1995, 1998).

Sancetta and Silvestri (1986) maintained that the modern subarctic water mass did not exist in the western Pacific, but a broad transition zone between warmer and cooler waters was present in the North Pacific, with a northern margin north of 48°N and a southern margin south of 41°N. Such a broad transition zone would have resulted in a northward spread of relatively warm, salty surface waters, which would lead to enhanced evaporation at the surface, to decreased vertical stratification of the water mass, and to an increased upward dif-

fusion of nutrient-rich deep waters, and accordingly fueled diatom production. Based on the diatom paleoclimatic ratios from the middle part of the Pliocene, Barron (1995) reconstructs warmer sea-surface temperatures distributed in the broad transition zone of the northwest Pacific.

On the other hand, the apparent decline in diatom productivity in middle latitude regions, such as the California margin and the coasts of Japan, indicates a reduced pole-to-equator thermal gradient resulting in a slackening of offshore winds and reduced upwelling. Based on the modern distribution of diatoms, it appears that the offshore intervals of diatom scarcity coincided with August sea-surface temperature of more than 17°C (Barron, 1992b). The onset of a period of climatically warmer high-latitude paleotemperatures and paleoceanographic circulation changes appears to link with a shoaling of the Isthmus of Panama, which may have induced major changes in diatom sedimentation in the Pacific at about 4.5 Ma.

At Event D of Barron (1998) after 2.7 Ma, diatom accumulation rates sharply declined at the higher latitudes of the North Pacific, coincident with a major increase in ice-rafted detritus and the onset of Northern Hemisphere glaciation. Increased vertical stratification of water masses resulted in a slackening in the upwelling of nutrient-rich deep waters in the northwest Pacific, and high diatom productivity probably shifted more toward the coasts of Asia and North America. Increased offshore winds appear to have enhanced upwelling and renewed diatom productivity off the coast of California at about the same time (Barron, 1981, 1992b). A true increase in diatom accumulation off California at about 2.7 Ma is suggested by the replacement of dissolved diatoms by well-preserved diatom assemblages at this time at DSDP Sites 467 and 469 as well as ODP Sites 1016, 1018, 1020, and 1022. Probably, this preservational change reflects enhanced diatom productivity due to an increase in zonal winds driving the upwelling along the California margin (Barron, 1981, 1992b, 1998).

Because the Isthmus of Panama apparently had completely emerged by 2.7 Ma, Event D in the high-latitude North Pacific was not directly related to the closure of the Central American Seaway. Rather, Barron (1998) indicates that major reorganization of surface- and intermediate-water masses at about 2.7 Ma would be the presumable trigger of contemporaneous changes in diatom sedimentation patterns that are documented in the North Pacific.

SUMMARY

Ocean-floor coring during Leg 167 provided a unique opportunity to examine the diatom assemblages from numerous near-continuous stratigraphic sequences from the California margin. Valuable middle Miocene through Pleistocene reference sections show that the standard diatom zonation of Yanagisawa and Akiba (1998) is of great use for North Pacific diatom biostratigraphy. When compared with one another and with published data, most of those middle through late Miocene diatom datum levels that have been widely used in the North Pacific for biostratigraphy appear to be isochronous within the level of resolution constrained by sample spacing. Reliable Miocene diatom datum levels in the North Pacific include the FCO of *D. simonsenii* (13.1 Ma), the FO of *D. praedimorpha* (12.9 Ma), the LCO of *D. praedimorpha* (11.5 Ma), the FO of *D. dimorpha* (9.9 Ma), the FO of *Thalassionema schraderi* (9.5 Ma), the LO of *D. dimorpha* (9.16 Ma), the LCO of *D. simonsenii* (8.6 Ma), both the FCO and LCO of *T. schraderi* (7.6 Ma), the LO of *Cavitatus jouseanus* (6.7–6.8 Ma), the LCO of *Rouxia californica* (6.65 Ma), the FCO of *Neodenticula kamtschatica* (6.4 Ma), and the FO of *T. oestrupii* (5.49 Ma).

Within the Pliocene, there is nothing more reliable among datum levels along the California margin covered by Leg 167. The somewhat inconstant occurrence of *Neodenticula kamtschatica* in Leg 167 samples precluded the authorization of the *N. kamtschatica* Zone (NPD 7B). Pliocene diatom assemblages in the California Current

basin are intermediate between those of subarctic and subtropical areas. Consequently, neither the present tropical nor the subarctic (high latitude) zonal schemes were applicable for this region.

At least 31 of the middle Miocene through Pleistocene diatom datum levels allow precise correlation along the length of the present-day California Current from Sites 1010 (30°N) to 1022 (40°N). The FO of *Proboscia barboi* (12.3 Ma) as a widely used Miocene diatom datum, however, is diachronous across latitude in the North Pacific. Within the Pliocene through Pleistocene, diachroneity is also documented for the FO of *Neodenticula koizumii* (3.53–3.95 Ma) and the LO of *Actinocyclus oculatus* (1.01–1.46 Ma).

A brief warming trend probably occurred between about 13.1 and 12.0 Ma in the area, as evidenced by the occurrence of relatively common warm-water taxa during this interval at Site 1010 (30°N) and Site 1022 (40°N). In addition, decreased diatom productivity along the California margin during most of the early Pliocene (~5.5–2.6 Ma) most likely reflects slackening of the California Current during a period of relative climatic warming. At Sites 1016, 1018, 1020, and 1022 off central-to-northern California, abundant and well-preserved diatoms returned at about 2.6 Ma near the base of Zone NPD 9, coincident with major cooling of high-latitude surface waters.

ACKNOWLEDGMENTS

I am grateful to John A. Barron, Itaru Koizumi, and Lona Dearmont for their critical reviews and suggestions for improving the manuscript. Funding for the research was partly supplied by the Grant-in-Aid for Scientific Research of the Ministry of Education, Science and Culture of Japan, No. 07640618, provided to T. Maruyama. I thank Mitch Lyle, Carl Richter, and the scientists and crew members of Leg 167 of the *JOIDES Resolution* for their support and encouragement.

REFERENCES

- Akiba, F., 1977. *Denticula kanayae* n. sp., and the diatom biostratigraphic significance of the *Denticula kanayae* Zone. *Bull. Tech. Lab. JAPEX*, 20:126–142. (in Japanese)
- , 1979. The morphology of *Denticula dimorpha* and its related species, and the Neogene diatom biostratigraphy of Japan. *Bull. Tech. Lab. JAPEX*, 22:9–55. (in Japanese)
- , 1982a. Late Quaternary diatom biostratigraphy of the Bellinghousen Sea, Antarctic Ocean. *Rep. Tech. Res. Cen. J.N.O.C.*, 16:31–74.
- , 1982b. Taxonomy and biostratigraphic significance of a new diatom, *Thalassionema schraderi*. *Bacillaria*, 5:43–61.
- , 1983. Revised Neogene diatom biostratigraphic zonation for middle-to-high latitudes of the North Pacific: evaluation of datum planes and age. *Gekkan Kaiyokagaku [Monthly Mar. Sci.]*, 15:717–725. (in Japanese)
- , 1986. Middle Miocene to Quaternary diatom biostratigraphy in the Nankai trough and Japan trench, and modified lower Miocene through Quaternary diatom zones for middle-to-high latitudes of the North Pacific. In Kagami, H., Karig, D.E., Coulbourn, W.T., et al., *Init. Repts. DSDP*, 87: Washington (U.S. Govt. Printing Office), 393–481.
- Akiba, F., Hiramatsu, C., and Yanagisawa, Y., 1993. A Cenozoic diatom genus *Cavitatus* Williams; an emended description and two new biostratigraphically useful species, *C. lanceolatus* and *C. rectus* from Japan. *Bull. Nat. Sci. Mus. Ser. C: Geol. Paleontol. (Tokyo)*, 19:11–39.
- Akiba, F., Hoshi, K., and Ichinoseki, T., 1982. Litho- and biostratigraphy of the Miocene Atsunai Group distributed in the southwestern part of the Kushiro Coal Field, eastern Hokkaido. *Bull. Tech. Lab. JAPEX*, 25:13–52. (in Japanese with English abstract)
- Akiba, F., and Ichinoseki, T., 1983. The Neogene micro- and chronostratigraphies in Hokkaido: special reference to those of the southwestern part of the Kushiro Coal Field area, eastern Hokkaido, Japan. *J. Jpn. Assoc. Pet. Tech.*, 48:49–61. (in Japanese with English abstract)
- Akiba, F., and Yanagisawa, Y., 1986. Taxonomy, morphology and phylogeny of the Neogene diatom zonal marker species in the middle-to-high latitudes of the North Pacific. In Kagami, H., Karig, D.E., Coulbourn, W.T., et al., *Init. Repts. DSDP*, 87: Washington (U.S. Govt. Printing Office), 483–554.
- Akiba, F., Yanagisawa, Y., and Ishi, T., 1982. Neogene diatom biostratigraphy of the Matsushima Area and its environs, Miyagi Prefecture, Northeast Japan. *Bull. Geol. Soc. Jpn.*, 33:215–239. (in Japanese with English abstract)
- Andrews, G.W., 1973. Systematic position and stratigraphic significance of the marine Miocene diatom *Raphidodiscus marylandicus* Christian. *Nova Hedwigia Beih.*, 45:231–250.
- , 1976. Miocene marine diatoms from the Choptank Formation, Calvert County, Maryland. *Geol. Surv. Prof. Pap U.S.*, 910:1–26.
- Baksi, A.K., 1993. A geomagnetic polarity time scale for the period 0–17 Ma, based on ⁴⁰Ar/³⁹Ar plateau ages for selected field reversals. *Geophys. Res. Lett.*, 20:1607–1610.
- Baldauf, J.G., and Barron, J.A., 1980. *Actinocyclus ingens* var. *nodus*: a new, stratigraphically useful diatom of the circum-North Pacific. *Micropaleontology*, 26:103–110.
- Baldauf, J.G., and Iwai, M., 1995. Neogene diatom biostratigraphy for the eastern equatorial Pacific Ocean, Leg 138. In Piasis, N.G., Mayer, L.A., Janecek, T.R., Palmer-Julson, A., and van Andel, T.H. (Eds.), *Proc. ODP, Sci. Results*, 138: College Station, TX (Ocean Drilling Program), 105–128.
- Barron, J.A., 1980a. Lower Miocene to Quaternary diatom biostratigraphy of Leg 57, off Northeastern Japan, Deep Sea Drilling Project. In von Huene, R., Nasu, N., et al., *Init. Repts. DSDP*, 56, 57 (Pt. 2): Washington (U.S. Govt. Printing Office), 641–685.
- , 1980b. Upper Pliocene and Quaternary diatom biostratigraphy of Deep Sea Drilling Project Leg 54, tropical eastern Pacific. In Rosendahl, B.R., Hekinian, R., et al., *Init. Repts. DSDP*, 54: Washington (U.S. Govt. Printing Office), 455–485.
- , 1981. Late Cenozoic diatom biostratigraphy and paleoceanography of the middle-latitude eastern North Pacific, Deep Sea Drilling Project Leg 63. In Yeats, R.S., Haq, B.U., et al., *Init. Repts. DSDP*, 63: Washington (U.S. Govt. Printing Office), 507–538.
- , 1983. Latest Oligocene through early middle Miocene diatom biostratigraphy of the eastern tropical Pacific. *Mar. Micropaleontol.*, 7:487–515.
- , 1985a. Late Eocene to Holocene diatom biostratigraphy of the equatorial Pacific Ocean, Deep Sea Drilling Project Leg 85. In Mayer, L., Theyer, F., Thomas, E., et al., *Init. Repts. DSDP*, 85: Washington (U.S. Govt. Printing Office), 413–456.
- , 1985b. Miocene to Holocene planktic diatoms. In Bolli, H.M., Saunders, J.B., and Perch-Nielsen, K. (Eds.), *Plankton Stratigraphy*: Cambridge (Cambridge Univ. Press), 763–809.
- , 1989. The late Cenozoic stratigraphic record and hiatuses of the northeast Pacific: results from the Deep Sea Drilling Project. In Winterer, E.L., Hussong, D.M., and Decker, R.W. (Eds.), *The Geology of North America (Vol. N): The Eastern Pacific Ocean and Hawaii*. Geol. Soc. Am., Geol. of North America Ser., 311–322.
- , 1992a. Neogene diatom datum levels in the equatorial and North Pacific. In Ishizaki, K., and Saito, T. (Eds.), *The Centenary of Japanese Micropaleontology*: Tokyo (Terra Sci. Publ.), 413–425.
- , 1992b. Paleooceanographic and tectonic controls on the Pliocene diatom record of California. In Tsuchi, R., and Ingle, J.C., Jr. (Eds.), *Pacific Neogene: Environment, Evolution, and Events*: Tokyo (Tokyo Univ. Press), 25–41.
- , 1995. High-resolution diatom paleoclimatology of the middle part of the Pliocene of the Northwest Pacific. In Rea, D.K., Basov, I.A., Scholl, D.W., and Allan, J.F. (Eds.), *Proc. ODP, Sci. Results*, 145: College Station, TX (Ocean Drilling Program), 43–53.
- , 1998. Late Neogene changes in diatom sedimentation in the North Pacific. *J. Asian Earth Sci.*, 16:85–95.
- Barron, J.A., and Baldauf, J.G., 1986. Diatom stratigraphy of the lower Pliocene part of the Sisquoc Formation, Harris Grade section, California. *Micropaleontology*, 32:357–371.
- , 1995. Cenozoic marine diatom biostratigraphy and applications to paleoclimatology and paleoceanography. In Blome, C.D., et al. (Eds.), *Siliceous Microfossils*. Paleontol. Soc. Short Courses Paleontol., 8:107–118.
- Barron, J.A., and Gladenkov, A.Y., 1995. Early Miocene to Pleistocene diatom stratigraphy of Leg 145. In Rea, D.K., Basov, I.A., Scholl, D.W., and Allan, J.F. (Eds.), *Proc. ODP, Sci. Results*, 145: College Station, TX (Ocean Drilling Program), 3–19.

- Berggren, W.A., Hilgen, F.J., Langereis, C.G., Kent, D.V., Obradovich, J.D., Raffi, I., Raymo, M.E., and Shackleton, N.J., 1995a. Late Neogene chronology: new perspectives in high-resolution stratigraphy. *Geol. Soc. Am. Bull.*, 107:1272–1287.
- Berggren, W.A., Kent, D.V., and Flynn, J.J., 1985a. Jurassic to Paleogene, Part 2. Paleogene geochronology and chronostratigraphy. In Snelling, N.J. (Ed.), *The Chronology of the Geological Record*. Geol. Soc. London Mem., 10:141–195.
- Berggren, W.A., Kent, D.V., Flynn, J.J., and van Couvering, J.A., 1985b. Cenozoic geochronology. *Geol. Soc. Am. Bull.*, 96:1407–1418.
- Berggren, W.A., Kent, D.V., Swisher, C.C., III, and Aubry, M.-P., 1995b. A revised Cenozoic geochronology and chronostratigraphy. In Berggren, W.A., Kent, D.V., Aubry, M.-P., and Hardenbol, J. (Eds.), *Geochronology, Time Scales and Global Stratigraphic Correlation*. Spec. Publ.—Soc. Econ. Paleontol. Mineral. (Soc. Sediment. Geol.), 54:129–212.
- Berggren, W.A., Kent, D.V., and Van Couvering, J.A., 1985c. The Neogene, Part 2. Neogene geochronology and chronostratigraphy. In Snelling, N.J. (Ed.), *The Chronology of the Geological Record*. Geol. Soc. London Mem., 10:211–260.
- Bodén, P., 1993. Taxonomy and stratigraphic occurrence of *Thalassiosira tetraoestrupii* sp. nov., and related species in upper Miocene and lower Pliocene sediments from the Norwegian Sea, North Atlantic and north-west Pacific. *Terra Nova*, 5:61–75.
- Brun, J., and Tempère, J., 1889. Diatomees Fossiles du Japon, especes marines et nouvelles des calcaires argileux des Sendai et de Yedo. *Soc. Phys. Hist. Geneve Mem.*, 30:1–75.
- Burckle, L.H., 1972. Late Cenozoic planktonic diatom zones from the eastern equatorial Pacific. In Simonsen, R. (Ed.), *First Symposium on Recent and Fossil Marine Diatoms. Nova Hedwigia Beih.*, 39:217–246.
- Burckle, L.H., Hammond, S.R., and Seyb, S.M., 1978. A stratigraphically important new diatom from the Pleistocene of the North Pacific. *Pacific Sci.*, 32:209–214.
- Burckle, L.H., and Opdyke, N.D., 1977. Late Neogene diatom correlations in the Circum-Pacific. In Ujiie, H., and Saito, T. (Eds.), *Proc. 1st Int. Congr. Pac. Neogene Stratigr.*: Tokyo (Kaiyo Shuppan), 255–284.
- , 1985. Latest Miocene/earliest Pliocene diatom correlation in the north Pacific. *Mem.—Geol. Soc. Am.*, 163:37–48.
- Burckle, L.H., Struz, A., and Emanuele, G., 1992. Dissolution and preservation of diatoms in the Sea of Japan and the effect on sediment thanatocoenosis. In Pisciotto, K.A., Ingle, J.C., Jr., von Breymann, M.T., Barron, J., et al., *Proc. ODP, Sci. Results*, 127/128 (Pt. 1): College Station, TX (Ocean Drilling Program), 309–316.
- Cande, S.C., and Kent, D.V., 1992. A new geomagnetic polarity time scale for the Late Cretaceous and Cenozoic. *J. Geophys. Res.*, 97:13917–13951.
- , 1995. Revised calibration of the geomagnetic polarity timescale for the Late Cretaceous and Cenozoic. *J. Geophys. Res.*, 100:6093–6095.
- Cleve-Euler, A., 1951–1955. Die Diatomeen von Schweden und Finnland. *K. Sven. Vetenskaps. Handl.*, Bd. 2, Teil 1: 1–163 (1951); Bd. 3, Teil 5: 1–153 (1952); Bd. 4, Teil 2: 1–158 (1953); Bd. 4, Teil 3: 1–255 (1953); Bd. 5, Teil 4: 1–232 (1955).
- Donahue, J.G., 1970. Pleistocene diatoms as climatic indicators in North Pacific sediments. In Hays, J.D. (Ed.), *Geological Investigations of the North Pacific*. Mem.—Geol. Soc. Am., 126:121–138.
- Fenner, J., Schrader, H.-J., and Wienigk, H., 1976. Diatom phytoplankton studies in the southern Pacific Ocean, composition and correlation to the Antarctic Convergence and its paleoecological significance. In Hollister, C.D., Craddock, C., et al., *Init. Repts. DSDP*, 35: Washington (U.S. Govt. Printing Office), 757–813.
- Fenner, J.M., 1991. Late Pliocene-Quaternary quantitative diatom stratigraphy in the Atlantic sector of the Southern Ocean. In Ciesielski, P.F., Kristoffersen, Y., et al., *Proc. ODP, Sci. Results*, 114: College Station, TX (Ocean Drilling Program), 97–121.
- Fryxell, G.A., and Hasle, G.R., 1972. *Thalassiosira eccentrica* (Ehrenberg) Cleve, *T. symmetrica* sp. nov., and some related centric diatoms. *J. Phycol.*, 8:297–317.
- Fryxell, G.A., Sims, P.A., and Watkins, T.P., 1986. *Azpeitia* (Bacillariophyceae): related genera and promorphology. *Syst. Bot. Monogr.*, 13:1–74.
- Gladkov, A.Y., and Barron, J.A., 1995. Oligocene and early middle Miocene diatom biostratigraphy of Hole 884B. In Rea, D.K., Basov, I.A., Scholl, D.W., and Allan, J.F. (Eds.), *Proc. ODP, Sci. Results*, 145: College Station, TX (Ocean Drilling Program), 21–41.
- Hanna, G.D., 1930. A revision of genus *Rouxia*. *J. Paleontol.*, 4:179–188.
- Harwood, D.M., and Maruyama, T., 1992. Middle Eocene to Pleistocene diatom biostratigraphy of Southern Ocean sediments from the Kerguelen Plateau, Leg 120. In Wise, S.W. Jr., Schlich, R., et al., *Proc. ODP, Sci. Results*, 120: College Station, TX (Ocean Drilling Program), 683–733.
- Hasle, G.R., and Fryxell, G.A., 1977. The genus *Thalassiosira*: some species with a linear areola array. *Nova Hedwigia Beih.*, 54:15–66.
- Heiden, H., and Kolbe, R.W., 1928. Die marinen Diatomeen der Deutschen Südpolar-Expedition 1901–1903. In von Drygalski, E. (Ed.), *Deutsche Südpolar-Expedition, 1901–1903* (Vol. 8): *Botanik*: Berlin (Walter de Gruyter), 447–715.
- Hemphill-Haley, E., and Fourtanier, E., 1995. A diatom record spanning 114,000 years from Site 893, Santa Barbara Basin. In Kennett, J.P., Baldauf, J.G., and Lyle, M. (Eds.), *Proc. ODP, Sci. Results*, 146 (Pt. 2): College Station, TX (Ocean Drilling Program), 233–249.
- Hendey, N.I., 1964. *An Introductory Account of the Smaller Algae of British Coastal Waters*. Fishery Investigations, Ser. 4, Pt. 5: *Bacillariophyceae (Diatoms)*: Koenigstein (Koeltz Scientific Books).
- Hustedt, F., 1927–1966. Die Kieselalgen Deutschland, Osrerreichs und der Schweiz unter Berücksichtigung der übrigen Länder Europas sowie der angrenzen zenden Meeresgebiete. In Rabenhorst, L. (Ed.), *Kryptogamen-Flora von Deutschland, Österreich und der Schweiz*: Teil 1, 1–272 (1927); Sect. 2. 273–464 (1928); Sect. 3, 465–608 (1929); Sect. 4, 609–784 (1930); Sect. 5, 785–920 (1930); Teil 2, Sect. 1. 1–176 (1931); Sect. 2, 177–320 (1932); Sect. 3, 321–432 (1933); Sect. 4, 433–576 (1933); Sect. 5, 577–736 (1937); Sect. 6, 737–845 (1959); Teil 3, Sect. 1, 1–160 (1961); Sect. 2. 161–348 (1962); Sect. 3, 349–556 (1964); Sect. 4, 557–816 (1966).
- , 1930. Bacillariophyta (Diatomeae). In Pascher, A. (Ed.), *Die Süswasser-Flora Mitteleuropas*: Jena (Gustav Fisher), 10:1–466.
- Jordan, R.W., and Priddle, J., 1991. Fossil members of the diatom genus *Probooscia*. *Diatom Res.*, 6:55–61.
- Jousé, A.P., 1961. Miocene and Pliocene marine diatoms from the Far East. *Bot. Mater. Spor. Rast., Bot. Inst., Akad. Nauk SSSR*, 16:59–70.
- , 1968. New species of diatoms in bottom sediment of the Pacific and the Sea of Okhotsk. *Nov. System. Plant. non Vascular 1965, Akad. Nauk SSSR*, 3:12–21.
- Kanaya, T., 1959. Miocene diatom assemblages from the Onnagawa Formation and their distribution in correlative formations in northeast Japan. *Sci. Rep. Tohoku Univ.*, Ser. 2, 30:1–130.
- Keller, G., and Barron, J.A., 1987. Paleodepth distribution of Neogene deep-sea hiatuses. *Paleoceanography*, 2:697–713.
- Koizumi, I., 1973a. The late Cenozoic diatoms of Sites 183–193, Leg 19 Deep Sea Drilling Project. In Creager, J.S., Scholl, D.W., et al., *Init. Repts. DSDP*, 19: Washington (U.S. Govt. Printing Office), 805–855.
- , 1973b. The stratigraphic ranges of marine planktonic diatoms and diatom biostratigraphy in Japan. *Mem. Geol. Soc. Jpn.*, 8:35–44.
- , 1975a. Diatom events in late Cenozoic deep-sea sequences in the North Pacific. *J. Geol. Soc. Jpn.*, 81:567–578.
- , 1975b. Late Cenozoic diatom biostratigraphy in the circum-North Pacific region. *J. Geol. Soc. Jpn.*, 81:611–627.
- , 1975c. Neogene diatoms from the northwestern Pacific Ocean, Deep Sea Drilling Project. In Larson, R.L., Moberly, R., et al., *Init. Repts. DSDP*, 32: Washington (U.S. Govt. Printing Office), 865–889.
- , 1975d. Neogene diatoms from the western margin of the Pacific Ocean Leg 31, Deep Sea Drilling Project. In Karig, D.E., Ingle, J.C., Jr., et al., *Init. Repts. DSDP*, 31: Washington (U.S. Govt. Printing Office), 779–819.
- , 1977. Diatom biostratigraphy in the North Pacific region. In Ujiie, H., and Saito, T. (Eds.), *Proc. 1st Int. Congr. Pac. Neogene Stratigr.*: Tokyo (Kaiyo Shuppan), 235–253.
- , 1980. Neogene diatoms from the Emperor Seamount Chain, Leg 55, Deep Sea Drilling Project. In Jackson, E.D., Koizumi, I., et al., *Init. Repts. DSDP*, 55: Washington, (U.S. Govt. Printing Office), 387–407.
- , 1985. Diatom biochronology for the Late Cenozoic northwest Pacific. *J. Geol. Soc. Jpn.*, 1:195–211.
- , 1992. Diatom biostratigraphy of the Japan Sea: Leg 127. In Pisciotto, K.A., Ingle, J.C., Jr., von Breymann, M.T., Barron, J., et al., *Proc. ODP, Sci. Results*, 127/128 (Pt. 1): College Station, TX (Ocean Drilling Program), 249–289.
- Koizumi, I., and Kanaya, T., 1976. Late Cenozoic marine diatom sequence from the Choshi district, Pacific coast, central Japan. In Takayanagi, Y., and Saito, T. (Eds.), *Progress in Micropaleontology*: New York (Micropaleontology Press), 144–159.

- Koizumi, I., and Tanimura, Y., 1985. Neogene diatom biostratigraphy of the middle latitude western North Pacific, Deep Sea Drilling Project Leg 86. In Heath, G.R., Burckle, L.H., et al., *Init. Repts. DSDP*, 86: Washington (U.S. Govt. Printing Office), 269–300.
- Koizumi, I., and Yanagisawa, Y., 1990. Evolutionary change in diatom morphology—an example from *Nitzschia fossilis* to *Pseudoenotia doliolus*. *Trans. Proc. Palaeontol. Soc. Jpn., New Ser.*, 157:347–359.
- Kolbe, R.W., 1955. Diatoms from equatorial Atlantic cores. *Rep. Swed. Deep-sea Exped., 1947–1948*, 7:149–184.
- Lohman, K.E., 1938. Pliocene diatoms from the Kettleman Hills, California. *Geol. Surv. Prof. Pap. U.S.*, 189-C:81–102.
- Lyle, M., Koizumi, I., Richter, C., et al., 1997. *Proc. ODP, Init. Repts.*, 167: College Station, TX (Ocean Drilling Program).
- Mammerickx, J., 1989. Bathymetry of the North Pacific Ocean: 3 maps. In Winterer, E.L., Hussong, D.M., and Decker, R.W., (Eds.), *The Eastern Pacific Ocean and Hawaii. The Geology of North America*, Geol. Soc. Am., Geol. of North Am. Ser., N.
- Maruyama, T., 1984a. Miocene diatom biostratigraphy of onshore sequences on the Pacific side of Northeast Japan, with reference to DSDP Hole 438A (Part 1). *Sci. Rep. Tohoku Univ., Ser. 2*, 54:141–164.
- , 1984b. Miocene diatom biostratigraphy of onshore sequences on the Pacific side of Northeast Japan, with reference to DSDP Hole 438A (Part 2). *Sci. Rep. Tohoku Univ., Ser. 2*, 55:77–140.
- , 1992. Diatom biometry of the Miocene index *Denticulopsis hyalina*. In Ishizaki, K., and Saito, T. (Eds.), *Centenary of Japanese Micropaleontology*: Tokyo (Terra Sci. Publ.), 427–437.
- Medlin, L.K., and Sims, P.A., 1993. The transfer of *Pseudoenotia doliolus* to *Fragilariopsis*. *Nova Hedwigia Beih.*, 106:323–334.
- Mertz, D., 1966. Mikropalaeontologische und sedimentologische Untersuchung der Pisco-Formation Suedperu. *Palaeontographica B*, 118:1–48.
- Motoyama, I., and Maruyama, T., 1998. Neogene diatom and radiolarian biochronology for the middle-to-high latitudes of the Northwest Pacific region: calibration to the Cande and Kent's geomagnetic polarity time scales (CK 92 and CK 95). *J. Geol. Soc. Jpn.*, 104:171–183. (in Japanese with English abstract)
- Mukhina, V.U., 1965. New species of diatom from the bottom sediments of the equatorial region of the Pacific. *Nov. System. Plant. non Vascular 1965*, *Akad. Nauk SSSR*, 11:22–25.
- Oreshkina, T.V., 1985. Diatom associations and the stratigraphy of the upper Cenozoic of the Pacific region near Kamchatka. *Izv. Akad. Nauk SSSR, Ser. Geol.*, 5:60–73. (in Russian)
- Poore, R.Z., McDougall, K., Barron, J.A., Brabb, E.E., and Kling, S.A., 1981. Microfossil biostratigraphy and biochronology of the type Relizian and Luisian Stages of California. In Garrison, R.E., Douglas, R.G., Pisciotta, K.E., Isaacs, C.M., and Ingle, J.C. (Eds.), *The Monterey Formation and Related Siliceous Rocks of California*. Proc. SEPM Res. Pacific Sect., Soc. Econ. Paleontol. Mineral., 15–41.
- Rattray, J., 1890. A revision of the genus *Actinocyclus* Ehr. *J. Quekett Microsc. Club, Ser. 2*, 4:137–212.
- Sancetta, C., 1982. Distribution of diatom species in surface sediments of the Bering and Okhotsk Seas. *Micropaleontology*, 28:221–257.
- Sancetta, C., and Silvestri, S., 1986. Pliocene-Pleistocene evolution of the North Pacific Ocean-atmosphere system, interpreted from fossil diatoms. *Paleoceanography*, 1:163–180.
- Schrader, H.-J., 1973a. Cenozoic diatoms from the Northeast Pacific, Leg 18. In Kulm, L.D., von Huene, R., et al., *Init. Repts. DSDP*, 18: Washington (U.S. Govt. Printing Office), 673–797.
- , 1973b. Stratigraphic distribution of marine species of the diatom *Denticula* in Neogene North Pacific sediments. *Micropaleontology*, 19:417–430.
- , 1974. Cenozoic marine planktonic diatom stratigraphy of the tropical Indian Ocean. In Fisher, R.L., Bunce, E.T., et al., *Init. Repts. DSDP*, 24: Washington (U.S. Govt. Printing Office), 887–967.
- Schrader, H.-J., and Fenner, J., 1976. Norwegian Sea Cenozoic diatom biostratigraphy and taxonomy. In Talwani, M., Udintsev, G., et al., *Init. Repts. DSDP*, 38: Washington (U.S. Govt. Printing Office), 921–1099.
- Sheshukova-Porentzkaya, V.S., 1959. On fossil diatom flora of South Sakhaline (Marine Neogene). *Bull. Leningrad Gos. Univ., Biol. Ser.*, 15:36–55. (in Russian with English abstract)
- , 1962. New and rare diatoms from formations of Sakhaline. *Leningrad Gos. Univ., Vest. 313, Biol. Inst. Ser. Biol., Nauk Vup.*, 49:203–211. (in Russian)
- Simonsen, R., 1979. The diatom system: ideas on phylogeny. *Bacillaria*, 2:9–71.
- Simonsen, R., and Kanaya, T., 1961. Notes on the marine species of the diatom genus *Denticula* Kütz. *Int. Rev. Gesamten Hydrobiol.*, 46:498–513.
- Takahashi, K., 1986. Seasonal fluxes of pelagic diatoms in the subarctic Pacific, 1982–1983. *Deep-sea Res.*, 33:1225–1251.
- Tanimura, Y., 1989. *Denticulopsis praehyalina*, sp. nov.: an early Middle Miocene pennate diatom from Dogo, Oki Islands, Southwest Japan. *Trans. Proc. Palaeontol. Soc. Jpn., New Ser.*, 155:169–177.
- , 1996. Fossil marine plicated *Thalassiosira*: taxonomy and an idea on phylogeny. *Diatom Res.*, 11:165–202.
- Watanabe, M., and Takahashi, M., 1997. Diatom biostratigraphy of the Middle Miocene Kinone and lower Amatsu Formations in the Boso Peninsula, central Japan. *J. Jpn. Assoc. Pet. Tech.*, 62:213–225. (in Japanese with English abstract)
- Wei, W., 1995. Revised age calibration points for the geomagnetic polarity time scale. *Geophys. Res. Lett.*, 22:957–960.
- Whiting, M.C., and Schrader, H.-J., 1985. *Actinocyclus ingens* Rattray: reinvestigation of a polymorphic species. *Micropaleontology*, 31:68–75.
- Yanagisawa, Y., 1995. Cenozoic diatom genus *Rossiella* Desikachary et Maheshwari: an emended description. *Trans. Proc. Palaeontol. Soc. Jpn., New Ser.*, 177:1–20.
- , 1996. Diatom biostratigraphy of the Neogene Taga Group in Otsu district, Kitaibaraki City, Ibaraki Prefecture, Japan. *Mem. Nat. Sci. Mus., Tokyo*, 29:41–59. (in Japanese with English abstract)
- Yanagisawa, Y., and Akiba, F., 1990. Taxonomy and phylogeny of the three marine diatom genera, *Crucidentacula*, *Denticulopsis* and *Neodenticula*. *Bull. Geol. Surv. Jpn.*, 41:197–301.
- , 1998. Refined Neogene diatom biostratigraphy for the northwest Pacific around Japan, with an introduction of code numbers for selected diatom biohorizons. *J. Geol. Soc. Jpn.*, 104:395–414.

Date of initial receipt: 13 October 1998

Date of acceptance: 17 June 1999

Ms 167SR-217

APPENDIX

Species List and Taxonomic Remarks

A list of all taxa used in this paper is documented. In general, only a reference to representative illustrations is provided, and the reader is referred to these references for a more precise taxonomic treatment. Original descriptions portrayed through good figures and detailed descriptions of the genera *Denticulopsis*, *Crucidentacula*, and *Neodenticula* are given in Akiba and Yanagisawa (1986) and Yanagisawa and Akiba (1990).

- Actinocyclus curvatulus* Janisch in Schmidt, 1878; Hustedt, 1929, teil 1, p. 538, fig. 307; Koizumi, 1973b, p. 831, pl. 1, figs. 1–6; Sancetta, 1982, p. 222, pl. 1, figs. 1–3.
- Actinocyclus ehrenbergii* Ralfs in Pritchard, 1861; Hustedt, 1929, teil 1, p. 525, fig. 298.
- Actinocyclus ehrenbergii* vars.; Hustedt, 1929, teil 1, p. 528–533, figs. 299–302.
- Actinocyclus ellipticus* Grunow in Van Heurck, 1881; Hustedt, 1929, teil 1, p. 533, fig. 303; Akiba, 1986, pl. 16, fig. 5.
- Actinocyclus ellipticus* f. *elongatus* (Grunow) Kolbe, 1955, p. 20, pl. 3, figs. 28, 31; Koizumi, 1980, pl. 1, fig. 21; Akiba, 1986, pl. 16, fig. 11.
- Actinocyclus ellipticus* var. *javanica* Reinhold, 1937; Barron, 1985a, pl. 7, fig. 12.
- Actinocyclus ellipticus* f. *lanceolata* Kolbe, 1955, p. 20, pl. 3, figs. 27; Koizumi, 1980, pl. 1, fig. 20; Akiba, 1986, pl. 16, fig. 10.
- Actinocyclus ingens* Rattray, 1890, p. 149, pl. 11, fig. 7; Koizumi, 1973b, p. 831, pl. 1, figs. 13–14, pl. 2, figs. 1–2.
- Remarks:** The species concept mainly includes *Actinocyclus ingens* f. *planus* Whiting and Schrader, 1985, p. 74, pl. 3, fig. 12.
- Actinocyclus ingens* f. *ingens* (Rattray) Whiting and Schrader, 1985, p. 74, pl. 1, fig. 1–2, pl. 2, figs. 4–10, pl. 3, fig. 13.
- Actinocyclus ingens* f. *nodus* (Baldauf) Whiting and Schrader, 1985, p. 74, pl. 1, fig. 3, pl. 2, fig. 11, pl. 3, fig. 14; as *Actinocyclus ingens* var. *nodus* Baldauf in Baldauf and Barron, 1980, p. 104, pl. 1, figs. 5–9.
- Actinocyclus ochotensis* Jousé, 1968, p. 17, pl. 2, figs. 2–5; Koizumi, 1973b, p. 831, pl. 2, figs. 3–7.
- Actinocyclus oculatus* Jousé, 1968, p. 18, pl. 2, figs. 6–7; Koizumi, 1973b, p. 831, pl. 2, figs. 8–9; Barron, 1980a, pl. 5, figs. 1, 3.
- Actinocyclus tenellus* (Jørgensen) Andrews, 1976, p. 14, pl. 3, figs. 8–9; as *Actinocyclus ehrenbergii* var. *tenella* (Jørgensen) Hustedt, 1929, teil 1, p. 530, figs. 302.
- Actinocyclus tsugaruensis* Kanaya, 1959, p. 99, pl. 8, figs. 5–8.
- Actinoptychus senarius* (Ehrenberg) Ehrenberg, 1843; Sancetta, 1982, p. 225, pl. 1, fig. 7; Akiba, 1986, p. 447, pl. 29, fig. 2.
- Actinoptychus splendens* (Shadbolt) Ralfs in Pritschard, 1861; Hustedt, 1929, teil 1, p. 478, fig. 265.
- Annellus californicus* Tempère in Tempère and Peragallo, 1908, p. 60; Barron, 1981, pls. 6–7, all figs.; Barron, 1985b, p. 780, figs. 12.8, 12.11.
- Asteromphalus robustus* Castracane, 1875; Hustedt, 1929, teil 1, p. 496, fig. 278; Koizumi, 1975b, pl. 3, fig. 5.
- Aulacoseira granulata* (Ehrenberg) Simonsen, 1979, p. 58; as *Melosira granulata* (Ehrenberg) Ralfs, Hustedt, 1927, teil 1, p. 248, fig. 104.
- Aulacoseira italica* (Ehrenberg) Simonsen, 1979, p. 60; as *Melosira italica* (Ehrenberg) Kützing, Hustedt, 1927, teil 1, p. 257, fig. 109.
- Azpeitia endoi* (Kanaya) P. A. Sims and G. Fryxell in Fryxell et al., 1986, p. 16, as *Coscinodiscus endoi* Kanaya, Koizumi and Tanimura, 1985, pl. 4, fig. 12.
- Azpeitia nodulifera* (Schmidt) G. Fryxell and P. A. Sims in Fryxell et al., 1986, p. 19, fig. 17; as *Coscinodiscus nodulifer* Schmidt; Akiba, 1986, pl. 2, figs. 6–7, pl. 3, fig. 6.
- Biddulphia aurita* (Lyngbye) Brébisson and Godey, 1838; Hustedt, 1930, teil 1, p. 846, fig. 501–502; Schrader, 1973a, pl. 13, figs. 1–3.

- Cavitatus jouseanus* (Sheshukova-Poretzkaya) Williams, 1989, p. 260; Akiba et al., 1993, p. 20, figs. 6.19–6.20; as *Synedra jouseana* Sheshukova-Poretzkaya, 1962, p. 208, fig. 4; Akiba, 1986, pl. 21, fig. 9.
- Cocconeis californica* Grunow, 1881; Hustedt, 1933, teil 2, p. 343, fig. 796.
- Cocconeis costata* Gregory, 1855; Hustedt, 1933, teil 2, p. 332, fig. 785.
- Cocconeis decipiens* Cleve, 1873; Hustedt, 1933, teil 2, p. 353, fig. 808.
- Cocconeis pellucida* Grunow, 1862; Hustedt, 1933, teil 2, p. 357, fig. 812.
- Cocconeis placentula* Ehrenberg, 1838; Hustedt, 1933, teil 2, p. 347–350, figs. 802–803.
- Cocconeis scutellum* Ehrenberg, 1838; Hustedt, 1933, teil 2, p. 337, fig. 790.
- Coscinodiscus asteromphalus* Ehrenberg, 1844; Hustedt, 1928, Teil 1, p. 452, fig. 250.
- Coscinodiscus lewisianus* Greville, 1866; Schrader, 1973a, pl. 8, figs. 1–6, 10, 15; Barron, 1985b, p. 781, fig. 9.10.
- Coscinodiscus marginatus* Ehrenberg, 1841; Hustedt, 1928, Teil 1, p. 416, fig. 223; Koizumi, 1975b, pl. 2, fig. 18; Akiba, 1986, pl. 1, figs. 1–4.
- Coscinodiscus marginatus* f. *fossilis* Jousé, 1961, p. 68, pl. 3, figs. 7–8; Koizumi, 1973b, p. 832, pl. 3, figs. 12–14; Schrader, 1973a, p. 703, pl. 20, figs. 12–13.
- Coscinodiscus oculus-iridis* Ehrenberg, 1839; Hustedt, 1928, teil 1, p. 454, fig. 252.
- Coscinodiscus radiatus* Ehrenberg, 1839; Hustedt, 1928, teil 1, p. 420, fig. 225.
- Coscinodiscus stellaris* Roper, 1858; Hustedt, 1928, teil 1, p. 396, fig. 207.
- Coscinodiscus symbolophorus* Grunow, 1884; Schrader, 1973a, p. 703, pl. 22, figs. 8–9 as *Coscinodiscus stellaris* Roper var. *symbolophorus* (Grunow) Jørgensen, Koizumi, 1973b, p. 832, pl. 4, figs. 5–6.
- Craspedodiscus coscinodiscus* Ehrenberg, 1844; Barron 1985b, p. 783, fig. 12.12.
- Crucidentacula nicobarica* (Grunow) Akiba and Yanagisawa, 1986, p. 486, pl. 1, fig. 9, pl. 2, figs. 1–7, pl. 5, figs. 1–9; Akiba, 1986, pl. 26, figs. 1–4; Yanagisawa and Akiba, 1990, p. 232, pl. 1, figs. 23–29.
- Remarks:** *Crucidentacula paranicobarica* vars. described by Akiba and Yanagisawa (1986) are tabulated together.
- Crucidentacula punctata* (Schrader) Akiba and Yanagisawa, 1986, p. 487, pl. 1, figs. 10–12, pl. 4, figs. 1–9; Yanagisawa and Akiba, 1990, p. 232, pl. 1, figs. 30–32.
- Cyclotella striata* (Kützing) Grunow, 1880; Hustedt, 1928, teil 1, p. 344, fig. 176.
- Denticulopsis dimorpha* (Schrader) Simonsen, 1979, p. 64; Akiba, 1986, pl. 27, figs. 1–13; Akiba and Yanagisawa, 1986, p. 488, pl. 15, figs. 1–25, pl. 16, figs. 1–11; Yanagisawa and Akiba, 1990, p. 254–257.
- Remarks:** The two varieties, var. *dimorpha* and var. *areolata*, are included here, so no effort was made to tabulate them separately.
- Denticulopsis hustedtii* (Simonsen and Kanaya) Simonsen emend. Yanagisawa and Akiba, 1990, p. 246, pl. 3, figs. 14–19, pl. 11, figs. 11–13; Akiba, 1986, pl. 28, figs. 16–17.
- Denticulopsis hyalina* (Schrader) Simonsen, 1979, p. 64; Akiba and Yanagisawa, 1986, p. 488, pl. 10, figs. 1–11, 14–16, pl. 11, figs. 1–10, pl. 12, figs. 1–5; Yanagisawa and Akiba, 1990, p. 240, pl. 2, figs. 14, 33–34, pl. 9, figs. 8–9.
- Denticulopsis katayamae* Maruyama, 1984a, p. 158, pl. 12, figs. 1–6, pl. 17, figs. 1–23 (not 14, 17); Akiba and Yanagisawa, 1986, p. 489, pl. 17, figs. 1–3, 6, pl. 19, figs. 6–9, pl. 20, figs. 1, 4–5, 7; Yanagisawa and Akiba, 1990, p. 245, pl. 3, figs. 12–13, 28, pl. 11, fig. 4.
- Denticulopsis lauta* (Bailey) Simonsen, 1979, p. 64; Akiba, 1986, pl. 26, figs. 15; Akiba and Yanagisawa, 1986, p. 489, pl. 7, fig. 29, pl. 9, figs. 2–9; Yanagisawa and Akiba, 1990, p. 235, pl. 2, figs. 6–8, 15, pl. 5, figs. 1–3, pl. 9, fig. 1.
- Denticulopsis miocenica* (Schrader) Simonsen, 1979, p. 65; Akiba, 1986, pl. 26, figs. 26–27; Akiba and Yanagisawa, 1986, p. 489, pl. 10, figs. 17–23, pl. 12, figs. 6–9; Yanagisawa and Akiba, 1990, p. 241, pl. 2, figs. 35–37.

- Denticulopsis praedimorpha* Barron ex Akiba, 1982a, p. 46, pl. 11, figs. 9-16, 18-27; Akiba and Yanagisawa, 1986, p. 489, pl. 13, figs. 1-2, 5-15, 17-23, 25-28, pl. 14, figs. 1-12; Yanagisawa and Akiba, 1990, p. 249-254.
- Remarks:** The four varieties and *D. barronii* are difficult to distinguish from one another in the light microscope, so no effort was made to tabulate them separately.
- Denticulopsis simonsenii* Yanagisawa and Akiba, 1990, p. 242, pl. 3, figs. 1-3, pl. 11, figs. 1, 5.
- Denticulopsis praelauta* Akiba and Koizumi in Akiba, 1986, p. 439 pl. 26, figs. 10-14; Akiba and Yanagisawa, 1986, p. 490, pl. 7, figs. 1-15, pl. 8, figs. 1-9; Yanagisawa and Akiba, 1990, p. 234, pl. 2, figs. 3-5, 16-18.
- Diploneis smithii* (Brébisson) Cleve, 1894; Hustedt, 1937, teil 2, p. 647, fig. 1051.
- Fragilariopsis doliola* (Wallich) Medlin and Sims, 1993; as *Pseudoeunotia doliolus* (Wallich) Grunow, 1880; Hustedt, 1932, teil 2, p. 259, fig. 737; Koizumi and Yanagisawa, 1990, p. 357, figs. 7.3-7.12, 8.
- Grammatophora angulosa* Ehrenberg, 1839; Hustedt, 1931, teil 2, p. 39, figs. 564a-k.
- Grammatophora oceanica* (Ehrenberg) Grunow, 1881; Hustedt, 1931, teil 2, p. 45, fig. 573.
- Hantzschia amphioxys* var. (Ehrenberg) Grunow, 1880; Hustedt, 1930, p. 394, figs. 747-750.
- Hemiaulus polymorphus* Grunow, 1884; Hustedt, 1930, teil 1, p. 880, fig. 525.
- Hemidiscus cuneiformis* Wallich, 1860; Hustedt, 1930, teil 1, p. 904, fig. 542; Koizumi, 1975a, pl. 4, fig. 2; Akiba, 1986, pl. 16, figs. 3-4.
- Mediaria splendida* Sheshukova-Poretzkaya, 1962, p. 210, figs. 2, 5; Koizumi, 1973b, pl. 7, figs. 5-6; Schrader, 1973a, pl. 3, figs. 14-15.
- Navicula lyra* Ehrenberg, 1841; Hustedt, 1964, teil 3, p. 500, figs. 1548-1555.
- Neodenticula kantschatica* (Zabelina) Akiba and Yanagisawa, 1986, p. 490, pl. 21, figs. 7-8, 13-19, 21, pl. 22, figs. 1-12; Akiba, 1986, pl. 25, figs. 15-27; Yanagisawa and Akiba, 1990, p. 259, pl. 7, figs. 27-37.
- Neodenticula koizumii* Akiba and Yanagisawa, 1986, p. 491, pl. 21, figs. 22-28, pl. 23, figs. 1-12, pl. 24, fig. 19; Yanagisawa and Akiba, 1990, p. 262, pl. 7, figs. 38-41.
- Neodenticula seminae* (Simonsen and Kanaya) Akiba and Yanagisawa, 1986, p. 491, pl. 24, figs. 1-11, pl. 26, figs. 1-10; Akiba, 1986, pl. 25, figs. 28-32; Yanagisawa and Akiba, 1990, p. 263 pl. 7, figs. 45-49.
- Neodenticula* sp. A, Akiba and Yanagisawa, 1986, p. 492, pl. 21, figs. 29-31, pl. 24, figs. 12-18, pl. 25, figs. 1-7.
- Nitzschia fossilis* (Frenguelli) Kanaya ex Schrader, 1973a; Koizumi and Kanaya, 1976, p. 155, pl. 1, figs. 11-14; Koizumi and Yanagisawa, 1990, p. 357, figs. 7-1, 7-2, 9.
- Nitzschia granulata* Grunow in Cleve and Möller, 1879; Lohman, 1938, pl. 22, fig. 10; Hendey, 1964, p. 278.
- Nitzschia heteropolica* Schrader, 1973a, pl. 26, figs. 1-2; Akiba, 1986, pl. 23, fig. 3.
- Nitzschia* cf. *jouseana* Burckle, 1972, p. 240, pl. 2, figs. 17-21; Schrader, 1974, pl. 7, figs. 14-23; Barron, 1980a, pl. 3, fig. 2; Akiba, 1986, pl. 23, Figs. 4, 11.
- Nitzschia marina* Grunow in Cleve and Grunow, 1880; Kolbe, 1955, p. 40, pl. 3, figs. 38-40; Schrader, 1973a, pl. 4 figs. 17-19; Koizumi and Tanimura, 1985, pl. 6, figs. 1-2; Akiba, 1986, pl. 22, fig. 12.
- Nitzschia navicularis* (Brébisson ex Kützing) Grunow, 1880; Hustedt, 1930, p. 401, fig. 763; Hendey, 1964, p. 276, pl. 39, figs. 3-5.
- Nitzschia pliocena* (Brun) Mertz, 1966; Koizumi, 1975b, p. 877, pl. 4, figs. 28-32; Akiba, 1986, pl. 23, figs. 6-9; Akiba and Yanagisawa, 1986, p. 496, pl. 40, figs. 1-7.
- Nitzschia porteri* Frenguelli, 1949; Schrader, 1973a, p. 707, pl. 5, figs. 35-36, 43-44.
- Nitzschia punctata* (Wm. Smith) Grunow; Hendey, 1964, p. 278, pl. 39, fig. 11.
- Nitzschia reinholdii* Kanaya ex Barron and Baldauf, 1986; Koizumi and Kanaya, 1976, p. 155, pl. 1, figs. 15-18; Koizumi and Tanimura, 1985, pl. 6, figs. 3-4; Akiba, 1986, pl. 22, figs. 4-5.
- Nitzschia rolandii* Schrader, 1973a, p. 708, pl. 5, figs. 31, pl. 26, figs. 3-4; Koizumi, 1980, p. 396, pl. 2, figs. 15-20; Akiba, 1986, pl. 25, figs. 1-6; Yanagisawa and Akiba, 1990, p. 258, pl. 7, figs. 17-26.
- Paralia sulcata* (Ehrenberg) Cleve, 1873; Hendey, 1964, p. 73, pl. 23, fig. 5; Sancetta, 1982, p. 235, pl. 3, figs. 13-15.
- Plagiogramma staurophorum* (Gregory) Heiberg, 1863; Hustedt, 1931, teil 2, p. 110, figs. 635; Hendey, 1964, p. 166, pl. 36, fig. 1.
- Proboscia barboi* (Brun) Jordan and Priddle, 1991, p. 56; Akiba and Yanagisawa, 1986, p. 497, pl. 42, figs. 3-5, 7, 10-11, pl. 44, figs. 1-8.
- Proboscia curvirostris* (Jousé) Jordan and Priddle, 1991, p. 57; Akiba and Yanagisawa, 1986, p. 497, pl. 42, figs. 1-2, pl. 45, figs. 1-6.
- Proboscia praebarboi* (Schrader) Jordan and Priddle, 1991, p. 57; Akiba and Yanagisawa, 1986, p. 497, pl. 42, figs. 8-9, pl. 43, figs. 1-9.
- Raphidodiscus marylandicus* Christian, 1886; Andrews, 1973, p. 231, pls. 1-5; Schrader and Fenner, 1976, pl. 7, fig. 16; Barron, 1983, p. 512, pl. 5, fig. 14.
- Rhaphoneis surirella* (Ehrenberg) Grunow in Van Heurck, 1880; Hustedt, 1931, teil 2, p. 173-174, fig. 679a-c; Schrader, 1973a, p. 709, pl. 25, figs. 4, 6.
- Rhizosolenia hebetata* f. *hiemalis* Gran, 1904; Hustedt, 1929, teil 1, p. 590, fig. 337; Koizumi, 1973b, pl. 5, figs. 34, 35; Schrader, 1973a, pl. 9, figs. 14-19.
- Rhizosolenia matuyamai* Burckle in Burckle et al., 1978, p. 213, figs. 3-6; Barron, 1980b, pl. 7, figs. 9-12.
- Rhizosolenia miocenica* Schrader, 1973a, p. 709, pl. 25, figs. 1, 11.
- Rhizosolenia styliformis* Brightwell, 1858; Hustedt, 1929, teil 1, p. 584, fig. 333; Schrader, 1973a, p. 710, pl. 10, figs. 18-21; Koizumi, 1975a, pl. 1, fig. 33.
- Rhopalodia gibba* (Ehrenberg) O. Müller, 1897; Hendey, 1964, p. 272.
- Rossiella paleacea* (Grunow) Desikachary and Maheshwari, 1958; Barron, 1985b, p. 790, figs. 9.6-9.7; Yanagisawa, 1995, p. 13, figs. 4.12-4.13, 15.1-15.8.
- Rouxia californica* M. Peragallo in Tempère and Peragallo, 1910; Hanna, 1930, p. 186, pl. 14, figs. 6, 7; Koizumi, 1975a, p. 802, pl. 1, fig. 52; Akiba, 1986, pl. 21, figs. 5-6.
- Stephanodiscus astraea* (Ehrenberg) Grunow; Hustedt, 1930, p. 110, fig. 85.
- Stephanopyxis dimorpha* Schrader, 1973a, p. 711, pl. 15, figs. 9-11, 19-20, pl. 16, figs. 1-3, 8-11, pl. 24, fig. 10; Hemphill-Haley and Fourtanier, 1995, pl. 3, figs. 4-5, 9-10.
- Stephanopyxis schenkii* Kanaya, 1959, p. 67, pl. 2, figs. 2-4; Koizumi, 1973b, pl. 6, figs. 11-12; Schrader and Fenner, 1976, pl. 19, figs. 7-8.
- Stephanopyxis turris* (Greville and Arnott) Ralfs, 1861; Hustedt, 1928, teil 1, p. 304, fig. 140; Koizumi, 1973b, p. 833, pl. 6, figs. 13-16; Schrader, 1973a, p. 711, pl. 15, figs. 1-7.
- Thalassionema hirosakiensis* (Kanaya) Schrader, 1973a, p. 711, pl. 23, figs. 31-33; Akiba, 1982b, p. 49, figs. 1-5.
- Thalassionema nitzschioides* Grunow, 1881; Hustedt, 1932, teil 2, p. 244, fig. 725; Koizumi, 1975a, pl. 1, figs. 50-51.
- Thalassionema nitzschioides* v. *parva* Heiden in Heiden and Kolbe, 1928, p. 564, pl. 35, fig. 118; Fenner et al., 1976, pl. 14, fig. 10.
- Thalassionema robusta* Schrader, 1973a, p. 712, pl. 23, figs. 24, 35-37.
- Thalassionema schraderei* Akiba, 1982b, p. 50, figs. 6-11; Koizumi and Tanimura, 1985, pl. 1, fig. 14; Akiba, 1986, pl. 21, figs. 13-16.
- Thalassiosira antiqua* (Grunow) Cleve-Euler, 1941; Cleve-Euler, 1951, p. 72, fig. 119a; Koizumi, 1973b, p. 834, pl. 7, fig. 12; Schrader, 1973a, pl. 11, fig. 25, pl. 25, fig. 19; Barron, 1980a, pl. 5, fig. 5; Akiba, 1986, pl. 12, figs. 1, 3-4.

- Thalassiosira convexa* Mukhina, 1965, p. 22, pl. 11, figs. 1–2; Koizumi, 1975a, pl. 4, figs. 15–20; Akiba, 1986, pl. 8, fig. 1.
- Thalassiosira eccentrica* (Ehrenberg) Cleve, 1904; Fryxell and Hasle, 1972, p. 300, pl. 1, figs. 1a–2, pl. 2, figs. 3–10, pl. 3, figs. 11–15, pl. 4, figs. 16–18; as *Coscinodiscus excentricus* Ehrenberg, Hustedt, 1928, teil 1, p. 388, figs. 201a–b.
- Thalassiosira grunowii* Akiba and Yanagisawa, 1986, p. 493, pl. 27, fig. 5, pl. 29, figs. 1–8, pl. 30, figs. 1–10; Tanimura, 1996, p. 178, figs. 18.29–18.34; as *Coscinodiscus plicatus* Grunow, 1884, p. 74, pl. 3, fig. 10.
- Thalassiosira hyalina* (Grunow) Gran, 1897; Hustedt, 1928, teil 1, p. 323, fig. 159; Koizumi, 1973b, p. 834, pl. 8, figs. 1?–2; Akiba, 1986, pl. 5, fig. 9.
- Thalassiosira leptopus* (Grunow) Hasle and Fryxell, 1977, p. 20, figs. 1–14; as *Coscinodiscus lineatus* Ehrenberg, Koizumi, 1975b, pl. 2, figs. 5–6.
- Thalassiosira marujamica* Sheshukova-Poretzkaya, 1959, p. 41, pl. 1, fig. 7; Akiba, 1986, p. 446, pl. 13, figs. 1–7; as *Thalassiosira nativa* Sheshukova-Poretzkaya sensu Barron, 1980a, pl. 6, figs. 8–9?.
- Thalassiosira manifesta* Sheshukova-Poretzkaya, 1964; Akiba, 1986, p. 446, pl. 9, figs. 1–3.
- Thalassiosira nidulus* (Tempère and Brun) Jousé, 1961, p. 6–3, pl. 3, figs. 4–5; Koizumi, 1973b, pl. 7, figs. 25–26.
- Thalassiosira oestrupii* (Ostenfeld) Proshkina-Lavrenko; Akiba, 1986, pl. 14, figs. 1–6.
- Remarks:** The Pliocene forms possibly include *T. tetraoestrupii* Bodén, 1993, p. 63, pl. 1, figs. A–G, and pl. 2, figs. A, B, H, and J. However, these two forms are too similar to discriminate from each other under the light microscope, so no effort was made to tabulate them individually.
- Thalassiosira* plicated spp. in Tanimura, 1996.
- Remarks:** Such marine plicated *Thalassiosira* as *T. californica*, *T. flexuosa*, and *T. kanayae* are not separated here.
- Thalassiosira praeyabei* (Schradler) Akiba and Yanagisawa, 1986, p. 492; Tanimura, 1996, p. 182, figs. 40–42; as *Coscinodiscus praeyabei* Schradler, 1973a, p. 703, pl. 6, fig. 16, pl. 7, figs. 17–20, 22–23.
- Thalassiosira temperei* (Burn) Akiba and Yanagisawa, 1986, p. 493, pl. 31, figs. 1–7; Tanimura, 1996, p. 182, figs. 17, 4752; as *Coscinodiscus temperei* Brun in Brun and Tempère, 1889, p. 33, pl. 8, fig. 2; Barron, 1985b, p. 782, figs. 10.5–10.6.
- Thalassiosira yabei* (Kanaya) Akiba and Yanagisawa, 1986, p. 493, pl. 27, figs. 1–2, pl. 28, figs. 1–9; Tanimura, 1996, p. 182, figs. 40–42; as *Coscinodiscus yabei* Kanaya, Koizumi and Tanimura, 1985, pl. 3, figs. 10–11.
- Thalassiosira zabelinae* Jousé, 1961, p. 66, pl. 2, figs. 1–7; Koizumi, 1973b, p. 834, pl. 8, figs. 10–12.
- Thalassiothrix longissima* Cleve and Grunow, 1880; Hustedt, 1932, teil 2, p. 247, fig. 726; Akiba, 1986, p. 447, pl. 21, fig. 18.